

DYNAMICS OF BAR IN THE BRAIDED RIVER JAMUNA

SHAMPA



DEPARTMENT OF WATER RESOURCES ENGINEERING

BANGLADESH UNIVERSITY OF ENGINEERING AND TECHNOLOGY

17 February, 2015

DYNAMICS OF BAR IN THE BRAIDED RIVER JAMUNA

A Thesis by

Shampa

In partial fulfillment of the requirement for the degree of

MASTER OF SCIENCE IN WATER RESOURCES ENGINEERING

DEPARTMENT OF WATER RESOURCES ENGINEERING

BANGLADESH UNIVERSITY OF ENGINEERING AND TECHNOLOGY

17 February, 2015

BANGLADESH UNIVERSITY OF ENGINEERING AND TECHNOLOGY

DEPARTMENT OF WATER RESOURCES ENGINEERING

The thesis titled 'DYNAMICS OF BAR IN THE BRAIDED RIVER JAMUNA' submitted by Shampa, Roll No. P 0411162003, Session: April 2011, has been accepted as satisfactory in partial fulfillment of the requirements for the degree of MASTER OF SCIENCE IN WATER RESOURCES ENGINEERING on 17 February, 2015.

BOARD OF EXAMINERS

.....

Dr. Mohammad Mostafa Ali
Associate Professor
Department of Water Resources Engineering
Bangladesh University of Engineering and Technology
Dhaka

Chairman
(Supervisor)

.....

Dr. Md. Sabbir Mostafa Khan
Professor and Head
Department of Water Resources Engineering
Bangladesh University of Engineering and Technology
Dhaka

Member
(Ex-officio)

.....

Dr. Md. Ataur Rahman
Professor
Department of Water Resources Engineering
Bangladesh University of Engineering and Technology
Dhaka

Member

.....

Dr. Md. Munsur Rahman
Professor
Institute of Water and Flood Management
Bangladesh University of Engineering and Technology
Dhaka

Member
(External)

CANDIDATE'S DECLARATION

It is hereby declared that this thesis or any part of it has not been submitted elsewhere for the award of any degree.

.....

Shampa,
Roll No. P 0411162003
Session: April 2011

ACKNOWLEDGEMENT

The author is grateful to the Almighty for successful completion of this thesis work. The author would like to express her sincere gratitude to her supervisor Dr. Mohammad Mostafa Ali (Assistant Professor, Department of Water Resources Engineering, Bangladesh University of Engineering and Technology), without whose constant supervision and endless support this research work would probably reach nowhere. His constant guidance, invaluable suggestions, motivation in difficult times and affectionate encouragement were extremely helpful in accomplishing this study.

The author expresses her sincere appreciation and deep gratitude to Prof. Md. Munir Rahman (Professor, Institute of Water and Flood Management, Bangladesh University of Engineering and Technology), Dr. Aminul Haque Sarker (Deputy Executive Director, CEGIS), Ms. Sara Nowreen (Assistant Professor, Institute of Water and Flood Management, Bangladesh University of Engineering and Technology) and Mr. Mahmood Khan (Junior Engineer, Institute of Water Modelling) for their enormous help in data collection and guidance.

The author thanks to Prof. Dr. Md. Sabbir Mostafa Khan (Professor and Head, Department of Water Resources Engineering, Bangladesh University of Engineering and Technology), Dr. Md. Aatur Rahman (Professor, Department of Water Resources Engineering, Bangladesh University of Engineering and Technology) and Prof. Md. Munir Rahman (Professor, Institute of Water and Flood Management, Bangladesh University of Engineering and Technology) for their kind review and suggestions, without these suggestions the successful completion of the thesis was quite impossible.

ABSTRACT

Braiding is one of the major river patterns of alluvial rivers. To respond to the pulsation of discharge and sediment load during the flood, the morphological features (bars and channels) of braided rivers experience major changes in area, shape and spatial distribution; that make the river network complex. Moreover, braided river network shows scale invariance property; the morphological and dynamical properties of a small part of a braided river can be applied to the larger part of it, from one braided river to another of different size, or from a laboratory model to a real braided river. Hence, this study focuses to understand the dynamics of the braided bar/island development process of braided river, Jamuna which is the downstream continuation of Brahmaputra river in Bangladesh.

Three types of data have been analyzed in this study- time series hydraulic data, data derived from the dry season satellite imagery analysis and the numerical modelling. The dry season satellite imagery analysis was basically used to understand the bar development process. At the same time the change of bar characteristic with time were also assessed using this data. Several hydraulic data such as water level, discharge, sediment, river cross section were used to assess the time series change of the bar development process. Numerical model was used to understand the detail of the development process of the bar at unsteady flow condition.

The bar development process in a dynamic river like Jamuna is very complex. This study indicated that, though during the last few decades river's discharge increased slightly and water level did not change significantly; river sediment load decreased drastically. As a response of the process, river reduces its water surface slope and increased its width. The bar area showed higher sensitivity to this process compared to the channel area. Large floods may not have a very significant role in increasing the bar area, but it contributes to the increase of sand area through lessening the vegetation coverage.

Temporal analysis of bars showed that at present maximum bars (53%) of the river are very young. The vegetation can cover bar area upto a limit of 70%. The vertical growth of bar stabilizes from 8 to 10 years. This study also found that the average height of the bars above low water level to be around 5 m which is comparable to the findings of several previous studies.

The numerical model study using Delft 3D indicated that several braided bar development phenomenon like adjacent channel shifting, formation of cross-bar channels and channel abandonment can be simulated through numerical model. This study also showed that several bar property like bar amplitude, aspect ratio are related to the active channel's (the channels that carry the 90% of the sediment in a cross-section) property of the river. With one unit change in active channel width-depth ratio both the bar amplitude and aspect ratio increased about 0.1%. The results of the numerical model also indicated that the average rate of sedimentation over the bar top during the wet season is 3.5 m/year which is comparable with the observed data (3.11 m/year during the young age).

Numerical model study also revealed that the growth of bars in lateral direction depend on the hydraulic property of the adjacent channel. The increment of channel length-width ratio also caused bar's length/width ratio increment. With one unit change in channel length-width ratio, bar's length/width ratio also increases more than 5%. With the change in discharge the adjacent channels adjust their sinuosity causing the lateral growth of bar. The growth of crossbar channel depends on the water depth that the bar experienced during monsoon. Adjacent channel abandonment process is mainly depend on the bifurcation angle with the main channel.

The process of braided bar development is as an essential part of the morpho-dynamics of the river. The river like Jamuna is subjected to future changes like climate anomalies, human interventions etc. If such changes occur hydro-morphological condition of the river will be altered. Finally this study recommends that before any interventions in the river, it should be considered that the river may not behave as the same as it do now. Hence detail study is needed prior to any intervention.

ACRONYMS AND ABBREVIATIONS

BWDB	Bangladesh Water Development Board
CEGIS	Center for Environmental and Geographic Information Services
d/s	Downstream of a river
DEM	Digital Elevation Model
FAP-6	Flood Action Plan 6
IWM	Institute of Water Modelling
m	meter
m ³ /s	Cubic meter per second
PWD	Public Works Department
H	Relative bar height
u/s	Upstream of a river

TABLE OF CONTENTS

ACKNOWLEDGEMENT	v
ABSTRACT.....	vi
ACRONYMS AND ABBREVIATIONS	viii
TABLE OF CONTENTS.....	ix
LIST OF FIGURES	xiii
LIST OF TABLES	xvi
Chapter 1 Introduction.....	1
1.1. Background and present state of the problem	1
1.2. Objectives.....	2
1.3. Structure of the report	3
Chapter 2 Literature Review.....	4
2.1 Introduction	4
2.2 Braiding process.....	5
2.3 Unit Processes in Braided River.....	6
2.3.1 Channel bifurcations	6
2.3.2 Confluences.....	7
2.3.3 Bar formation	8
2.3.4 Avulsions	8
2.3.5 Incision of bars.....	8
2.3.6 Channels migration	9
2.4 Complexities Associates in Reproducing the Braided Phenomenon	9
2.4.1 Strong nonlinearities	9
2.4.2 Unsteadiness	9
2.4.3 Time scales.....	9
2.4.4 Gravitational effects on sediment transport	10
2.4.5 Partially transporting cross sections.....	10

2.4.6	Secondary flows.....	10
2.4.7	Finite length effects.....	10
2.5	Braided Bar Development Process in Braided River.....	10
2.5.1	Factors Determining Bar Dimensions and Dynamics in Braided Rivers	13
2.6	Computational models of braided rivers.....	15
2.7	Other Earlier studies related to bar dynamics of the Jamuna River.....	16
Chapter 3	Study Area	18
3.1	Introduction.....	18
3.2	Geophysical setting.....	19
3.3	Hydro-morphological status.....	22
3.3.1	Flow Regime.....	22
3.3.2	Sediment Regime.....	24
3.4	Morpho-dynamics of the River.....	25
3.4.1	Long-term development.....	25
3.4.2	Recent development.....	32
3.4.3	Bedform types and dynamics.....	35
3.5	Human Interventions in Brahmaputra Basin.....	35
Chapter 4	Data Used and Methodology.....	37
4.1	Data Used.....	37
4.1.1	Water level.....	37
4.1.2	Discharge.....	38
4.1.3	Sediment.....	38
4.1.4	Cross-section.....	39
4.1.5	Satellite images.....	39
4.1.6	Topographic survey data.....	39
4.2	Methodology.....	39
4.2.1	Satellite imagery processing and classification.....	41

4.2.2	Selection of study bar.....	45
4.2.3	Assessing the age of bars	45
4.2.4	Assessing the relative bar height (H) with respect to low water level.....	45
4.2.5	Assessing Active braided index (ABI)	46
4.2.6	Assessing Active Channel Width.....	46
4.2.7	Assessing Bar Length and Amplitude.....	47
4.2.8	Assessing Bar Shape	47
4.2.9	Numerical Model Description.....	47
Chapter 5	Results and Discussions.....	54
5.1	Changes in River Flow and Sediment Regime.....	54
5.2	Changes in river spatial characteristics	60
5.3	Relation between the Water Surface Slope and Bar Dynamics	61
5.4	Relation between Sediment load and Bar dynamics	62
5.5	Temporal Development of Bars	63
5.5.1	Ages of the bars	63
5.5.2	Vegetation colonization on the bar	64
5.6	Vertical growth of bar	65
5.6.1	Vertical growth of a structurally intervened and a non- intervened bar	68
5.7	Bar dynamics in lateral direction	69
5.8.1	Spatial Development of bar	69
5.8.2	Unit process related to the development of bar	71
5.8	Numerical Modelling of braiding process.....	75
5.9.1	Calibration and verification of the Numerical Model.....	76
5.9.2	Overall planform of the river	79
5.9.3	Reach-scale River hydraulic property and Bar	80
5.9.4	Relation between Adjacent Channel Characteristics and Bar.....	85
5.9.5	Development of crossbar channel.....	87

5.9.6	Channel abandonment and growth of bar	89
5.9	Discussions.....	90
Chapter 6	Conclusions and Recommendations	95
6.1	Conclusions	95
6.2	Recommendations	96
Reference	98

LIST OF FIGURES

Figure 2-1 : Classification of alluvial channels (redrawn from Leopold and Wolman, 1957)..5	5
Figure 2-2: Landsat photograph of the Brahmaputra River various kinds of channel pattern. (Reproduced from Bridge, 1993).....5	5
Figure 2 -3: (a) central bar braiding mechanism, (b) alternating point bar chute cutoff, (c) dissection of multiple row bars (redrawn from Ashmore, 1991).....7	7
Figure 2-4: Avulsion and incision of a new channel (redrawn from Ashmore, 1991)8	8
Figure 2-5: Braided bar development process (reproduced from Asworth, 2000)12	12
Figure 2-6: A typical neutral curve for alternate-bar formation (reproduced from Colombini et al., 1986)14	14
Figure 3-1: Map showing the study area.....18	18
Figure 3-2: Longitudinal profile of Brahmaputra River (reproduced from Jagers, 2003).....19	19
Figure 3 -3: Tectonic map of the Indo-Australian and Euro-Asian Plates (reproduced from Rashid, 1991).....20	20
Figure 3 -4: Mean daily discharge hydrograph of the river at Bahadurabad (from 1956 to 2006)22	22
Figure 3-5 : Mean daily water level hydrograph at Bahadurabad (from 1956 to 2006).....23	23
Figure 3 -6: Average water surface slope at the date of annual minimum water level (from 1956 to 2006)23	23
Figure 3 -7: Shifting of the rivers of Bengal basin (based on Paleogeographic map of the Ganges-Brahmaputra delta (reproduced from Sarker et al., 2013 after Goodbred and Kuehl, 2000a)26	26
Figure 3-8: (a) Maps illustrating the position of the Jamuna River from 1776 to 1978: (A) 1776; (B) 1828; (C) 1843; (D) 1978. (Reproduced from Gupta et al., 2007).....28	28
Figure 3-9: Reproduction of Rennel's Map of 1776 (redrawn from Gupta et al., 2007).....29	29
Figure 3-10: Westward migration of Jamuna (reproduced from CEGIS, 2007)31	31
Figure 3 -11: Length-averaged bankline migration of the Jamuna River (reproduced from Sarker, 2009).....32	32
Figure 3-12: Riverbank erosion of Jamuna from 1973-09 (reproduced from CEGIS, 2010)..33	33
Figure 3-13: Rate of Erosion along the Jamuna River at different periods (reproduced from CEGIS, 2010).....34	34
Figure 3 -14: Change of braiding index of the Jamuna River over time (reproduced from CEGIS, 2010).....34	34

Figure 4-1: BWDB Discharge, Water level and X-sec location along Jamuna.....	38
Figure 4-2: Methodology of the study	40
Figure 4-3: Selection of study bar.....	44
Figure 4-4: Definition diagram for relative bar height	46
Figure 4-5: Model Grid and Bathymetry	51
Figure 4-6: The upstream and downstream boundary conditions of the model	52
Figure 4-7: Comparisons of measured and predicted values of sediment load	53
Figure 5-1: Changes in (A) maximum annual discharge, (B) minimum annual discharge and (C) mean annual discharge of the Jamuna River over time	56
Figure 5-2: Changes in (A) maximum annual water level (B) minimum water level (C) mean annual water level of the Jamuna River over time.....	57
Figure 5-3: Changes in water surface slope over time (at dry period).....	58
Figure 5-4: Changes in (A) maximum annual Bedmaterial load (B) minimum Bedmaterial load (C) mean annual Bedmaterial load (D) mean annual Wash load of the Jamuna River over time	59
Figure 5-5: Average width of Jamuna with time	60
Figure 5-6: Yearly variation of Area of Water and Bar within the bankline with annual maximum and minimum flow.....	61
Figure 5-7: Changes in bar and channel area with the slope	62
Figure 5-8: Changes in bar and channel area with the sediment load	62
Figure 5-10: Ages of bar area in the study area.....	63
Figure 5-9: Ages of the bars of the study area	63
Figure 5-11: Typical and low level vegetation	64
Figure 5-12: The bar area and its vegetation coverage with time.....	65
Figure 5-13: Vegetation coverage of land with age.....	65
Figure 5-14: Box plot of relative height of the selected bars against age.....	66
Figure 5-15: Relationship between Relative heights of the selected bars against age.....	67
Figure 5-17: Predicted and observed relative height with age.....	67
Figure 5-16: Location of topographic survey of Bar at Chowhali.....	67
Figure 5-19: Relationship between Relative heights and age of a structurally intervened and non-intervened bar	68
Figure 5-18: Location of selected bar to assess the effect of structural intervention	68
Figure 5-20: Development of a mid-channel bar over time.....	69
Figure 5-21: Development of a cluster of bars into a bar over time	70

Figure 5-22: Adjacent Channel shifting process and lateral growth of bar	71
Figure 5-23: Growth of crossbar channel	73
Figure 5-24: Channel abandonment and growth of the bar	74
Figure 5-25 Planform of 2011 and initial bathymetry of the river	75
Figure 5-26: Calibration of the numerical model	77
Figure 5-27: Water level calibration at Sirajgonj	78
Figure 5-28: Sediment calibration at Bahadurabad	78
Figure 5-29: Verification of the model for the year 2012 at Sirajganj	78
Figure 5-30: Comparison between the planform of 2012 and numerical model	79
Figure 5-31: Change of ABI and ACW during the simulated period	80
Figure 5-32: Relation between braided index and river width/depth ratio	81
Figure 5-33: Relation between bar amplitude and different hydraulic parameters	81
Figure 5-34: Relation between bar length and different hydraulic parameters	82
Figure 5-35: Relation between bar amplitude ratio and active B_c/h_c	83
Figure 5-36: Relation between bar aspect ratio and active B_c/h_c	83
Figure 5-37: Cumulative sedimentation/erosion in the numerical model.....	84
Figure 5-38: Net sedimentation/erosion within the bankline.....	85
Figure 5-39: Cumulative sedimentation on the bar top	85
Figure 5-40: Channel shifting process and reproduction in numerical modelling.....	86
Figure 5-41: Relation between bar and channel hydraulic property where W_b = Width of the bar (m) W_c = Width of the Channel (m) L_b =Length of the bar (m) L_c =Length of the channel (m).....	87
Figure 5-42: Velocity vector in main and cross-bar channel.....	87
Figure 5-43: Development of crossbar channel and reproduction of the process in the numerical model.....	88
Figure 5-44: Relation between water depth, bed shear stress and crossbar channel area.....	89
Figure 5-45: Channel abandonment process and reproduction in numerical modelling	89
Figure 5-46: Relation between bifurcation angle and percentage of flow.....	90

LIST OF TABLES

Table 3-1: The annual average sediment load as measured during 1966-1969 by the BWDB (source Delft Hydraulics and DHI, 1996a).....	24
Table 3-2: Total suspended sediment load in the Jamuna River	25
Table 3-3: Average Width and Position of the Jamuna River (ISPAN, 1993).....	31
Table 4-1: List of data used for the study	37
Table 4-2: Extent of study and main data source.....	41
Table 4-3: List of Satellite images with acquisition date.....	42
Table 4-4: Boundary Sediment load	52
Table 4-5: Parameters used in the Sensitivity Analysis.....	53

Chapter 1

Introduction

1.1. Background and present state of the problem

Braided rivers are morphologically very dynamic and complex in nature (Schumm, 1977; Hooke et al., 1997). The system of a braided network is being characterized by strong nonlinearities, unsteadiness; time scaled difficulties, gravitational effects on sediment transport, partially transporting cross sections, secondary flows and finite length effects which add to the complexity to understand the network (Thorne et al., 1997). Moreover, the change of river morphology due to extrinsic and intrinsic factors adds to the new dimension to the complexity (Sarker et al., 2011). But at the same time the rivers of the world exhibit a remarkable similarity, regardless of size. There is a neat progression of shapes and dimensions from the smallest rill to the Mississippi or the Amazon. There are, of course, differences among rivers in various climates and geological settings, but such differences seem overshadowed by similarities (Leopold, 1994). Georgiou and Sapozhnikov (2001) showed that there are fundamental statistical similarities between small and large parts of a braided river and between one braided river and other both in terms of static morphology and evolutionary dynamics. Hence, understanding the morphological and dynamical properties of a small part of a braided river is crucial when applying the knowledge to a larger part of it, from one braided river to another of different size, or from a laboratory model to a real braided river. Therefore, this study focuses the dynamics development process of braided bar/island in the Jamuna River.

The Jamuna, downstream continuation of the Brahmaputra River in Bangladesh, is almost an un-trained large braided river, complex in nature and possibly showing chaotic behavior (Repetto, 2000). The river experiences a very high discharge during monsoon (more than $100,000 \text{ m}^3/\text{s}$) and a very low flow at dry season (about $4,000 \text{ m}^3/\text{s}$) (CEGIS, 2010). But like the world's other great braided rivers, Brahmaputra-Jamuna is currently subject to extreme development pressures amplified by climate change and the need for improved approaches to river engineering and adaptive management rising day-by-day (Sarker et al., 2013).

The present river management approaches (structural interventions and others) suffer from the lack of understanding of the river behavior (Sarker et al., 2013). Moreover, the river provides substantial eco-system services, which are often ignored while making of any intervention. Furthermore, the islands of Jamuna provide livelihood for a large number of people, with a population density of 402 persons/km² which is nearly half of the country's density (Sarker et al., 2003). Most of their livelihood is based on agriculture but their land fertility and cropping pattern are highly dependent on river, as a result of erosion and sand deposition (Sarker et al., 2003 and Uddin et al., 2011). About 98% of the bar/island people experience the threats of migration or relocation due to bar/island erosion (Imran et al., 2002). The dynamics of bar/island also affect the mainland people as the initiation or incision process of bar is closely related to the river widening or narrowing process (Delft Hydraulics and DHI, 1996). So to protect the people and vital ecosystem in a sustainable manner, it is important to know the natural development process of bar/island and its dynamics.

Several studies have been done on Jamuna River. But most of them address the overall channel morphology (FAP 24; Goodbred and Kuehl, S.A.; 2000a, Klaassen and Masselink, 1992), bifurcation (Ashworth et al., 2000; Richardson and Thorne, 2001), riverbank erosion (Coleman, 1969; Thorne et al., 1995; Ashworth et al., 2000; CEGIS, 2007) and structural interventions (Rahman et al., 1998, Rasheduzzaman et al., 2007, Uddin et al., 2012). Yet understanding of fluvial processes is still limited and knowledge of the morpho-dynamics is even sparser (Thorne, 1997; Gupta, 2007). A very few study have been done on river bar/island development process (Ashworth et al., 2000; Sarker et al., 2003; Schuurman et al., 2013) and most of them cover the social aspect of char/island dwellers (Zaman, 1991; Sarker et al., 2003) and a certain stage of bar/island development process (Richardson et al., 1996; Richardson & Thorne, 1998). Therefore, an attempt has been made through this study to understand the dynamics of braided bar/island in line with the river dynamics.

1.2. Objectives

The main goal of this study is to understand the development process of braided bar/island in Jamuna River. The specific objectives are

- To assess the temporal developments of selected bars/islands of the Jamuna River both in horizontal and vertical planes.

- To assess the relationship of horizontal and vertical developments of selected bars/islands with different hydraulic parameters.
- To assess the competency of a 2-D morphology model in simulating bar/island development processes in a braided river.

1.3. Structure of the report

This report contains six chapters. The first chapter provides an introduction that includes the background and objectives of this study. The second chapter elucidates the overall morphological process of bar development with the earlier studies. The third chapter describes the details of the study area. The fourth chapter explains the details of the data and methodology used in this study. The results and discussion on the bar dynamics are described in chapter five. Finally chapter six describes the conclusions and the recommendations.

Chapter 2

Literature Review

2.1 Introduction

River pattern and fluvial processes evolved simultaneously. These fluvio-morphological processes work through mutual adjustment unless they attain a self-stabilization state (Rosgen, 1994). Although the physical laws governing the formation of a channel of a great river are the same that form a tiny one; different types of river are seen in the world (Leopold and Wolman, 1957). Not only rivers differ among themselves but also through time, and one river can vary significantly in a downstream direction (Schumm, 2005). A river is shaped by its flow, quantity and characteristics of the sediment it is carried, character and composition of its bed and bank material and the uniqueness of the valley over which it is flowing (Leopold et al., 1964). Natural controls (e.g. rocks, vegetation) and human interventions (e.g. embankments, bridges) may influence the shape of the river (Delft Hydraulic and DHI, 1996a). However, the effects of natural controls are limited to an alluvial river - a river which has formed its channel in the sediments that is transported or has been transported by its sediment (Schumm and Winkley, 1994). Surprisingly, large alluvial rivers can vary greatly in morphology as it goes towards downstream, although hydrologic conditions are not greatly different (Schumm, 2005). The channel patterns of the alluvial rivers may be braided, meandering or straight which is shown in Figure 2-1 (Leopold and Wolman, 1957). Brice (1982, 1983) added another pattern which is anabranching or anastomosing. Among them the braided river, being a system of numerous alluvial channels that divide and rejoin around bars and islands, forming an intertwining structure that resembles a braid; are morphologically very dynamic and complex in nature (Schumm, 1977; Hooke, 1997; Thorne, 1997; Efi Sapozhnikov, 2000; Sarker et al., 2011). Although a vast amount of research has been directed toward understanding braided rivers, we still do not completely understand the relationship between controlling independent variables and braided-river morphology (Germanoski and Schumm 1993).

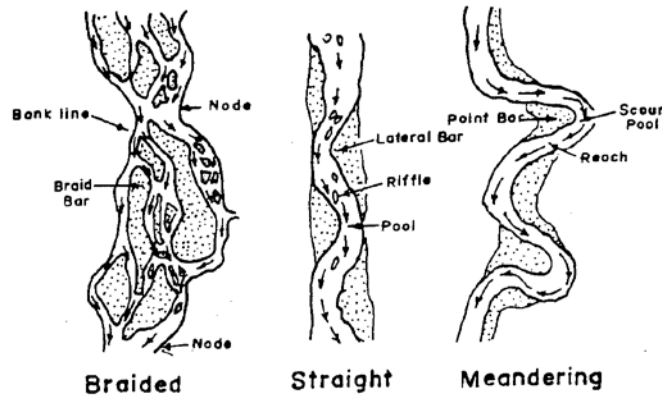


Figure 2-1 : Classification of alluvial channels (redrawn from Leopold and Wolman, 1957)

2.2 Braiding process

As mentioned earlier the term 'braiding' is generally meant the splitting of channels around bars (islands). Another type of river "anastomosing" has also splitting channels (Brice 1964, 1984). The definitive feature of anastomosing (anabranching) channel segments is that they are longer than a curved channel segment around a single braid or point bar and their width-scale flow patterns behave independently of adjacent segments, in contrast to braided channel segments around bars (e.g. Fig 2-2). Thus anastomosed channel segments contain their own bars in accordance with imposed discharge and sediment load, enabling definition of braiding index and sinuosity for each segment. Anastomosing is therefore more similar to terms like distributive and tributive (e.g. Schumm 1985). This type of river has the individual segments are undivided, sinuous channels separated by areas of floodplain much larger than the largest

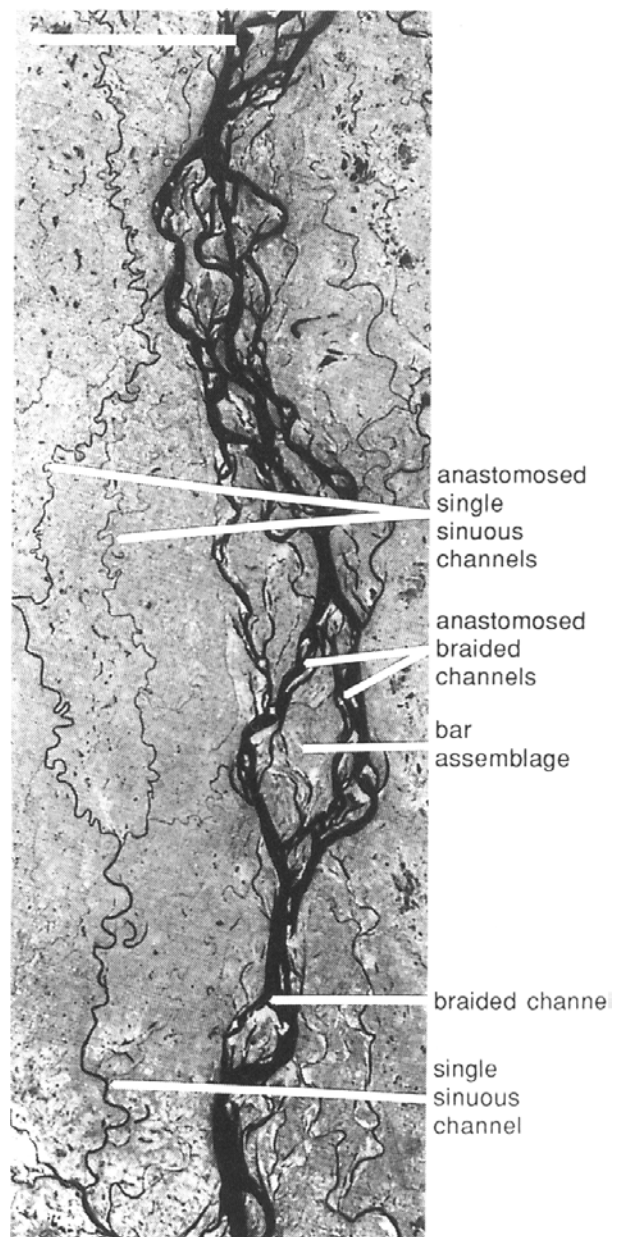


Figure 2-2: Landsat photograph of the Brahmaputra River various kinds of channel pattern. (Reproduced from Bridge, 1993)

bars present (e.g. Fig 2-2).

The fundamental causes of braiding are still unclear. However braiding seems to occur when the flow and bank are sufficiently unconstrained (laterally); the channels can change their width freely (Bridge, 1993). Furthermore, braiding occurs in the presence of huge bedload transport in comparison with that suspended load. Murray & Paola (1994) define the braiding process as the fundamental instability of laterally unconstrained free-surface flow over cohesionless beds.

Ashmore (1982, 1991) identifies six single unit processes governing the generation and development of the braided network. His two experimental works provide a detailed description of these unit processes, which are summarized as follows.

2.3 Unit Processes in Braided River

2.3.1 Channel bifurcations

Channel bifurcations are the formative process in braided systems; Ashmore (1991) describes the possible mechanisms through which bifurcation may develop are i) Central bar mechanism and dissection of transverse unit bar ii) Chute cutoff mechanism iii) Multiple bars mechanism.

Central bar mechanism and dissection of transverse unit bar are the two most commonly documented processes of braiding generation and have been first described by Leopold & Wolman (1957). These processes imply the development of a submerged central bar, initiated from a symmetrical transverse unit bar, whose downstream margin is usually marked by the accumulation of the coarsest fraction of bedload. Figure 2-3a shows the typical development of this process. The presence of the unit bar, forces the flow to diverge and the central nucleus (submerged bar) is eventually exposed. Immediately downstream of the bar, the divided flows produce scour pools against the opposite banks. Ashmore (1991) suggests that the distinction between the central bar mechanism and the dissection of transverse unit bar is essentially due to higher sediment mobility which characterizes the latter process.

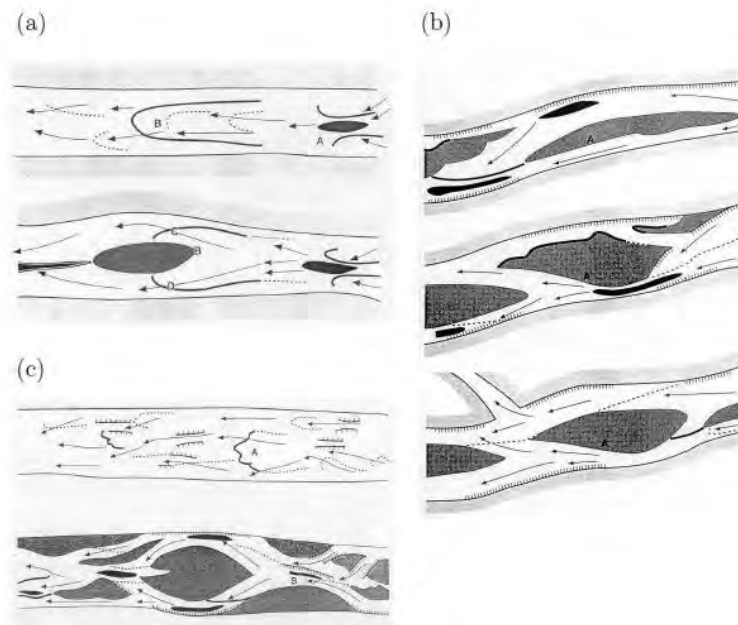


Figure 2-3: (a) central bar braiding mechanism, (b) alternating point bar chute cutoff, (c) dissection of multiple row bars (redrawn from Ashmore, 1991)

The chute cutoff mechanism indicates the chute cutoff of point bars in low-sinuosity channels. Figure 2-3b shows an example of alternating point bar cutoff. A transverse alternating point bar in a weakly curved channel is transformed into a more complex bed form by lateral accretion as migratory sheets that move along the channel. The rapid point bar accretion and concave bank erosion immediately upstream of the chute causes more flow to be directed over the point bar. Multiple bars mechanism was first documented by Fujita & Muramoto (1988). This particular mechanism appears to be a special case that applies only to channels with very high values of the width/depth ratio. The initial bed configuration, consisting of numerous multiple bars, is gradually converted to fewer larger bars which concentrate the flow into scour (Figure 2-3c)

2.3.2 Confluences

Another important unit process is channel confluences. When the flow of two bifurcated channels converge; a scour hole may generate due to the strong secondary currents. According to Mosley (1976), the scour depth is controlled by the angle of incidence of the two channels and by the proportion of the total discharge flowing in each branch. The hole tends to parallel the alignment of the dominant channel.

2.3.3 Bar formation

In single branches of braided rivers alternating bars develop, similar to those of the straight channels. Though their formation may be associated to an inherent instability of the flow sediment system, their development is crucially affected by local flow conditions like curvature and local widening. Channels confluences and alternating bars development are mainly responsible for the generation of scour holes. Details about the bar formation process will be described later in this chapter.

2.3.4 Avulsions

Channel avulsions are typical events in a fully developed braiding. They occur under a variety of circumstances. The presence of bars plays a crucial role on the generation of avulsions both inducing bank erosion and raising the local water level allowing overtopping of the channels sides. When the water finds a definite path across the surface the incision of a new channel may occur (Figure 2-4).

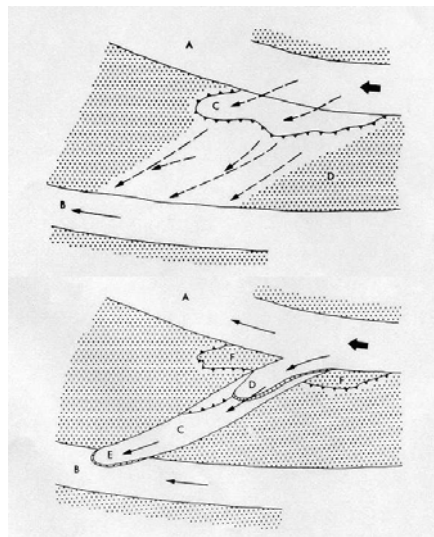


Figure 2-4: Avulsion and incision of a new channel (redrawn from Ashmore, 1991)

2.3.5 Incision of bars

In braided networks large bars are often split due to the generation of an axial trough which displays a accelerated sediment transport. This phenomenon usually occurs during declining water discharge, being triggered by the concentration of flow along one line.

2.3.6 Channels migration

Single channels in braided networks are subjected to migration which is similar to the meandering rivers. In general, the bank erosion occurs on a time scale which is of the same order of the scale of the deformation of the bed. However, channel migration in braided rivers is typically much faster than in meandering channels.

In the present work the attention is focused on bar growth process of the braided systems. The growth of the braided bar influence almost all the unit process but more closely related with the channel bifurcations, bar formation and incision of bars mechanisms. Several researchers adopted different methodologies and sources (e.g. physical modeling, field observation, satellite image, numerical modeling) to explain the characteristics of the braided scheme but the braided network presents several difficulties; the system being characterized by numerous complicating features like - Strong nonlinearities, Unsteadiness, Time scales, Gravitational effects on sediment transport, Partially transporting cross sections, Secondary flows, Finite length effects etc. (Repetto, 2000) which are summarized below.

2.4 Complexities Associates in Reproducing the Braided Phenomenon

2.4.1 Strong nonlinearities

Braided systems are subjected by strong non-linearity. The interactions between free responses of the system (due to an inherent instability of free surface turbulent flow over an erodible bed) and forced responses (induced by physical constraints, such as curvature, width variations, confluences) crucially affect the topographic behavior of the network.

2.4.2 Unsteadiness

Braided river systems exhibit strong unsteadiness in flow field and sediment transport. An equilibrium configuration of the system does not seem to exist, rather a recursive process of formation and obliteration of bed forms and planimetric structures is always observed.

2.4.3 Time scales

In braided streams the time scales of bed and bank erosion are comparable. The full coupling between bed and planform evolution is another characteristics of the braided streams. Furthermore, bank erosion induces a net effect on sediment transport.

2.4.4 Gravitational effects on sediment transport

Gravitational effects on bedload transport have been found to play a fundamental role in river morphodynamics, since they affect both the instability process which leads to bar development and the equilibrium configuration of bedforms (Fredsoe, 1978; Colombini et al., 1987). In braided systems, the presence of strong local depositions and scours induced by channel migration and confluences, implies that their effects have to be taken into account in detail.

2.4.5 Partially transporting cross sections

Small values of Shields stress which falls close to the critical value even at high stages is another major phenomenon of the braided stream. Typically only some branches are simultaneously active. Furthermore, in a single channel, sediment transport may occur only in a limited part of the cross section; hence, the possibility of partial transport of sediment within the cross section must be accounted to model the network.

2.4.6 Secondary flows

Like the other alluvial rivers depositional and scour phenomena in are often associated with the development of secondary flows; bed deformation often developed by the centrifugal effect induced by curvature of streamlines of depth averaged flow and by inertial effects associated with flow adjustments to spatial variations of channel geometry.

2.4.7 Finite length effects

The relatively small length of each branch at the same time continuous interplay of channels, imply that the condition of infinite longitudinal domain. When investigating the bar development in rivers, it is hard to reproduce this phenomenon in single branches of braided systems. Nevertheless, upstream and downstream influences may crucially affect water and sediment motion in each channel.

2.5 Braided Bar Development Process in Braided River

Braided rivers are fascinating because of their complicated patterns and dynamics. Within the group of braided rivers, there is a large diversity of particle sizes, bar shapes, and tendencies to avulse, wander, or form anabranches. Both bar dimensions and braiding intensity are known to depend on the width-depth ratio of the braidplain, as shown by field observations,

flume experiments, and linear analyses based on analytical physics (Bernini, et al., 2006). Asworth (2000) identifies the key development stages of a braided bar based on the field observations of a bar of the Jamuna river, Bangladesh. These stages are summarized below.

Stage 1

A Mid-channel bar starts to grow downstream of a major flow convergence. Bar initiation was probably caused by an increase in discharge from one of the tributary anabranches and large scale sediment input from the bank erosion immediately upstream of the zone of bar deposition (Figure 2-5(1)).

Stage 2

As dunes are ubiquitous in the Jamuna at all flow stages (Roden, 1998). It is also likely that the initial bar core was formed by a series of amalgamated large dunes, which may have evolved into a bar front with an angle-of-repose slipface (Figure 2-5(2)).

Stage 3

After deposition of a central bar nucleus, bar growth continues through a combination of several depositional processes. The principal mechanism of sand braid-bar growth is through the amalgamation of large dunes that form a central bar nucleus. Bar-top aggradations continues through both dune superimposition and development of “accretionary dune front” upto a certain height (3-m-high in case of Jamuna). Amalgamation of smaller dunes are found in shallower flow on the bar-top (Figure 2-5(3)).

Stage 4

At low flow, the bar widens through lateral accretion produced by dune migration around and onto the margins of the bar. Lateral accretion at the bar-tail may form two or more protruding ‘limbs’ that provide a zone of low flow velocity, which permits deposition of substantial quantities of fine-grained sediment (i.e. silts and clays) (Figure 2-5(4)).

Stage 5

As bar evolution continues, one anabranch becomes dominant, is enlarged and supplies sediment for deposition within the anabranch. This deposition deflects the flow across the bartail and constructs a broad depositional front attached to the bar-tail. Emergence of bars

along this depositional front gives the reach a morphology, that resembles an alternate bar (Figure 2-5(5)).

Stage 6

From the observations of a mid channel braid bar of Jamuna, Asworth (2000) concludes that the morphological evolution of the sand braid-bar will be dominated by cross-stratification formed by dunes and sets of cross-strata produced by slipface accretion at bar margins. The general similarity in bar dynamics and alluvial architecture between the Jamuna and past models of braid-bar deposition proposed for smaller sand-bed rivers (e.g. Cant & Walker, 1978; Bridge et al., 1986, 1998) suggests a scale invariance in some aspects of braid-bar deposition across several orders.

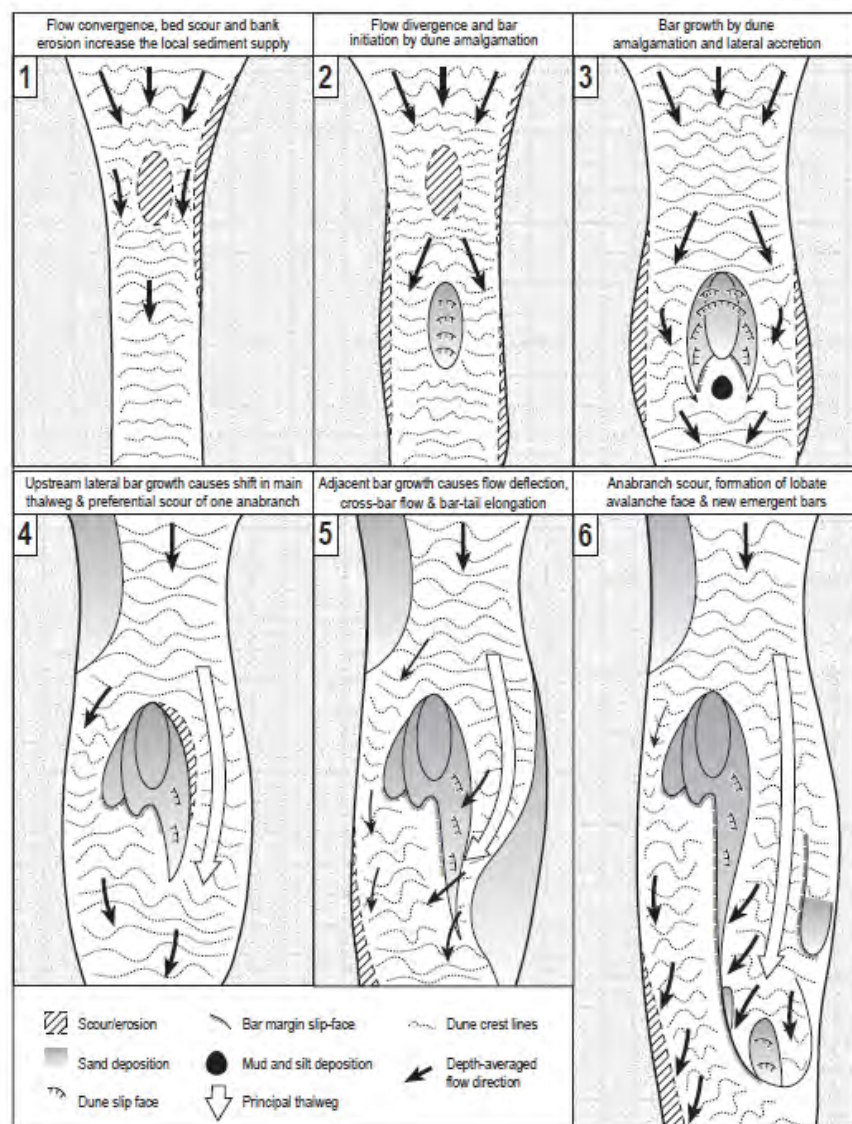


Figure 2-5: Braided bar development process (reproduced from Asworth, 2000)

Schuurman et al. (2013) summarized the factors that determine Bar Dimensions and Dynamics in Braided Rivers. These factors are described in the following sections.

2.5.1 Factors Determining Bar Dimensions and Dynamics in Braided Rivers

At a high width-depth ratio, midchannel bars form spontaneously from minor perturbations in the bed (Fujita, 1989; Ashmore, 1991). With fully developed bars, a higher braiding intensity is caused by dissection of midchannel bars by over-bar flow (Ashmore, 1991). At a lower width-depth ratio, weak braiding initiates by chute cutoffs (Ashmore, 1991; Federici and Seminara, 2003; Bertoldi et al., 2009; Kleinhans and Berg, 2011). Furthermore, braidplain widening results in higher braiding intensity (e.g., Ashworth et al., 2000; Rice et al., 2009). Two types of bars are distinguished: unit bars and compound bars (e.g., Rice et al., 2009). Unit bars are relatively simple, whereas compound bars have more complicated morphology and were built up from multiple bars. A compound bar changes shape during development in contrast to a unit bar that maintains its shape while migrating. Furthermore, the upstream part of compound bars commonly is the oldest and highest part with steep erosive upstream edges bifurcating the river, whereas unit bars commonly have a relatively high downstream part with a steep downstream slope. One or two bar tails commonly form by deposition at the lee-side of compound bars sourced partly by erosion of the upstream side of the bar (Bridge, 1993; Best et al., 2003, 2006; Rice et al., 2009; Ashworth et al., 2011).

Although these phenomena are well known and often observed, there exists no quantitative model for the dimensions and dynamics of compound bars, whereas incipient unit bar wavelength can perhaps be predicted by linear analyses. Many flume experiments have shown that discharge magnitude variation, such as a hydrograph, is not necessary for river braiding or for maintaining dynamics in braided rivers (e.g., Fujita, 1989; Ashmore, 1991). This suggests that the key requirements for development of a braided river are a movable bed and a sufficiently wide braidplain (e.g., Parker, 1976; Blondeaux and Seminara, 1985; Tubino et al., 1999; Crosato and Mosselman, 2009; Kleinhans and Berg, 2011). However, bar initiation in numerical modeling and linear analyses requires at least a small initial perturbation to induce nonuniformity in the flow field and thus nonuniformity in sediment transport.

The formative conditions of braided streams with non-dimensional parameters were first proposed by Ikeda (1973). He proposed

$$U^*/U_{c*} < 1.4(BI/h) \quad (2.1)$$

Where, B is the full channel width, h the mean depth, U^* the shear velocity and U_{c*} the critical shear velocity. Later, Muramoto and Fujita (1977, 1978) applied dimensional analysis and found the formative condition

$$(h/d) (B/d)^{2/3} < 0.15 \text{ for } 1 < U^*/U_{c*} < 12 \quad (2.2)$$

Where d is representative grain size. Colombini et al (1986) proposed a typical neutral curve for alternate-bar formation which is shown in Figure 2-6. Here, β is the width ratio of the channel and β_c is its 'critical' value below which bars would not form and λ is the bar length.

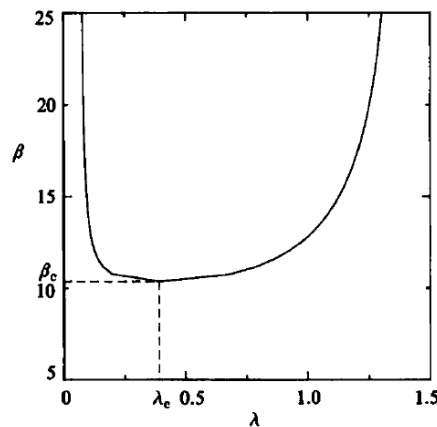


Figure 2-6: A typical neutral curve for alternate-bar formation (reproduced from Colombini et al., 1986)

To specify the bar dimension different semi-empirical formulae was developed by Ikeda (1984, 1990) and Yalin (1992). The bar height was expressed by

$$H_b/h_o = 9.34(B/d)^{-0.45} \exp [f(B/h_o)] \quad (2.3)$$

$$f(B/h_o) = 2.53 \operatorname{erf} \left[\frac{\{\log_{10} (B/h_o) - 1.22\}}{0.594} \right]$$

from Ikeda (1990) where H_b = bar height (m), h_o = flow depth for the uniform basic flow (m), d = sediment particle diameter (m)

Yalin (1992) proposed

$$H_b/h_o = 0.18(B/h_o)(B/d)^{-0.45} \quad (2.4)$$

To specify bar length, Ikeda (1990) proposed

$$\lambda/B = 5.3(B/h_o)(B/d)^{-0.45} \quad (2.5)$$

where λ = bar length (m)

The functional relationship between bar length and channel width derived by Yalin (1992)

$$\lambda/B=6 \quad (2.6)$$

2.6 Computational models of braided rivers

During the last few decades, the demand for reliable methods to analyze and predict braided river behavior has grown considerably. Small-scale laboratory braided river models and computational models play a key role in the research of braided river dynamics as they offer the possibility to generate and observe the evolution of a braided river model in great detail over a sufficiently long time period for known initial and boundary conditions. These models thus reveal various aspects of braided rivers that cannot easily be assessed in natural braided rivers, such as the constant interaction between planform and topographic characteristics and their collective response to variations in hydraulic and geometric conditions. As a consequence, an increased awareness that braided river dynamics which cannot be described by the development of the channel structure independently has emerged (Ashmore, 2000; Murray and Paola, 1997; Furbish, 2003).

However, progress in developing physical and computational models as a base to study the dynamic behaviour of braided rivers, as well as the coupled behaviour between flow and topographic characteristics, also raises the demand for appropriate model evaluation tools that capture these multiple aspects of braided river morpho-dynamics. Present quantitative methods for model evaluation concentrate mainly on static flow or planform properties, but the evaluation of topography and dynamics is, at present, primarily restricted to qualitative assessment (Sapozhnikov et al., 1998; Murray and Paola, 1997, 1998; Paola, 2000; Thomas and Nicholas, 2002; Jagers, 2003). Essentially the problem is to find quantitative criteria that characterize braided rivers and allow modellers to assess the extent to which model output reproduces the morphology, dynamics and response to external forcing, of 'real' braiding.

Nicholas et al. (2013) attempted the numerical simulation of bar and island morphodynamics in a branching mega rivers. Their study can be considered as a first attempt to assess physics-based morphodynamic modeling of large rivers over centennial time scales is feasible or not, and whether it can contribute to understanding of bar and island morphodynamics. They use 2D HSTAR model to simulate the river. They concluded that the model results were sensitive to the parameterization of the processes and to the representation

of bed roughness. Moreover, considerable uncertainty surrounds several modeling parameterizations and the associated benefits of accounting for the effects on flow and sediment transport of spatial and temporal variations in alluvial bed forms. Development and evaluation of more robust parameterizations requires the collection of high-resolution process data sets and critically, DEMs of river bathymetry collected over a range of time scales (from days to decades). Such data are required to resolve the interactions between process-form feedbacks operating at bed form, bar, and whole river scales.

Schuurman et al. (2013) tried to determine the capability of a widely used physics-based model to produce key characteristics of braided sand-bed rivers such as bar and channel dimensions, braiding intensity and shape of bars, and the channel network. They used Delft 3D software to simulate the river and concluded that the morphological model results are very sensitive to the constitutive relation for bed slope effects and also to the type and parameter values of the constitutive relations for flow resistance and sediment transport. Regardless of the sensitivity, the model reproduced important characteristics of braided rivers like the quasi-regular pattern of low-amplitude bars showed a wavelength that is in good agreement with predictions by linear stability theories. Furthermore, the model was able to produce the characteristic morphology of compound bars and channels showing a great variety of morphological features found in natural braided rivers, including bar-tail limbs, crossbar channels, and scour holes. Also, multiple mechanisms for bifurcation initiation, bifurcation closure, bar migration, and bar growth occurring in the model are comparable to observations in nature and flume experiments.

2.7 Other Earlier studies related to bar dynamics of the Jamuna River

A few studies, mainly in the 1990s, have been carried out on the physical processes on the bars of the Jamuna River. The purposes and methodologies for carrying out the studies are differed from each other. ISPAN (1995) studied the physical environment of the bars of the major rivers in Bangladesh including the Jamuna. The main purpose of the study was to build up information and knowledge on the physical processes using Remote Sensing and GIS technology for reducing the sufferings of the most vulnerable groups of people living in the fragile bars. Using the experience of ISPAN, EGIS (1997) attempted to assess bar topography using time-series satellite images. The purpose of the study was to generate bar topography for predicting the future development of the chars. Delft Hydraulics and DHI (1996a) carried

out a research on the formation processes of mid-channel bar (island char) in conjunction with the flow structure and bedforms of the Jamuna River.

ISPAN (1995) studied the morphological dynamics of the Jamuna River using historical maps and time-series satellite images. They related the dynamics of the river with the dynamics of the bars. They defined islands as vegetated islands. They have made an inventory of the bars in the major rivers of Bangladesh and classified the bars as island chars and attached chars. ISPAN (1995) were used satellite images to assess the ages of bars that existed in the early 1990s, along with the persistence of islands and incidences of bars. According to them the average age of 38% of the bars, observed in 1992 dry season satellite image, were within three years and they found that only 14% of the bars were older than 20 years. EGIS (1997), Hasan et al. (1999) and Sarker et al. (2003) updated the analysis of ISPAN (1995) works. Both of them attempted to relate the dynamics of the bars with the lives and livelihoods of the islands dwellers. They extended the analyses of bar ages and persistence for the bars appearing on satellite images of 2000. They found that the ages of more than 56% of the bar areas were within three years and only 6% of char areas above 19 years. They further found that 34% of the bars persisted for 3 to 6 years, which was the highest among other groups of years.

EGIS (1997) found that the average relative elevation of chars increased up to the age of 7 and later reached almost a steady state with a certain range of uncertainty. Uncertainty of relative elevation is very high at the initial stage of bar development. Delft Hydraulics and DHI (1996a) in collaboration with the University of Leeds, UK studied the evolution of mid-channel in the Jamuna River. Their research was mainly concentrated to the evolution of a mid-channel bar in the left anabranch of the Jamuna River upstream of Bahadurabad.

Chapter 3

Study Area

3.1 Introduction

The river reach of the Brahmaputra River flowing from the international border between Bangladesh and India to the confluence with the Ganges at Aricha is referred as the Jamuna in Bangladesh. Being originated from Chemayungdung glacier near the mount Kailas of the Himalayas; the Brahmaputra drains almost 3000 km of China, India and Bangladesh. The river starts its journey at an altitude of 5100 m from the Chemayungdung glacier of the Himalayas (Figure 3-1 and 3-2). Then it flows for about 1400 km in an easterly direction across the Tibetan plateau, which is bordered by the Himalayas in the south and the Gandis Mountains in the north, while it descends to 3000 m. In this reach the river is known as the Tsangpo or Yarlung Zangbo (Jiang) River. At an altitude of 200 m above sea level it leaves the Himalayan range as the Dihang River (Jagers, 2003). At Assam province in India, the river meets the Lohit and Dibang River and takes its name as the Brahmaputra. Then the river flows to the west and near the international border between India and Bangladesh at the ninety degrees east meridian, it makes a sharp left turn, goes south and enters Bangladesh from where the river is known as the Jamuna.

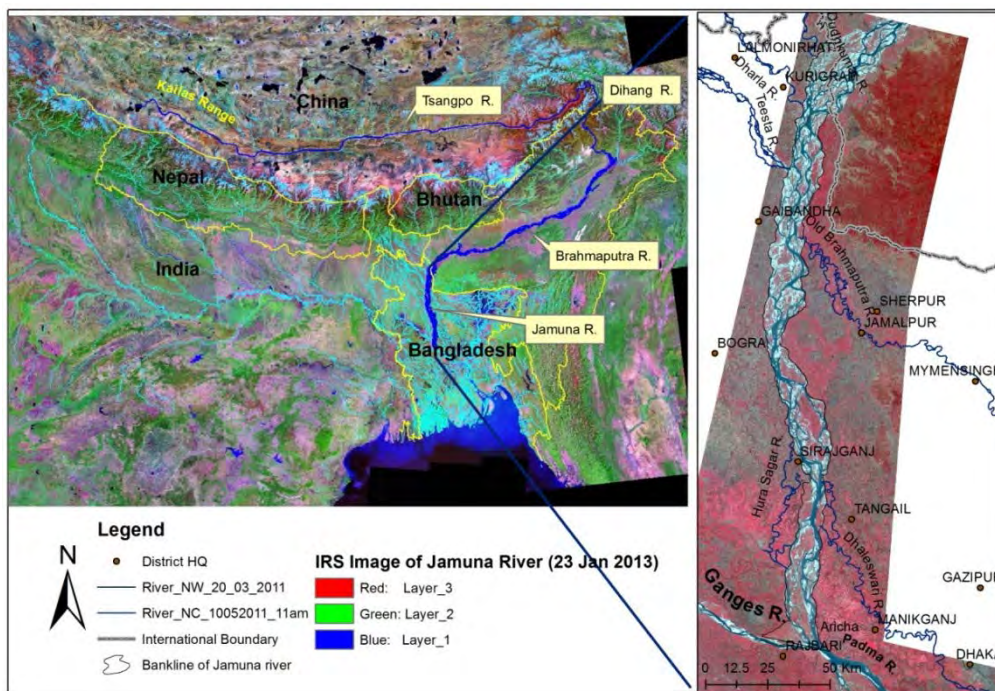


Figure 3-1: Map showing the study area

After a while (near the left bank of the river at Gaibandha district), the river splits into the Old Brahmaputra River and the Jamuna River, the latter currently being the main branch. The Jamuna River meets with the Ganges River near Aricha and the combined flow is known as the Padma River. After flowing 100 km, the Padma merges with the Upper Meghna River and together taking the name as Lower Meghna River, discharges into the Bay of Bengal.

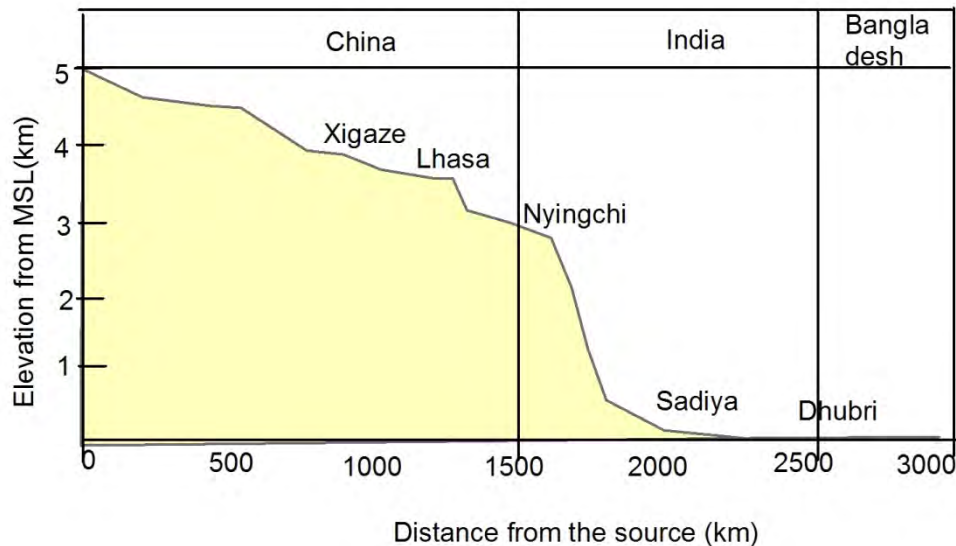


Figure 3-2: Longitudinal profile of Brahmaputra River (reproduced from Jagers, 2003)

On the right bank it meets four tributaries inside Bangladesh- the Dudhkumar, the Dharla, the Teesta and the Hurasagar (Figure 3-1). It has only one distributary on the left bank- the Dhaleswari. The aerial distances from the international border with India to the confluence along the right and left banks are 240 and 220 km respectively (Jagres, 2003). The average width of the river within Bangladesh is 12 km (Jagres, 2003). The river is braided in planform.

3.2 Geophysical setting

The geology of the basin of the Brahmaputra River is predominant by the Tectonic activities (Gupta, 2008). The Indo-Australian Plate was separated from the Euro-Asian Plate by the Tethys Sea prior to the Palaeocene (65 million years before present). Figure 3-3 shows the position of the Indo-Australian and Euro-Asian Plates. During the Eocene (54 to 38 million years BP) the Indo-Australian Plate collided with the southern edge of the Euro-Asian Plate (Rashid, 1991). Since then, the Indo-Australian Plate has advanced northwards about 2000 km, passing beneath the Euro-Asian Plate, uplifting it and crumpling its southern edge to

form the Tibetan Plateau and the Himalayas respectively (Rashid, 1991). Every year India migrates to the north into Asia by approximately 5 cm. A part of this convergence is taken up in the Himalayas (1 cm/year raise); the remainder is expected to be absorbed in the Altun Tagh Mountains (West China), the Tien Shan Mountains (Northwest China), and the eastward motion of China and Mongolia (Molnar, 1977; Pendick, 1996). This tectonic motion has been and will be an important factor in the evolution of the Jamuna River by influencing its sediment load, planform and course.

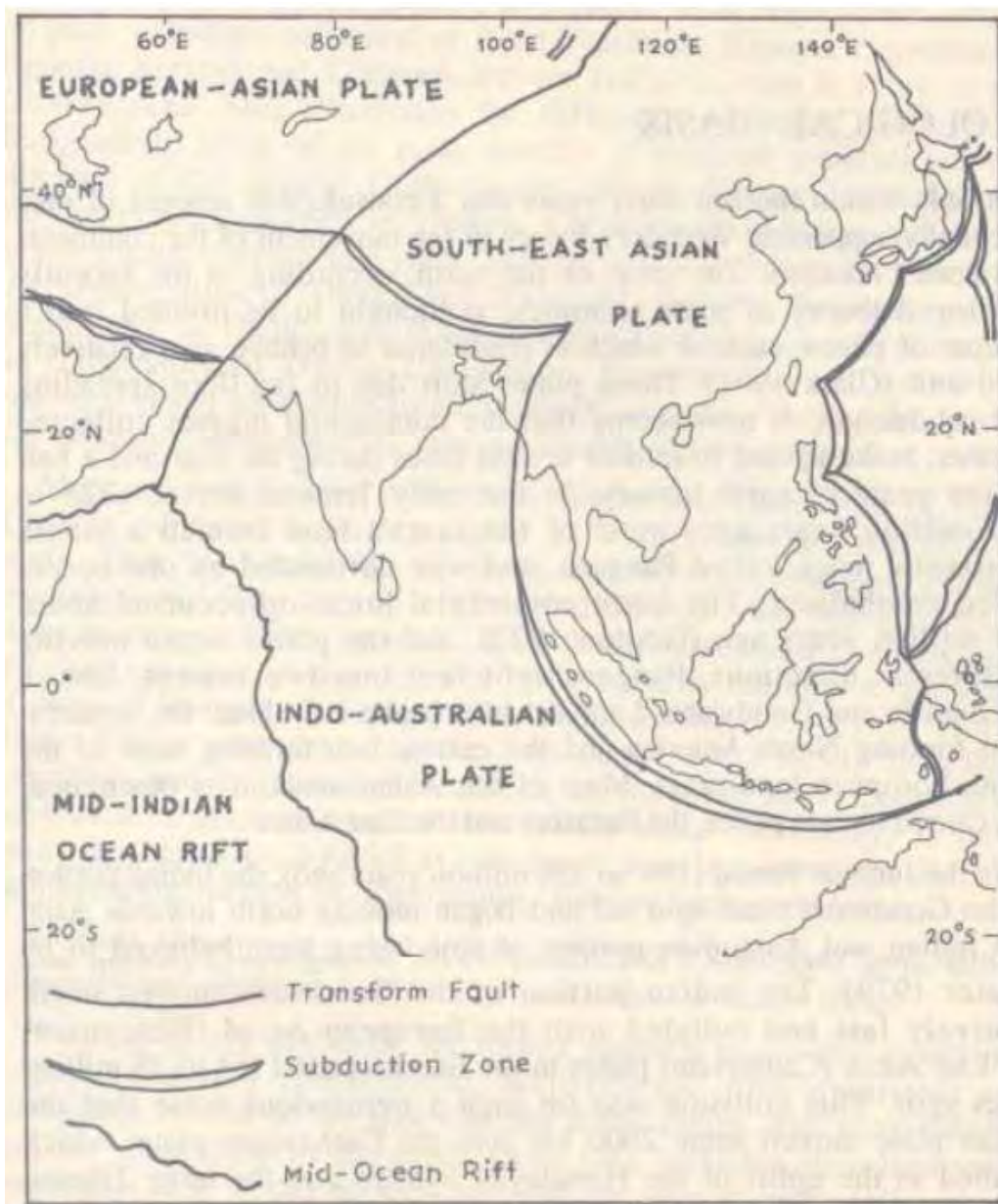


Figure 3-3: Tectonic map of the Indo-Australian and Euro-Asian Plates (reproduced from Rashid, 1991)

However, the Jamuna River is flowing in a region of significant tectonic activity which is continuously occurring like Himalayan uplift and development of the Bengal basin (Alam, M.K. and Hossain, M.M., 1988; Barua, 1994; Goodbred et al., 2003). The underlying structure of Bengal basin controls the location of the major river systems of Bangladesh has been hypothesized by several researchers (Morgan and McIntire, 1959; Umitsu, 1993; Barua, 1994). Morgan and McIntire (1959) suggested there is a 'zone of weakness' along the present course of the Ganga–Jamuna–Padma Rivers due to either a subsiding trough or a fault at depth. However, the evidence on which this suggestion was based was indirect and the seismic investigation is also low to ascertain the exact subsurface controls on river channel migration and long-term evolution. But FAP24 (1996b) indicated that the region is now suffering the major seismic activity since the past 100 years, as an evidence they showed that last 20 earthquakes were below the magnitude of 7 in Richter scale only one exception of the great 1950 Assam earthquake measuring Richter magnitude 8.6 and affecting up to 52 000 km² of territory in Assam (Sarker and Thorne, 2006). Seijmonsbergen (1999) showed that many structural lineaments, running broadly NW–SE and SW–NE, which can be recognized from physical features on the floodplain, and concludes these are small faults that can influence local migration of the channels.

Ongoing subsidence in the Bengal Basin, combined with high rates of Himalayan uplift set the tectonic and climatic context for the large water and sediment discharges in the rivers of Bangladesh (Goodbred and Kuehl, 2000 a, b). Allison (1998), in a review of the geologic and environmental framework of the Ganga-Brahmaputra Delta, highlighted that the uplifted Pleistocene terraces of the Barind and Madhupur tracts act as the first-order controls on the courses of the Jamuna. Barua (1994) also presented a synthesis of the major environmental controls on Bangladesh's river systems and, together with the major controlling factors of regional tectonics; climate, sea-level rise and vegetation were also highlighted as the controls by the 'fluvial loading'. The nature of sea-level rise, together with other anthropogenic effects on the river such as flood control and water usage, is clearly affecting the river in the twenty-first century (Begum and Fleming, 1997; Choudhury et al., 1997; Mirza et al., 2001; Mirza, 2002).

3.3 Hydro-morphological status

3.3.1 Flow Regime

The catchment area of the Jamuna River is almost 560 000 km² with approximately 8.1 % of the drainage basin area being within Bangladesh and it receives an average of 1900 mm rainfall year⁻¹ (Gupta, 2007). The rise in the hydrograph of the Jamuna begins due to Himalayan snowmelt in May, but the hydrograph is dominated by monsoon rainfall which is concentrated during the period of June to October. During the rest of the year the flow is generated from the base flow and snow melt in the Himalayas (CEGIS, 2010). Figure 3-4 shows the mean annual hydrograph of the river at Bahadurabad which is prepared from the daily discharge data from 1956 to 2006. It indicates that in dry period the average flow is about 5000 m³/s and flood season it goes up to 50000 m³/s. Such a big variation of the discharge may be one of the causes of heavy dynamicity of the river.

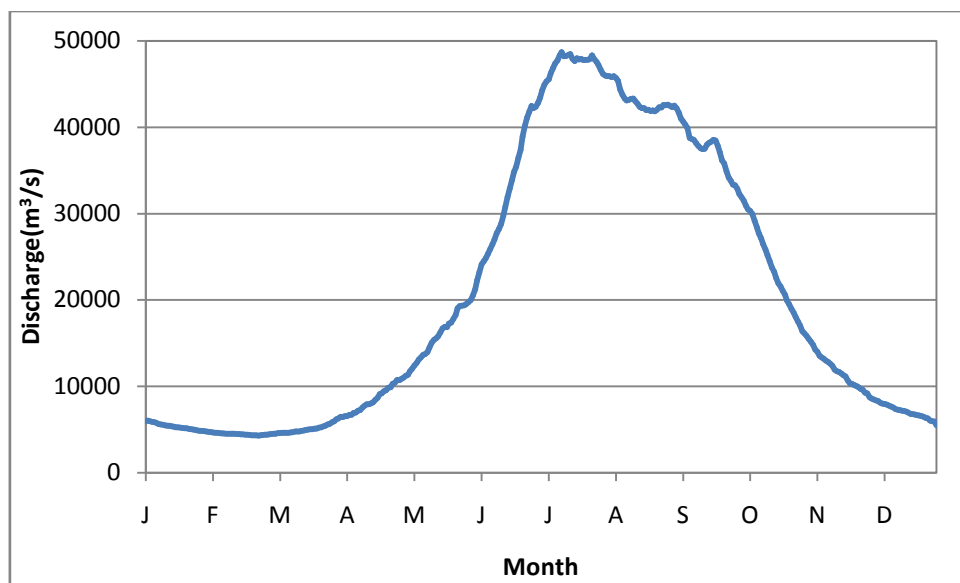


Figure 3-4: Mean daily discharge hydrograph of the river at Bahadurabad (from 1956 to 2006)

Like the flow hydrograph the mean annual water level hydrograph of the river also shows the peaks in July- August and the maximum value goes up to about 18.5 m PWD at Bahadurabad (Figure 3-5). The analysis of daily water level data from 1956 to 2006 also shows that the mean minimum annual water level at Bahadurabad is found 12.5 m PWD during February-March (Figure 3-5).

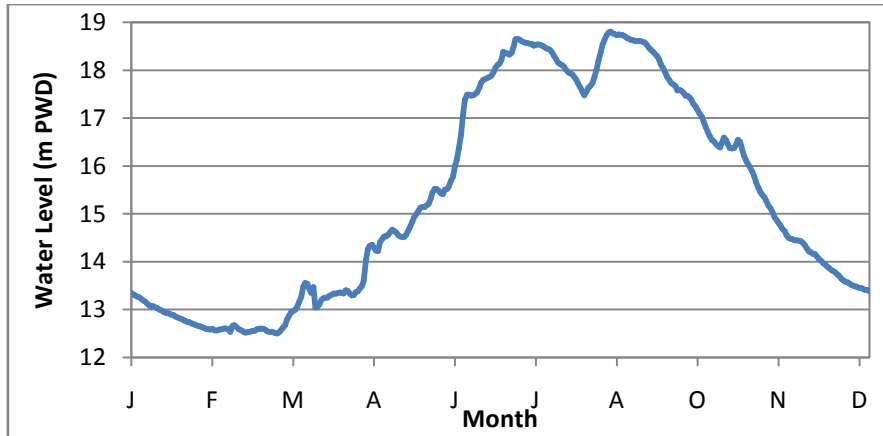


Figure 3-5 : Mean daily water level hydrograph at Bahadurabad (from 1956 to 2006)

The average bed slope of this river is 7.5 cm/km (CEGIS, 2010). In fact, bed slope varies from the upstream to the downstream reach. The upper section has an 8.5 cm/km slope while at the downstream section the slope is 6.0 cm/km (CEGIS, 2010). The average water surface slope is 8 cm/km. Figure 3-6 shows the mean annual minimum water level at different stations and the corresponding slope for the period 1956 to 2006. Though the river exhibits comparatively high slope in the u/s direction, the slope reduces near the confluences of Ganges at Aricha where the water surface slope is 5.9 cm/km.

Delft Hydraulics and DHI (1996) estimated the bankfull discharge of the Jamuna River and found that it is between the range 45,000 to 50,000 m³/s. According to the regime relations derived by FAP 24, the regime width of this river (if a channel carries 100% of discharge) at bankfull stage is 4 km and the average depth is 7.1 m if bankfull discharge is considered to be 50,000 m³/s.

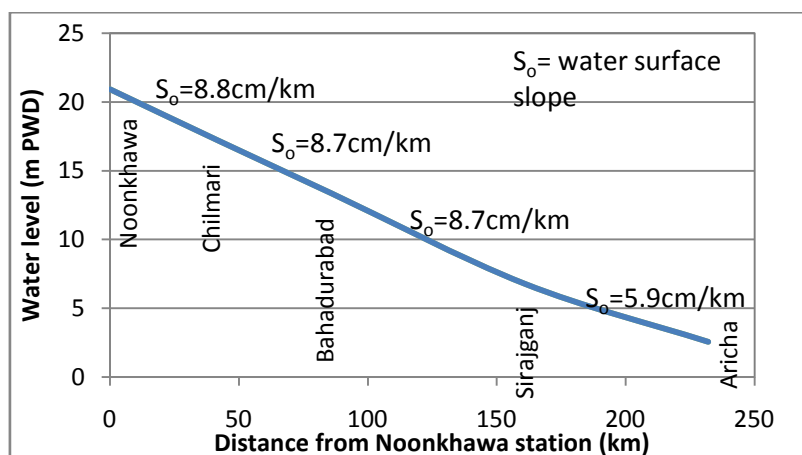


Figure 3-6: Average water surface slope at the date of annual minimum water level (from 1956 to 2006)

3.3.2 Sediment Regime

In Jamuna, the majority of the bed materials consist of fine sand and bed material is transported in suspension mode. The suspended load that derives from the catchments of the river consists of silt and clay (FAP 6). Sarker (2009) analyzed the size of bed material (D_{50}) at Bahadurabad and found the value in an average of 0.20 mm.

Holeman (1968) estimated the sediment load in the Brahmaputra which was 1.6 billion tons/year. But he did not mention the time period of measurement. Holeman's article also did not mention the locations of sediment gauging station. Colman (1969) stated that the total suspended load was 610 billion tons/year. However, BWDB measurements in the late 1960s showed that the suspended sediment load in both the Jamuna and the Ganges were 1047 million ton/y. Table 3-1 shows the annual average sediment load as measured during 1966-1969 by the BWDB. But the analysis of bed material load measured by the BWDB showed that the sediment load in the Jamuna River had reduced more substantially during the 1980s than in the late 1960s (Delft Hydraulic and DHI, 1996a). Sarker and Thorne (2006) related the reduction in bed material load in the Jamuna and Padma rivers to the propagation of sediment wave through the Brahmaputra-Jamuna-Padma-Lower Meghna River system due to huge landslides in the Himalayas caused by the 1950 Assam earthquake.

Table 3-1: The annual average sediment load as measured during 1966-1969 by the BWDB (source Delft Hydraulics and DHI, 1996a)

Period	Type of sediment	Sediment load in Jamuna (m ton/yr)
1966-1969	$S_{\text{wash load}}$	335
	$S_{\text{susp. bed}}$	220
	Total S_s	555

The measurements of FAP 24 in the early 1990s shows that suspended bed material load in this river were much less than in the 1960s as measured by BWDB. The slight decrease in wash load in the Jamuna might be due to the continuation of the reduction in wash load since the

1950 earthquake, which overrules the assumption of increased sediment due to intensive agricultural practices in the Assam valley (CEGIS, 2010).

Table 3-2 shows the sediment load estimated by different authors/studies based on the sediment gauging of different agencies at different periods. The amount of sediment in the Jamuna has been changing over time. Except the sediment load mentioned by Holeman (1968), all other studies provided estimates of annual average sediment load in the Jamuna and Ganges rivers that varied between 1 to 1.1 billion tons/y.

Table 3-2: Total suspended sediment load in the Jamuna River

Source	Period of Sediment Record	Suspended Sediment (m ton/yr)
Holeman (1968)	-	800
Coleman (1969)	1958-1962	610
BWDB (1972)	1966-1969	553
Delft Hydraulics/DHI (1996c)	1993-1996	402

3.4 Morpho-dynamics of the River

Jamuna is a wide braided river; maintaining a almost a fixed and wide corridor which is generally aligned in north-south direction. The average width of the river was 8 km during early 1970s, which is now more than 12 km. The river shows a tendency of shifting towards the west during the whole of the eighties and much of the nineties. The bank materials mainly consist of non-cohesive sediments and have almost similar characteristics in terms of erodibility (Thorne et al., 1993). Since the river is the most dynamic river in Bangladesh, it causes huge erosion every year. Here the evolution of the river is described into two phases – Long-term and short term.

3.4.1 Long-term development

Several studies (Umitsu, 1993; Khan and Kudrass, 1999; Khan and Islam, 2008; Goodbred and Kuehl, 2000a and Goodbred and Kuehl, 2000b) revealed the long term development of

the river. Goodbred and Kuehl (2000a & b) studied the development of the Ganges-Brahmaputra delta during the Holocene using borehole and carbon dates from borehole and vibracores; and using these sources they demonstrated the development of the Jamuna River. The early development of the river were closely related to that time Sea Level Rise and tectonic activity of the of Bengal basin. They have prepared a Paleo-geographic map of the Ganges-Brahmaputra delta which indicates the repeated switching of the river course between the present “Old Brahmaputra” and “Jamuna” (Figure 3-7).

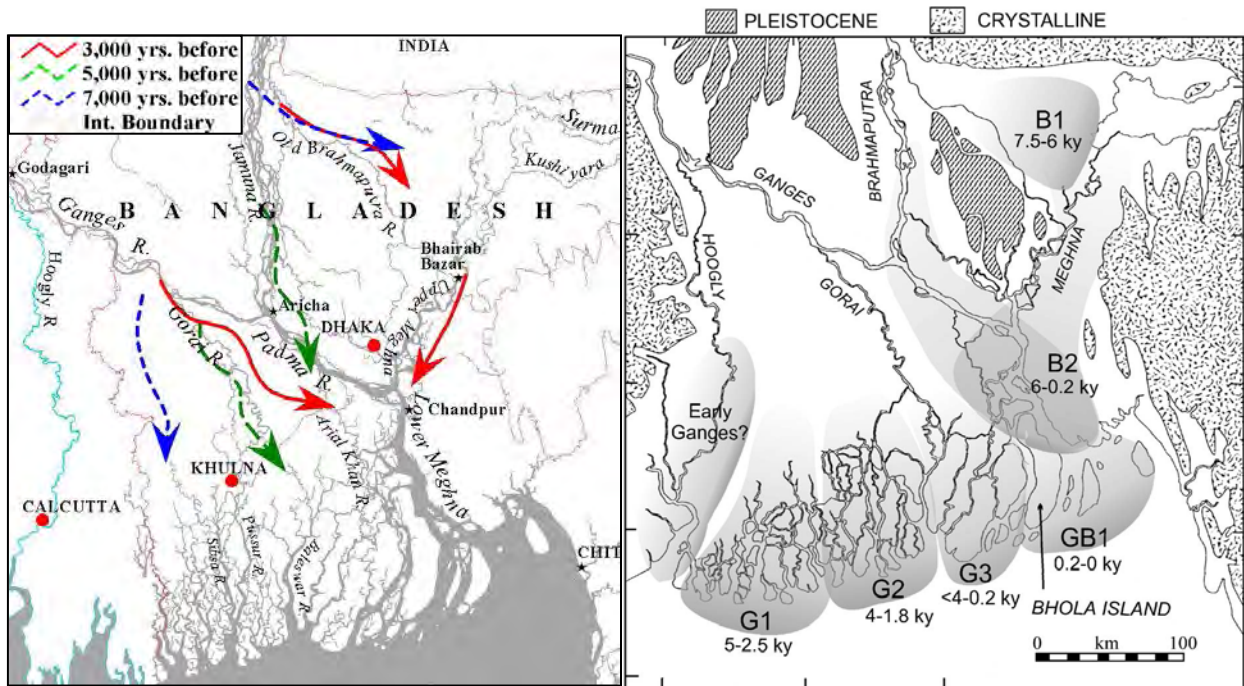


Figure 3-7: Shifting of the rivers of Bengal basin (based on Paleo-geographic map of the Ganges-Brahmaputra delta (reproduced from Sarker et al., 2013 after Goodbred and Kuehl, 2000a)

If it is focused only to the century scale development of the river, it also showed very dynamic characteristics. The course of the Jamuna River shows large scale changes over the past 250 years, with an evidence of both a vulsion in the period 1776–1850 and a westward migration of the Jamuna channel belt since this date. The avulsion of the Jamuna has been described by several authors, with Bristow (1999) presenting the most recent summary of theories for the trigger of the change in channel belt location.

Prior to 1843, the Jamuna flowed within the river which is now termed the ‘ Old Brahmaputra’ (Figure 3-8), east of the Madhupur Tract, and joined with the Upper Meghna River. Sometime between 1830 and 1860 avulsion of the river course occurred and caused a maximum of ~80 km of lateral shifting of the river course from the east to the west of the

Madhupur Tract (Figure 3-8) (Best et al., 2007). Several studies have discussed about this avulsion and suggested a number of reasons including tectonic activity (Winkley et al., 1994), switches in the upstream course of the Teesta River (Morgan and McIntire, 1959), the influence of increased discharge (Coleman, 1969), catastrophic floods (La Touche, 1910) and capturing the old course (Bristow, 1999). Analyzing the map between 1776 and 1843, Bristow (1999) concluded that the river avulsion was more likely to be gradual than catastrophic. As the reason he indicated that bank erosion; he pointed out a large mid-channel bar, causing diversion of the channel into an existing floodplain channel. The map of Rennell (1776) clearly shows a sequence of large bars near the offtake of the present Jamuna (Figure 3-9) suggesting local sediment overload and diversion of flow against the banks. Best et al. (2007) concluded that significant flow may have previously been diverted down the Jamuna offtake, since the right bank at this point showed two large embayments that would divert water to the offtake (Figure 3-9, label x).

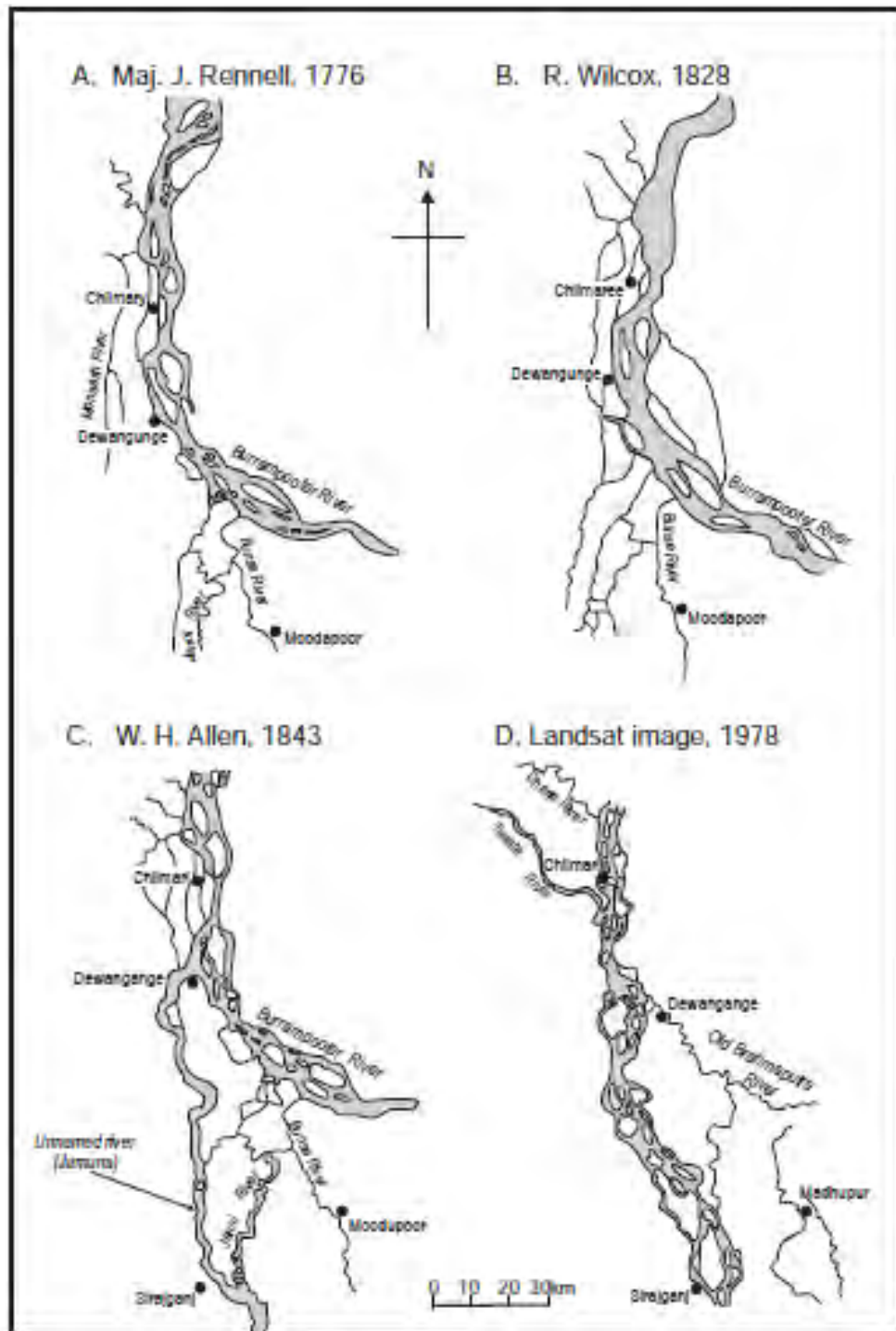


Figure 3-8: (a) Maps illustrating the position of the Jamuna River from 1776 to 1978: (A) 1776; (B) 1828; (C) 1843; (D) 1978. (Reproduced from Gupta et al., 2007)

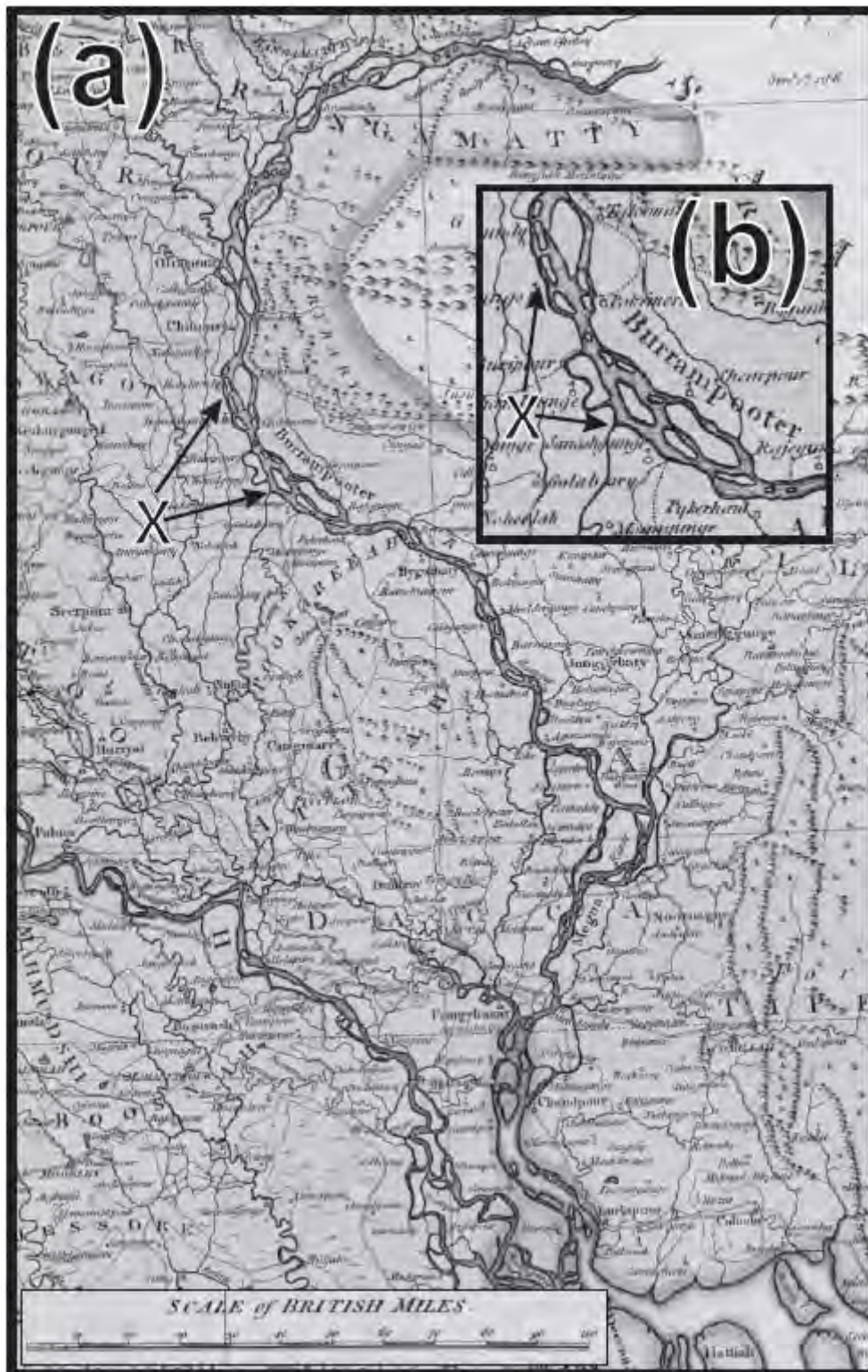


Figure 3-9: Reproduction of Rennel's Map of 1776 (redrawn from Gupta et al., 2007)

Another significant century scale change of the river is the gradual westward migration of the braided belt of the river (Coleman, 1969; Sarker, 1996; Khan and Islam, 2003). The braided belt has widened since the early twentieth century (FAP24, 1996c; Sarker, 1996; EGIS, 1997,

Figure 3-10). Movement of the banklines of the Jamuna River during the last 200 years was comprehensively studied by FAP 19 (Flood Action Plan, project 19) and the results were published in ISPAN (1993). It indicated that in 1830 the Jamuna River had a meandering planform and followed a course that was for most likely to the present east (left) bank. In 1914 the planform remained meandering, but the river had shifted noticeably westward and the average width of the channel (5.55 km) was somewhat narrower than displayed in 1830 (6.24 km) (as shown in Table 3-3). Between 1914 and 1953 the river continued its westward migration while widening significantly and its planform turned to braiding from meandering. By 1973, the average width of the river had reduced slightly, but rapid westward migration had continued. Between 1973 and 1992 the rate of increase of the average width accelerated to a very high level (Figure 3 -11), although the rate of westward migration slowed right down. The average westward migration rate of the centerline of the Jamuna River between 1830 and 1992 was 28 my⁻¹, while the rate of migration of the west bank was about 50 my⁻¹ (ISPAN, 1993). The difference in the two rates reflects the impacts of the processes of westward migration and channel widening, which operated simultaneously during much of this period.

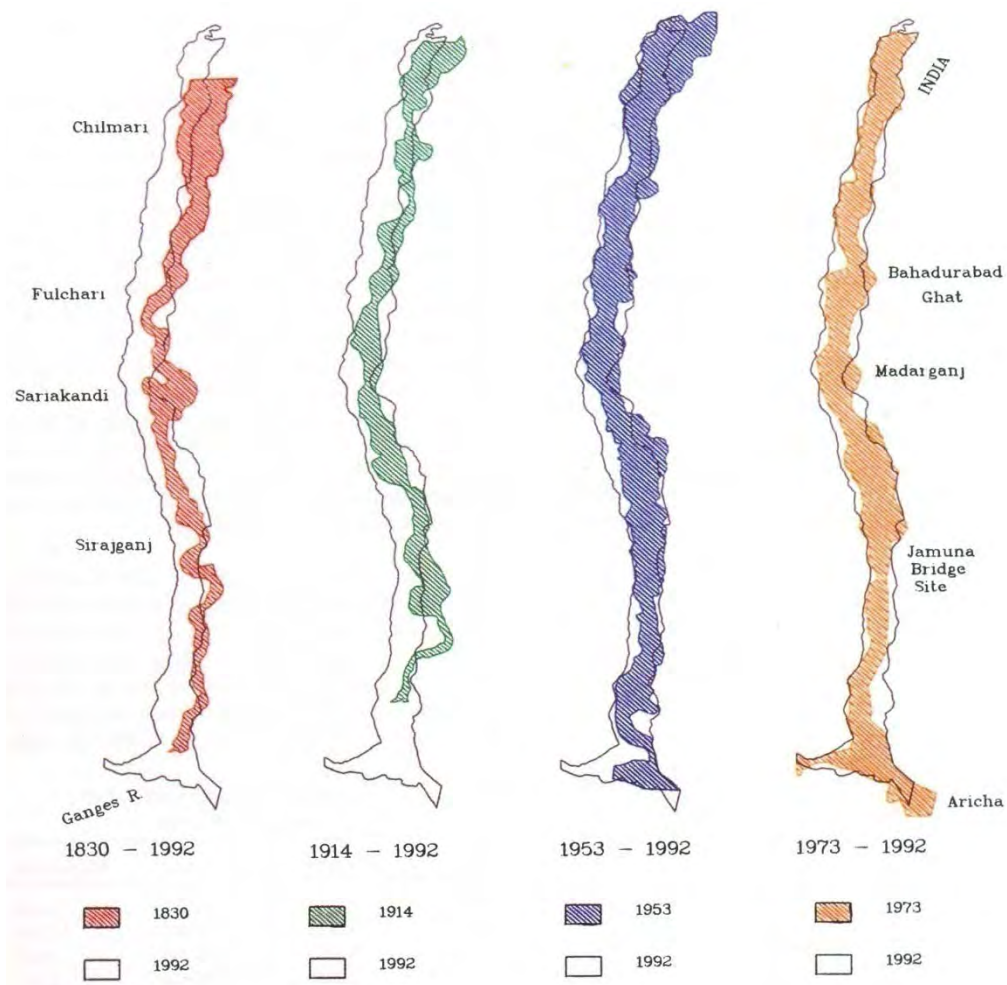


Figure 3-10: Westward migration of Jamuna (reproduced from CEGIS, 2007)

Table 3-3: Average Width and Position of the Jamuna River (ISPAN, 1993)

Year	Average width (km)	Westward mig ration of average eas ting o ft he centerline, co mpare t o i ts position in 1830 (km)
1830	6.24	--
1914	5.55	1.9
1953	9.05	3.6
1973	8.08	4.5
1992	10.61	4.6

3.4.2 Recent development

Being one of the largest braided rivers, ranking fifth considering discharge (Thorne et al., 1993); the river shows significant morphological changes in decadal scale too. As mentioned before, the total width of the river has been changing over time which has been hoped to be continued in recent time as well. But CEGIS (2010) indicated that since the 1990s the rate of widening has been reduced substantially. During the process of widening, both banks have been migrating outwards (Figure 3-11). Migration of the left bank ceased from the early 1990s while the westward migration of the right bank has continued. Due to the construction of several bank protection works in the recent past, the rate of westward migration has also been retarded. The probable reasons for such widening have been indicated by CEGIS (2007) and Sarker and Thorne (2006). To some extent, the construction of different types of bank protection structures along both banks has also contributed to reducing the rate of widening.

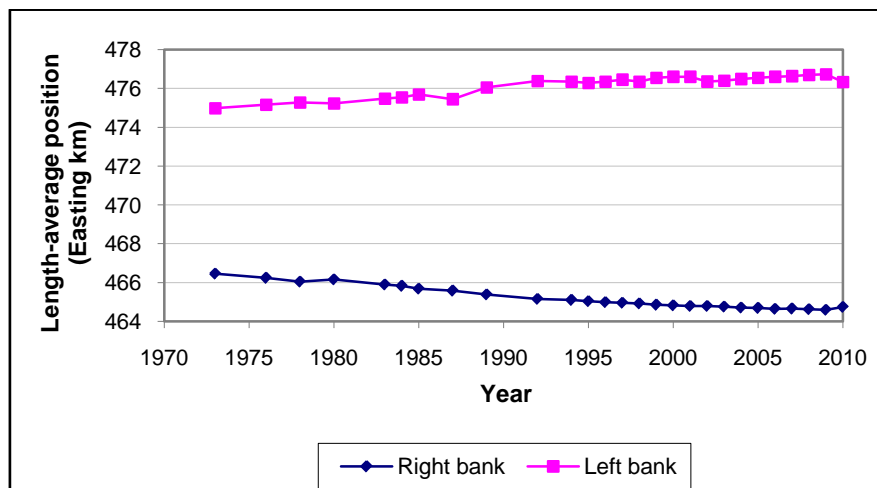


Figure 3-11: Length-averaged bankline migration of the Jamuna River (reproduced from Sarker, 2009)

Erosion has been the dominating process in this river during the last few decades (Figure 3-12 and Figure 3-13). Since 1973, a large amount of floodplain (90,830 ha) has been engulfed by the river, with only a small amount of land (10,140 ha) gained during this period. In the 1970s the rate of erosion was less than 4,000 ha/y, which increased to 4,900 ha/y in the 1980s. Later, in one and a half decade the rate of erosion decreased significantly. In the 2000s the annual average rate of erosion was found to be less than 2,000 ha/y (CEGIS, 2011). With the reduction in the widening rate, the annual rate of erosion also decreased in the current decade.

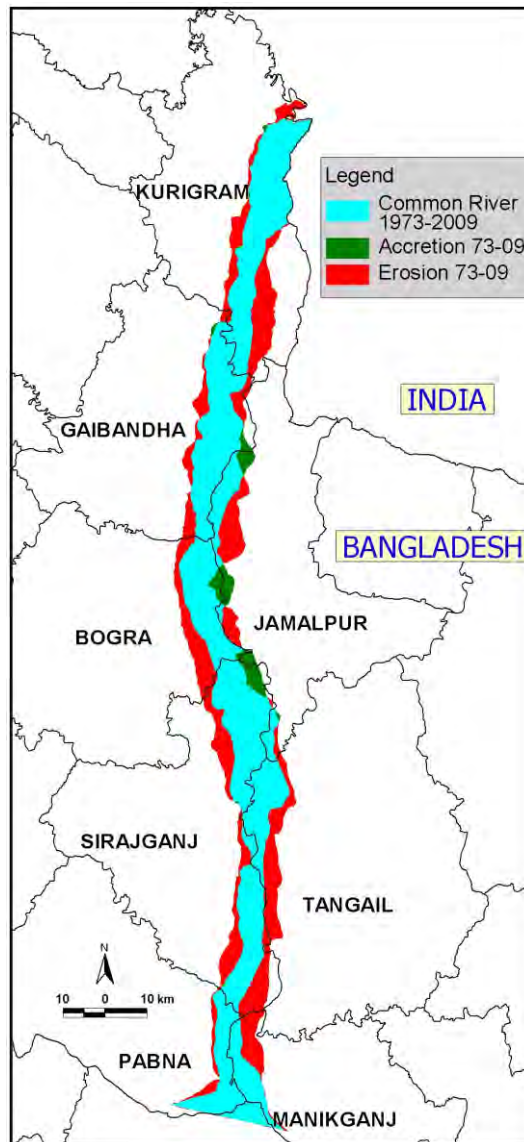


Figure 3-12: Riverbank erosion of Jamuna from 1973-09 (reproduced from CEGIS, 2010)

Several bank protection structures were constructed at the end of the last decade and early in the current decade such as the guide bunds of the Jamuna Bridge, hard points of Sirajganj, Sariakandi, Bhupur, Bahadurabad and several other structures, which have contribution in reducing the erosion rate and bankline migration. Compared to the length of the banklines of the Jamuna River, the influence area of the bank protection structures is not such that it could reduce the rate of erosion two fold or more (CEGIS, 2011). Hence it can be said that the large scale reduction in the annual rate of erosion is mainly related to the ongoing morphological processes. Since the widening rate reduced in the early 1990s and continued at a lower rate, bank erosion also reduced in the same period.

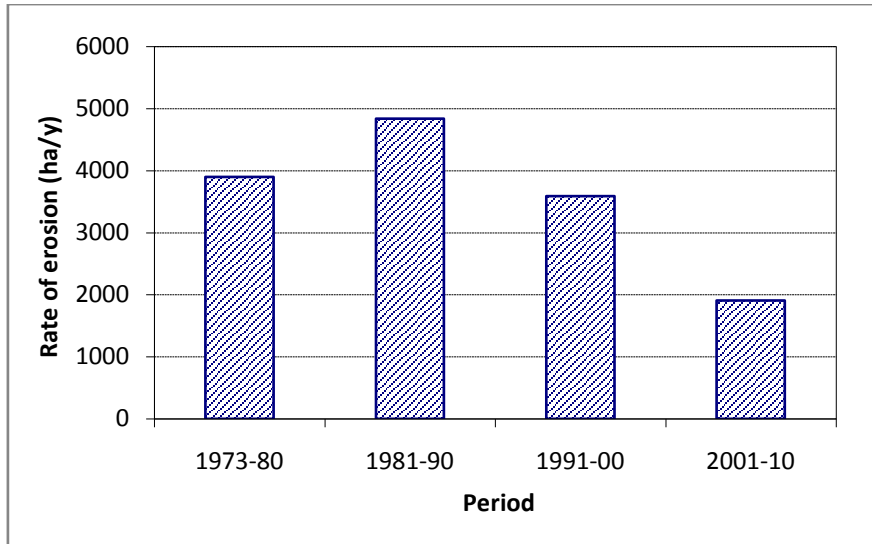


Figure 3-13: Rate of Erosion along the Jamuna River at different periods (reproduced from CEGIS, 2010)

CEGIS (2010) analyzed the braiding intensity of the river based on the method as suggested by Howard et al. (1970). The resultant data show that the braiding index of this river increased from the early 1980s to mid 1990s (Figure 3-14). During this period, the average braiding index of this river was 2.6. After this period it started to reduce. This may have happened due to the propagation of the sediment wave generated by huge landslides resulting from the 1950 Assam earthquake as suggested by Sarker and Thorne (2006).

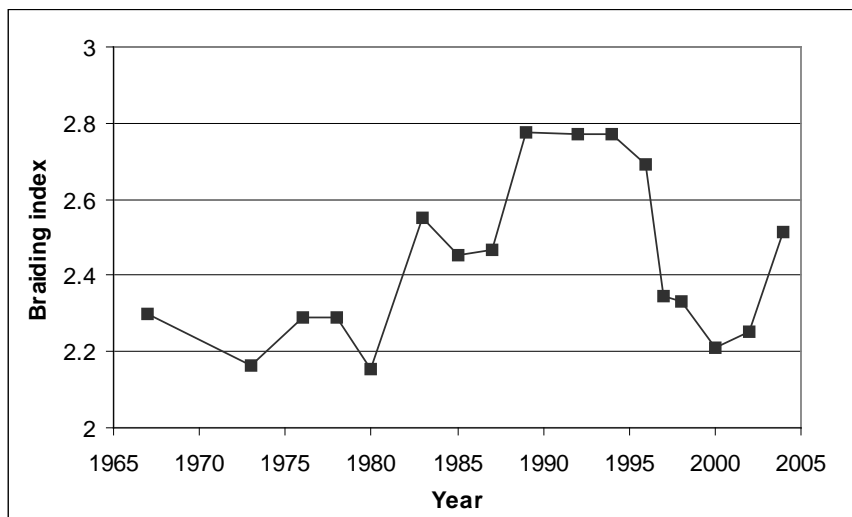


Figure 3-14: Change of braiding index of the Jamuna River over time (reproduced from CEGIS, 2010)

4.4.3 *Bedform types and dynamics*

Sediment is carried as bed, suspended and wash load by this river (Klaassen et al., 1988). However, the bed load, although this fraction is only 10 % of the total sediment load, is critical in generating a wide array of bedforms of different scale that drive channel change and migration. Bed material transport occurs at all flow stages in the Jamuna and the role of high-stage flood flow and subsequent reworking, or modification, of the high-stage deposits becomes significant on the falling limb of the flood hydrograph (Best et al., 2007).

Among the smaller-scale bedforms (ripples, dunes and megaripples), sand dunes are the predominant in the Jamuna at all flow stages and in all parts of the channel (FAP24, 1996c; Roden, 1998). They also act as the nucleus of many larger scale bars and are a key component of the sedimentary facies (Best et al., 2003). Best et al., 2007 indicated that at Bahadurabad and Sirajganj over 40 % of the bed is occupied by dunes at any flow stage, and this figure may rise to nearly 100 % (Roden, 1998). Ripples and smaller dunes are commonly superimposed on larger dunes, but upper-stage plane beds are rare and largely restricted to fast, shallow flows on bar-tops. Dune height and wavelength ranges from 0.10 to 6 m and 2 to 331 m respectively.

The Large-Scale Bedforms (bars and Islands) goes up to 15 km in length and with heights up to the adjacent floodplain level. The Jamuna contains all sizes of sand bars ranging from tens of metres to several kilometers in length. The most common bar types are the scroll (or point) bar and mid-channel (compound braid) bar (Bristow, 1987; Ashworth et al., 2000).

3.5 Human Interventions in Brahmaputra Basin

From the Holocene period, as a result of the transition from food appropriation to food production, the human interventions in river basin has increased and intensified (Ter-Stepanian, 1988). One of the major consequences of that was increased agriculture production, a large-scale conversion of forested areas to agriculture lands, leading to increased soil erosion. Rivers in Asia have been centers of ancient civilizations and it is likely that the human influence on soil erosion (Heun et al., 1997). In order to sustain the ever growing population and to meet water and energy requirements of the rapidly growing economies, most of the large rivers in Asian region have been regulated all along their courses, over the past few decades. Brahmaputra is not an exception of that. For example, on the upper reaches of Yarlung Tsangpo-Brahmaputra, China has completed 10 dams, 3 under

construction, 7 under a ctive consideration and 8 more proposed¹. Gupta (2012) shows that annual during this Holocene sediment flux reduces almost 60% in the GBM basin in which the effect of human intervention has a great contribution.

¹ <http://www.tibetanplateau.blogspot.com/2010/05/damming-tibets-yarlung-tsangpo.html>

Chapter 4

Data Used and Methodology

4.1 Data Used

Several types of data such as satellite images, cross-profile data, water level, discharge and river bathymetry data have been used for conducting the study. A list of the data is given in Table 4.1. A brief description of the used data is given in the following paragraphs.

Table 4-1: List of data used for the study

Data	Source	Period
Water level	NWRD	1940-2009
Discharge	NWRD	1940-2009
Sediment	NWRD	1968-2010 (Discrete type)
Cross-section	NWRD and BWDB	1958- 2011
Satellite Image	CEGIS archive	1973-2013
Bar Topography	CEGIS	March, 2013
Bathymetry	IWM	2011 and 2012

4.1.1 Water level

BWDB maintains water level gauging stations in the Jamuna River at nineteen locations (as shown in Figure 4-1). Time-series water level data of these gauging stations since the 1940s have been used in this study. The checking of data due to the gauge level datum shifting has been done in this study. If such an error has been noticed it was corrected by comparing with the previous time series data. Annual flood level and minimum water level have been analyzed from the time-series data. However, there were gaps in the time-series data. If such gaps were of several days (more than 5 successive days) during the monsoon (June to September) and dry season (January to March) the maximum and minimum water levels were not considered for that particular year.

4.1.2 Discharge

There is only one discharge gauging station of BWDB in the Jamuna which is located at Bahadurabad Transit. There were three other discharge gauging stations along the river, but measurements at these stations have only been performed for periods of 1 to 3 years. Hence, only long-term discharge data for the Jamuna River measured at Bahadurabad have been used in this research.

To determine the discharge, BWDB uses the velocity-area method. Ott current meters are used to measure the flow velocity at different verticals and at each vertical, the velocity is measured at 0.2 and 0.8 of the depth. However, like the water level data annual flood and minimum flow have been analyzed from the time-series data. As like as the water level, if there were gaps in the time-series data of several days (more than 5 successive days) during the monsoon (June to September) and dry season (January to March) the maximum and minimum water levels were not considered for that particular year.

4.1.3 Sediment

The BWDB measures the suspended sediment transport at Bahadurabad. Bed load is not measured by BWDB. In sampling suspended sediment transport, BWDB uses the Brinkley silt sampler. BWDB divides the suspended sediment samples into two fractions: the suspended bed material load or silt and clay fraction with particle diameter larger than 0.063 mm, and the wash load or silt and clay fraction, with particle

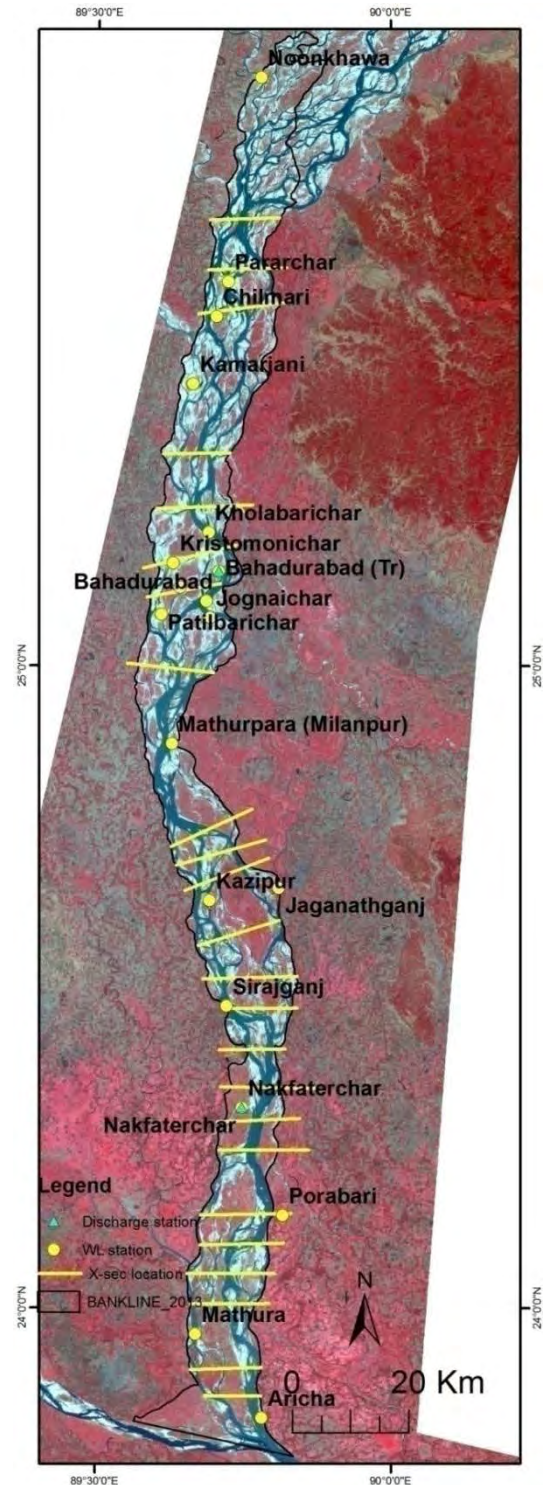


Figure 4-1: BWDB Discharge, Water level and X-sec location along Jamuna

diameter smaller than 0.063 mm. As wash load plays a minor role in channel adjustments compared to that played by the bed material load, only the suspended bed material fraction of the measured load has been considered in this study.

Sediment transport measurements are generally made in conjunction with discharge measurements, with point samples of suspended sediment being collected at each alternate vertical assigned for flow velocity measurements. The quality of measured sediment load data depends on the instrument used, the gauging procedure employed and natural variability at the gauging location.

4.1.4 Cross-section

The Bangladesh Water Development Board (BWDB) established a river survey network covering major and minor rivers for the whole country in the mid-1960s. The network comprises 667 monumented river cross-sections, and the interval of the cross-sections is 6,436 m (4 miles). Figure 4.1 shows the cross-section measuring location along the Jamuna.

4.1.5 Satellite images

From 1973-2013 total thirty satellite images with the spatial resolution of 30*30 m were used in this study. Among them, eight was derived from Landsat MSS, eight was from Landsat TM, three from Landsat ETM+ and other was derived from IRS LISS. These geo-referenced images were collected from CEGIS archive.

4.1.6 Topographic survey data

The topographic survey data of a bar near Chowhali thana was collected from CEGIS. The bar elevation data were gathered through spot leveling using Total Station. Public Works Department (PWD) data have been used as reference level. The elevation data were collected around 200m*200m interval. Bar elevation survey was done in the first week of March 2013. Isohyets surfaces were generated using ARC-GIS interface for further analysis.

4.2 Methodology

Three types of data have been analyzed in this study- time series hydraulic data, data derived dry season satellite imagery analysis and the results of the numerical modeling. Figure 4-2 shows the general methodology of the study. From the dry season satellite imagery, analysis was basically used to understand the bar development process at the same time the change of

bar characteristic with time were also assessed. Several hydraulic data such as water level, discharge, sediment river cross section were used to assess the time series change of the process. Numerical model was used to understand the detail of the bar development process.

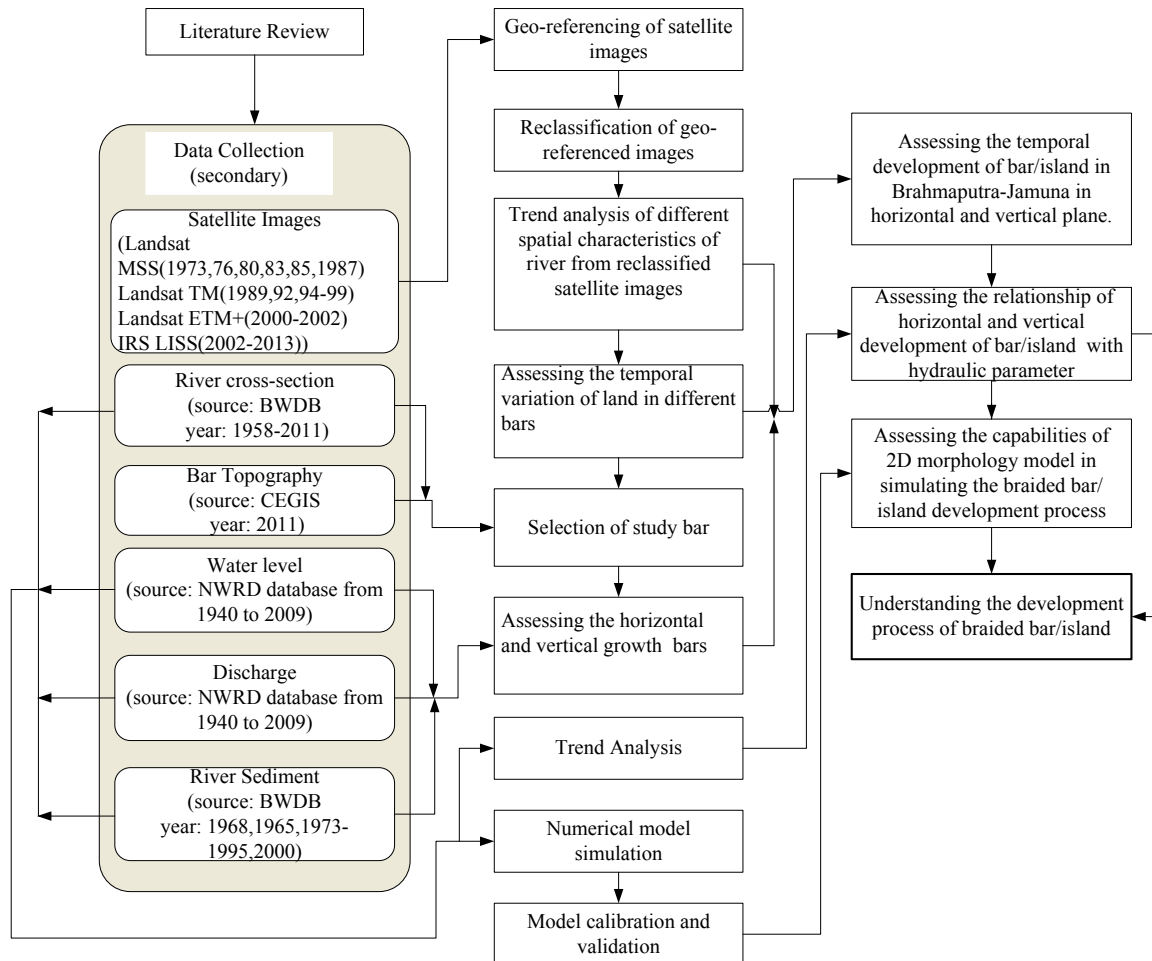


Figure 4-2: Methodology of the study

This study was performed focusing three specific objectives which have been discussed in Chapter one. However, all types of analysis were not performed for all types of bar. Table 4-2 shows the summary of the extent of the study and which type of analysis were used to understand the certain part of the bar growth process. However, the details of the methodology have been discussed in the following sections.

Table 4-2: Extent of study and main data source

Objectives	Extent of Study	Main Source of analysis
Temporal Development	All bars in the study area	Time Series hydraulic data and RS data
Vertical and Lateral Development	Selected bars	BWDB x-sec data, CEGIS topographic data and Numerical Modelling
Competency of a 2D morphology model in simulating bar/island	Selected bars	Numerical model and RS data

4.2.1 Satellite imagery processing and classification

Processing

Processing and analysis of the satellite images were performed using standard image processing software provided in ERDAS IMAGINE. ArcGIS software was used for vector analysis. Geo-referenced satellite images of the Jamuna River between 1973 and 2013 were acquired from CEGIS archives which already were geo-referenced using a set of reference points taken from 1:50,000 high-resolution color maps of SPOT satellite images acquired in 1989. Permanent features, such as road intersections, airport runways or large buildings were selected on the SPOT maps and used as reference points. The image type and acquisition dates and corresponding water level at Aricha are shown in Table 4-3.

Since there are a few such features within the river corridor, and this is especially true for reference points that can be identified on the lower resolution MSS images, other features such as ponds and uniquely shaped water bodies were used. Twenty-five or more GCPs were used in each pair of satellite images to geo-reference the river corridor area. For each reference point, the ground coordinates were obtained from the SPOT maps and entered into a data file together with the input coordinates of the same reference point identified in the digital satellite image. The coordinate pairs were used to compute a first order transformation matrix, which was applied to the entire digital satellite image to compute rectified coordinates for each image pixel. For each image transformation, a Root Mean Square (RMS) error was calculated: a measure of the accuracy of the geo-referencing procedure. The maximum RMS

error was 1.2 pixels for the MSS and 1.5 pixels for the TM images; this corresponds to a ground distance of 96 m and 45 m for the MSS and TM images, respectively. Each raw satellite image was resampled, using the nearest neighbor algorithm, and transformed into a file referenced to the Bangladesh Transverse Mercator (BTM) projection. The BTM projection, described by ISPAN (1992), has the following features:

Ellipsoid : Everest 1830

Projection : Transverse Mercator

Central meridian : 90 0E

False easting : 500,000 m

False northing : -2,000,000 m

Table 4-3: List of Satellite images with acquisition date

Image Type	Image acquisition dates	Water Level at Aricha (m PWD)
Landsat MSS	21/2/1973	3.16
Landsat MSS	10/01/1976	3.46
Landsat MSS	22/02/1978	3.02
Landsat MSS	21/02/1980	2.67
Landsat MSS	05/02/1983	2.44
Landsat MSS	25/02/1984	2.38
Landsat MSS	25/02/1985	2.42
Landsat MSS	07/02/1987	2.82
Landsat TM	28/02/1989	2.91
Landsat TM	08/03/1992	2.77

Image Type	Image acquisition dates	Water Level at Aricha (m PWD)
Landsat TM	25/01/1994	2.82
Landsat TM	28/01/1995	2.38
Landsat TM	31/01/1996	3.13
Landsat TM	18/02/1997	2.73
Landsat TM	05/02/1998	2.93
Landsat TM	23/01/1999	3.13
Landsat ETM+	19/02/2000	2.64
Landsat ETM+	28/01/2001	2.58
Landsat ETM+	24/02/2002	2.33
IRS LISS	08/03/2003	2.59
IRS LISS	16/02/2004	2.91
IRS LISS	17/01/2005	3.07
IRS LISS	-/-/2008	
IRS LISS	14/01/2007	2.92
IRS LISS	9/12/2007	4.22
IRS LISS	13/02/2009	2.69
IRS LISS	15/01/2010	
IRS LISS	03/12/2011	
IRS LISS	25/02/2012	

Image Type	Image acquisition dates	Water Level at Aricha (m PWD)
IRS LISS	23/01/2013	

Classification

The digital satellite images were classified using image processing techniques to enable the assignment of land cover classes to areas with similar spectral characteristics. For each of the Landsat MSS satellite image pairs, the procedure involved stretching and scaling the range of digital values by histogram matching to the 1976 image for Jamuna River. This modification of the data resulted in images with similar spectral characteristics which simplified classification and interpretation of the historic images. A series of tests was carried out using statistical clustering to derive a set of signatures that was used to classify the images. The tests were successful for seven of the eight MSS images of the Jamuna River, but the 1980 MSS image of the Jamuna River had to be classified using a slightly different signature.

Each Landsat TM, ETM+ and LISS III image of the Jamuna was classified independently using an iterative classification procedure. An unsupervised classification algorithm was used to derive signature statistics which were examined by an image processing analyst, modified as appropriate and used with a maximum likelihood classifier. Results were examined and acceptable classes were assigned to land cover categories. Image pixels corresponding to inadequate classes were digitally extracted, resubmitted to the unsupervised clustering routine and reclassified. Four broad land cover classes were assigned to each of the 20 image pairs acquired between 1973 and 2013 in the time-series of the Jamuna River: water, sand, cultivated land and vegetated land. From 1973 to 2013 thirty classified images were analyzed among which the images from 1978-2013 were newly classified. The rest of the images were taken from CEGIS

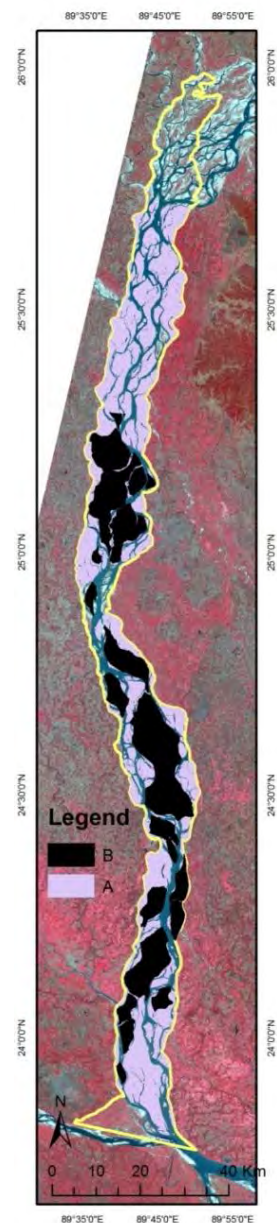


Figure 4-3: Selection of study bar

archives which were already classified for different previous studies. The images of 2000, 2001, 2002, 2006, 2007, 2008, 2010, 2011, 2012 and 2013 were previously classified as land and water but for this study they were classified as vegetated area, sand and water. The accuracy of the satellite image classification was considered although it was impossible to assess the historic images which date back to 1973. However, since the image processing techniques and land cover classes used were very similar to those developed in an earlier river morphology study, the extensive field assessment carried out in 1992 should be indicative of the accuracy expected under the present study. The 1992 field effort, as described by ISPAN (1995), involved several visits to the Jamuna River where fluvial processes, land cover, and agronomic practices were observed and documented. Two hundred and forty-five sites along the entire course of the river within Bangladesh were visited. An overall accuracy of 88% was found for three broad classes: water, sand and vegetated area.

4.2.2 Selection of study bar

In the study region where the BWDB cross-section data were available, the bars of that region were selected for assessing the Vertical and Lateral Development. In Figure 4-3 the both A and B marked bars were selected for assessing vertical and lateral development whether the B marked bars were used for numerical model results analysis.

4.2.3 Assessing the age of bars

The classified image of 2013 was set as base level for determining the age of vegetated area, sand and water. The successive images of previous years were superimposed to assess the changes in the bars (vegetated area+ sand) and water. Newly added bars were marked as one year old bars.

4.2.4 Assessing the relative bar height (H) with respect to low water level

Hasan et al. (1999) illustrated a methodology to determine the height of bar with respect to the low water level. In this study to assess the relative bar height the methodology used by Hasan et al. (1999) was followed. Elevations of the selected bars in respect of PWD data were obtained from BWDB survey data. Later elevations of the bars were expressed as relative height in respect of low water level. In the Jamuna River, an annual minimum water level generally exists from mid-February to mid-March every year. Lowest water level of that year was used as the reference level to assess the relative height of a particular location of the

bar. The difference between the minimum water level and the elevation of respective places gives the relative height of that place. Definition diagram for relative height are shown in Figure 4-4.

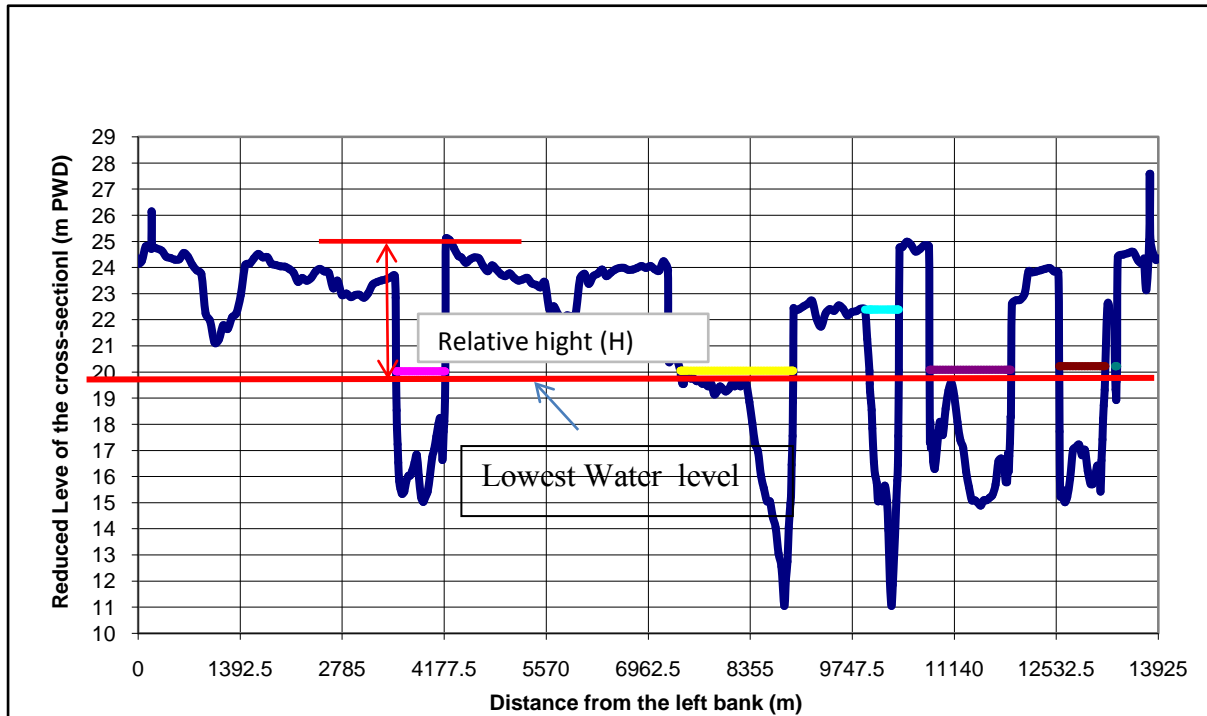


Figure 4-4: Definition diagram for relative bar height

4.2.5 Assessing Active braided index (ABI)

The total braided index (TBI) of the Jamuna river was assessed by many researchers (i.e. Klaassen and Vermeer, 1988; Halcrow, 1991; Bridge, 1993; Egozi and Ashmore, 2008). The active braiding index (ABI) only includes active channels with significant sediment transport, herein defined as higher than the cross-sectional average value, whereas the TBI includes both active and inactive channels. According to Bertoldi et al. (2009), the ABI provides a better description of the state of a braided river than the TBI. In this study ABI of the simulated river was calculated.

4.2.6 Assessing Active Channel Width

In relation to the ABI and to study the growth of bars, the active channel width was analyzed. The active channel width was defined as Schuurman et al (2013) i.e. the percentage of the channel width in which significant sediment transport occurred according to the, here defined as

$$F_{\text{active}} = \sum W_{\text{active}} / W * 100 (\%)$$

Here, F_{active} (%) the active channel width, W the total channel Width, and W_{active} the sum of widths of active channels in cross section (m).

4.2.7 *Assessing Bar Length and Amplitude*

There are several ways to determine the bar length. In this study the bar length was determined by identifying the bars as individual objects and measuring their longest axis. This method is previously used by Schuurman et al (2013). Bar amplitude was defined by the average difference of the bar crest level and the trough level.

4.2.8 *Assessing Bar Shape*

Two ratios were used to describe bar shape: length-width ratio (aspect ratio) and perimeter-area ratio (Kelly, 2006; Meshkova and Carling, 2013). In this study aspect ratio was used as an indicator of bar shape.

4.2.9 *Numerical Model Description*

4.2.9.1 Delft 3D Model

In this study the physics-based nonlinear morphodynamic model names as Delft3D was used. Delft3D solves the two dimensional depth-averaged flow equations and computes sediment transport and bed level change. It can also solve three-dimensional flow, but for the sake of computational efficiency, we use it in the two-dimensional mode with a parameterization for the effect of flow curvature and spiral flow on near-bed shear stress direction. The Delft3D model has been applied in a wide range of scientific projects for river, estuarine, and coastal systems (e.g., Roelvink, 2006; Van Marren, 2007; Van der Wegen and Roelvink, 2008; Crosato and Saleh, 2010; Crosato et al., 2011, 2012). Moreover, the model has proven to be reliable and accurate in the demanding practice of river engineering. The standard issue of Delft3D (version 3.28.5.01) was used, hence full optimizations of the model capacities.

Delft3D has been validated for a large number of well-documented cases, including well-documented flume experiments and on the river Rhine. Langendoen (2001) compared a number of models and found that Delft3D, together with Mike21C and concluded, it contains the most rigorous theoretical foundation for modeling sediment transport and morphological change.

In Delft3D, the hydrodynamics are modeled by applying conservation of momentum and mass assuming hydrostatic pressure:

Conservation of momentum in x -direction:

$$\frac{\partial u}{\partial t} + u \frac{\partial u}{\partial x} + v \frac{\partial u}{\partial y} + g \frac{\partial \eta}{\partial x} - fv + \frac{gu|U|}{c^2(d+\eta)} - \frac{F_x}{\rho(d+\eta)} - \nu_t \left(\frac{\partial^2 u}{\partial x^2} + \frac{\partial^2 u}{\partial y^2} \right) = 0 \quad (4.1)$$

Conservation of momentum in y -direction:

$$\frac{\partial v}{\partial t} + u \frac{\partial v}{\partial x} + v \frac{\partial v}{\partial y} + g \frac{\partial \eta}{\partial y} - fu + \frac{gv|U|}{c^2(d+\eta)} - \frac{F_y}{\rho(d+\eta)} - \nu_t \left(\frac{\partial^2 v}{\partial x^2} + \frac{\partial^2 v}{\partial y^2} \right) = 0 \quad (4.2)$$

Conservation of mass, also known as the sediment continuity equation:

$$\frac{\partial \eta}{\partial t} + \frac{\partial[(d+\eta)u]}{\partial x} + \frac{\partial[(d+\eta)v]}{\partial y} = 0 \quad (4.3)$$

Where

η = water level elevation (m)

d = still water depth (m)

u, v = velocity in the x - and y -directions, respectively ($\text{m}\cdot\text{s}^{-1}$)

U = magnitude of total depth-averaged current velocity ($\text{m}\cdot\text{s}^{-1}$)

$F_{x,y}$ = x - and y - components of external forces (Pa): surface and bottom stress

f = Coriolis parameter $2\Omega \sin \theta$, where Ω is the earth's angular velocity and θ is the geographic latitude ($\text{rad}\cdot\text{s}^{-1}$)

g = acceleration due to gravity ($\text{m}\cdot\text{s}^{-2}$)

ρ = water density ($\text{kg}\cdot\text{m}^{-3}$)

ν_t = eddy viscosity ($\text{m}^2.\text{s}^{-1}$)

c = Chézy coefficient ($\text{m}^{1/2}.\text{s}^{-1}$)

The horizontal turbulent dispersive transport of momentum is computed using a prescribed eddy viscosity coefficient. A quadratic friction law is assumed to give the current shear stress (τ) at the seabed that is induced by turbulent flow:

$$\tau = \rho \frac{g}{c^2} |U|^2 \quad (4.4)$$

Where

$|U|$ = the magnitude of the depth-average flow ($\text{m}.\text{s}^{-1}$)

c = Chézy coefficient ($\text{m}^{1/2}.\text{s}^{-1}$)

In Delft3D-FLOW the roughness factor may be determined according to three different formulations, namely Manning's formulation, the Chézy formulation and White Colebrook's formulation. For the Chézy formulation, the user specifies the coefficient 'c'.

For predicting the sediment load, several transport formula (i.e. of Engelund and Hansen, 1967; Meyer-Peter and Mueller, 1948; Van Rijn, 1984, 2000) can be used in the model. For non-cohesive sediment if one uses Van Rijn (1984) then the following approach is adopted in Delft 3D.

The sediment transport predictor of Van Rijn distinguishes between bed load transport $q_{\theta,b}$ and suspended-load transport $q_{\theta,s}$:

$$q_{\theta} = q_{\theta,b} + q_{\theta,s} \quad (4.5)$$

The bed load transport rate $q_{\theta,b}$ is computed by

$$q_{\theta,b} = \begin{cases} 0.53(\Delta g^* d_{50}^3)^{0.5} (D^*)^{-3} (\mu_{cT} - \tau_c)^{2.1} & \text{if } (\mu_{cT} - \tau_c) < 3 \\ 0.1(\Delta g^* d_{50}^3)^{0.5} (D^*)^{-3} (\mu_{cT} - \tau_c)^{1.5} & \text{if } (\mu_{cT} - \tau_c) \geq 3 \end{cases} \quad (4.6)$$

in which the critical shear stress τ_c is based on the critical Shields number, τ is the bed shear stress, μ_c is the ratio between total bed roughness C and grain-related bed roughness Cd_{90} :

$$\mu_c = C/Cd_{90}$$

Where, $D_{90} = 1.5D_{50}$, and the dimensionless particle parameter D^* is computed by

$$D^* = D_{50} (\Delta g / \nu^2) \quad (4.7)$$

Where, ν is the dynamic viscosity (m^2/s). The suspended-load transport $q_{0,s}$ is computed by

$$q_{0,s} = fsUhC_a \quad (4.8)$$

In which C_a is the reference concentration and fs is a shape factor for the vertical distribution of suspended sediment (Van Rijn, 1984). The bed slope effect is only applied to the bed load sediment transport and no lag between sediment transport capacity and suspended sediment concentration is applied. After each time step, the bed level is updated using the Exner equation for mass conservation of sediment:

$$\Delta Z_b / \Delta t = Morfac (\Delta q_x / \Delta x + \Delta q_y / \Delta y) \quad (4.9)$$

In which MorFac is an acceleration factor, which reduces computational time. Application of this factor is valid, as the adaptation time of morphology is larger than the adaptation time of flow. Consequently, the bed level change within a hydrodynamic time step Δt is negligible even with $MorFac \gg 1$ and the flow field adapts quickly to any change in bed topography (Roelvink, 2006; Crosato et al., 2011). In the Delft 3D model, in horizontal direction an irregularly spaced, orthogonal, curvilinear grid can be used. For 3D simulations the model uses the sigma co-ordinate approach in the vertical direction (Delft Hydraulics, 1999). A sigma-coordinate system scales the vertical coordinate relative to the local water column depth, resulting in a constant number of layers over the entire model domain (Robson, 2008; Van Ballegooyen et al., 2004). The relative layer thicknesses may also be non-uniformly distributed to allow for increased vertical resolution in the region of interest. For a detailed description of the hydrodynamics and numerical scheme of Delft3D, see Lesser et al., (2004), Van der Wegen and Roelvink (2008), and Deltares (2009).

4.2.9.2 Model Schematization

Grid

The numerical model was simulated for 165 km long river reach with a average width of 13 km; started from 15 km upstream from the Bahadurabad station and ended at 1.5 km upstream of Aricha station. The reach was discretized by 884*137 grid cells. Therefore, the average dimension of each grid cell was 185m*95m. The choice of grid resolution was a balance between computational time, scale of the processes, and desired level of detail. The assumption working behind the choice of the grid cell size was to cover the one bar/ channel with at least three grid cells (i.e. the size of the smallest bar in emerged in 2013 was around 600m*378m).

Bathymetry

The initial bathymetry data used in the model was collected from Institute of Water Modeling (IWM) with a resolution of 350 m*100 m. The data was measured with respect to PWD datum. Bathymetry data was collected during the monsoon period of the year 2011. Figure 4-5 shows the grid and initial bathymetry of the model.

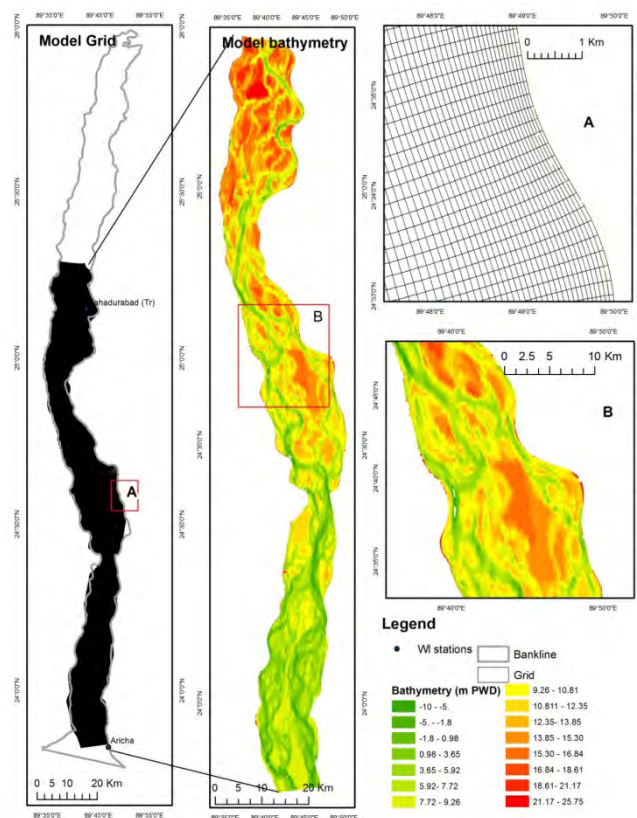


Figure 4-5: Model Grid and Bathymetry

Boundary Condition

The model was simulated for 4.5 months only from the 1st of June, 2011 to 15th of October, 2011. For the upstream boundary, the discharge data of Bahadurabad was considered and the water level of Aricha station was chosen for the downstream boundary. Figure 4-6 shows the upstream and downstream boundary of the model. As the sediment boundary the monthly average sediment data (1968-2001) was given as the input which is shown in Table 4-4.

Table 4-4: Boundary Sediment load

Month	Sediment load (kg/s)
June	210.4355
July	179.6984
August	214.1194
September	206.3134
October	158.407

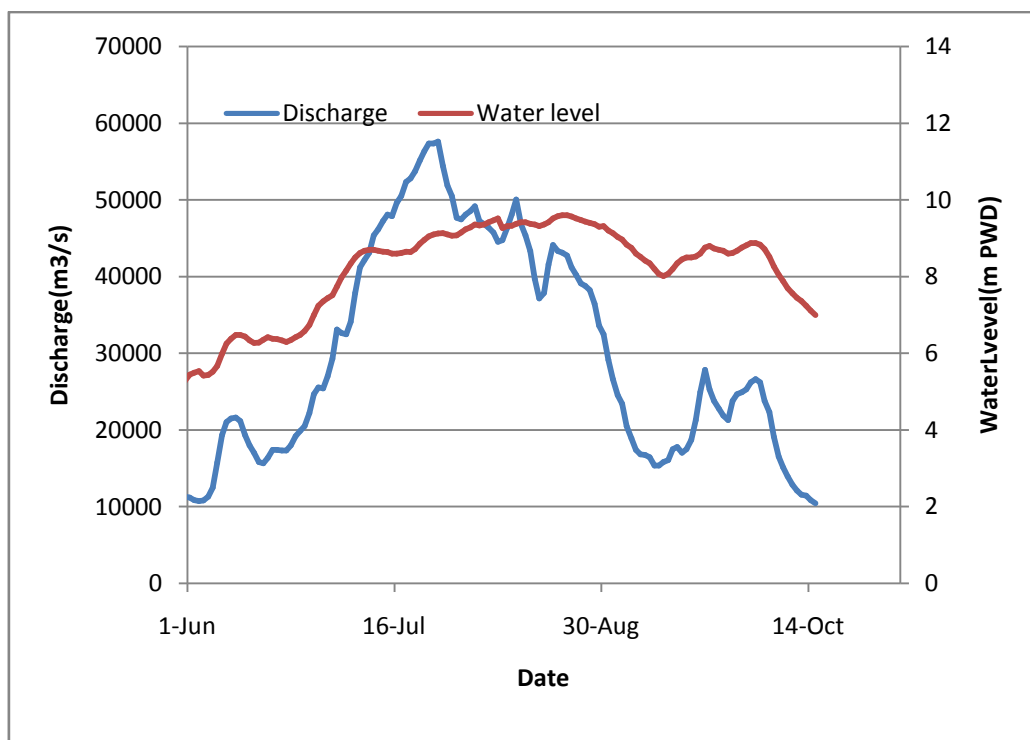


Figure 4-6: The upstream and downstream boundary conditions of the model

Morphological and Physical Parameters

Based on the analysis of FAP-6 data Kabir and Ahmed (1996) estimated the sediment load using different predictor formulae. Their observation is presented in Figure 4-7. They concluded that Van Rijn approach predicts well in case of Jamuna during monsoon. Therefore, for this model Van Rijn formula was used assuming the sp. density 2650 kg/m^3 and the mean sediment diameter, $d_{50} 277 \mu\text{m}$ (FAP-6; Kabir and Ahmed, 1996). The water density and horizontal eddy viscosity were assumed 1000 kg/m^3 and $10 \text{ m}^2/\text{s}$ respectively. For assuming the appropriate value of roughness (Manning's n) and Morfac (Exner equation) sensitivity analysis was done using the combination of the parameter described in Table 4-5. Manning's $n=0.027$ and Morfac= 10 were taken finally as they produce the better results.

Table 4-5: Parameters used in the Sensitivity Analysis

Parameter	Low	Middle	High
Manning's n	0.025	0.026	0.027
Morfac	1	10,25	50

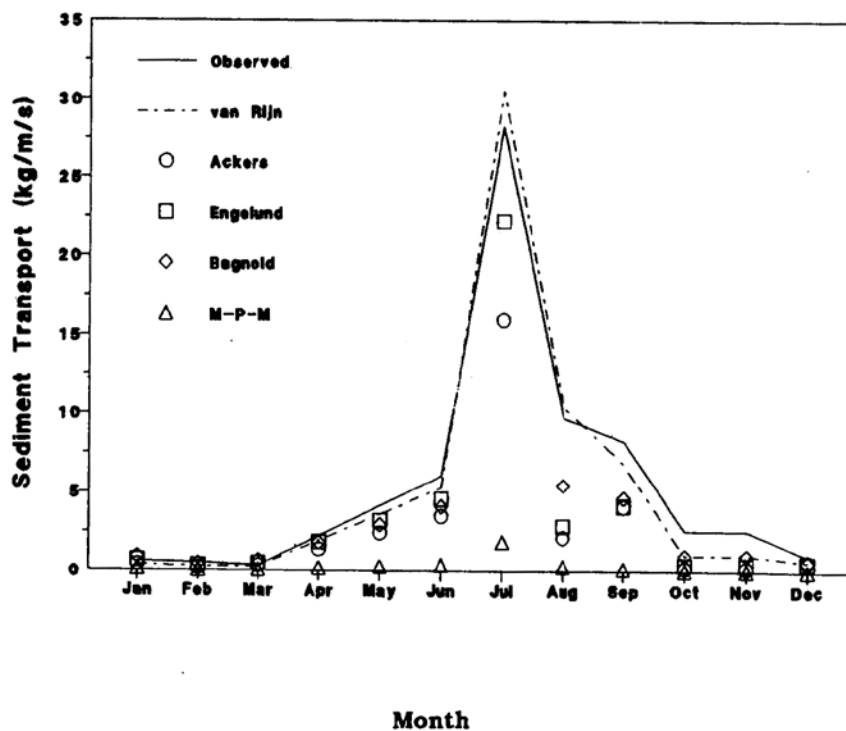


Figure 4-7: Comparisons of measured and predicted values of sediment load

Using different formulae at Bahadurabad (reproduced from Kabir and Ahmed, 1996)

Chapter 5

Results and Discussions

5.1 Changes in River Flow and Sediment Regime

The analysis of the discharge data measured in the Jamuna River at Bahadurabad by the BWDB from 1956 to 2006 is presented in Figure 5-1. The mean annual flood flow in the Jamuna River is about $70,000 \text{ m}^3/\text{s}$ but the maximum annual floods vary in magnitude from $40,000 \text{ m}^3/\text{s}$ to more than $100,000 \text{ m}^3/\text{s}$ (Figure 5-1 A). Variability in maximum annual flood was less in the 1960s and 1970s than the following decades. The standard deviation of maximum annual flood was $6105.6 \text{ m}^3/\text{s}$ in the 1960s but in recent decades this value goes to $16834.6 \text{ m}^3/\text{s}$, almost three times higher than the value of 1960s. There is an increasing trend in the magnitude of maximum annual flood with time; it increases at a rate of $113 \text{ m}^3/\text{s}$ in each year.

The average minimum annual flow in the Jamuna River is about $4,000 \text{ m}^3/\text{s}$ with a standard deviation of $740.9 \text{ m}^3/\text{s}$ (Figure 5-1 B). The minimum annual flow shows slight increasing trend for the last five decades. The minimum annual flow is rising at a rate of $47 \text{ m}^3/\text{s}$ in each year. The mean annual discharge is about $20,000 \text{ m}^3/\text{s}$ having the standard deviation of $2910.4 \text{ m}^3/\text{s}$ and like the maximum flood flow, only a small increase is apparent during the last five decades (Figure 5-1 C). The mean annual flow is increasing at a rate of $57 \text{ m}^3/\text{s}$ in each year.

Figure 5-2 shows the analysis of the water level data from measured from 1950 to 2009 in the Jamuna River at Bahadurabad by the BWDB. The annual maximum, minimum and mean water levels show a very small variation including the decadal change. The maximum water level varies between 18 m PWD to 21 m PWD during the last few decades at Bahadurabad (Figure 5-2 A). The mean of maximum annual water level from 1950 to 2009 was 19.8m PWD with a standard deviation 0.398 m PWD. The trend of variation during this period was almost steady. The average of mean annual water level is about 16 m PWD and it fluctuates between 15.5 m PWD to 17 m PWD annually (Figure 5-2 B). These data shows a slight increasing trend but the magnitude of increasing is small, only 0.014m per year with the standard deviation of 0.34 m PWD. The average of minimum annual water level at Bahadurabad is about 13 m PWD. Like the annual maximum water level it also varies almost

2 m from its mean (Figure 5-2 C). The annual minimum water level data also shows an increasing trend at an amount 0.006 m in each year with the standard deviation of 0.44 m PWD.

The change in river's average water surface slope over time from Noonkhawa to Aricha is shown in Figure 5-3 (the locations of water level stations are shown in Figure 4-1). The data shows a decreasing trend; on an average reduction of water level 0.017cm/km in every year. The average slope of the water surface 8 cm/km during the last five decades which is described in sec 3.3.1. However, the water surface slope was 8.24 cm/km during 1980s but in 2000s it was on an average 7.55 cm/km. After 2005 it shows an increasing trend; the value goes to on an average 7.86 cm/km.

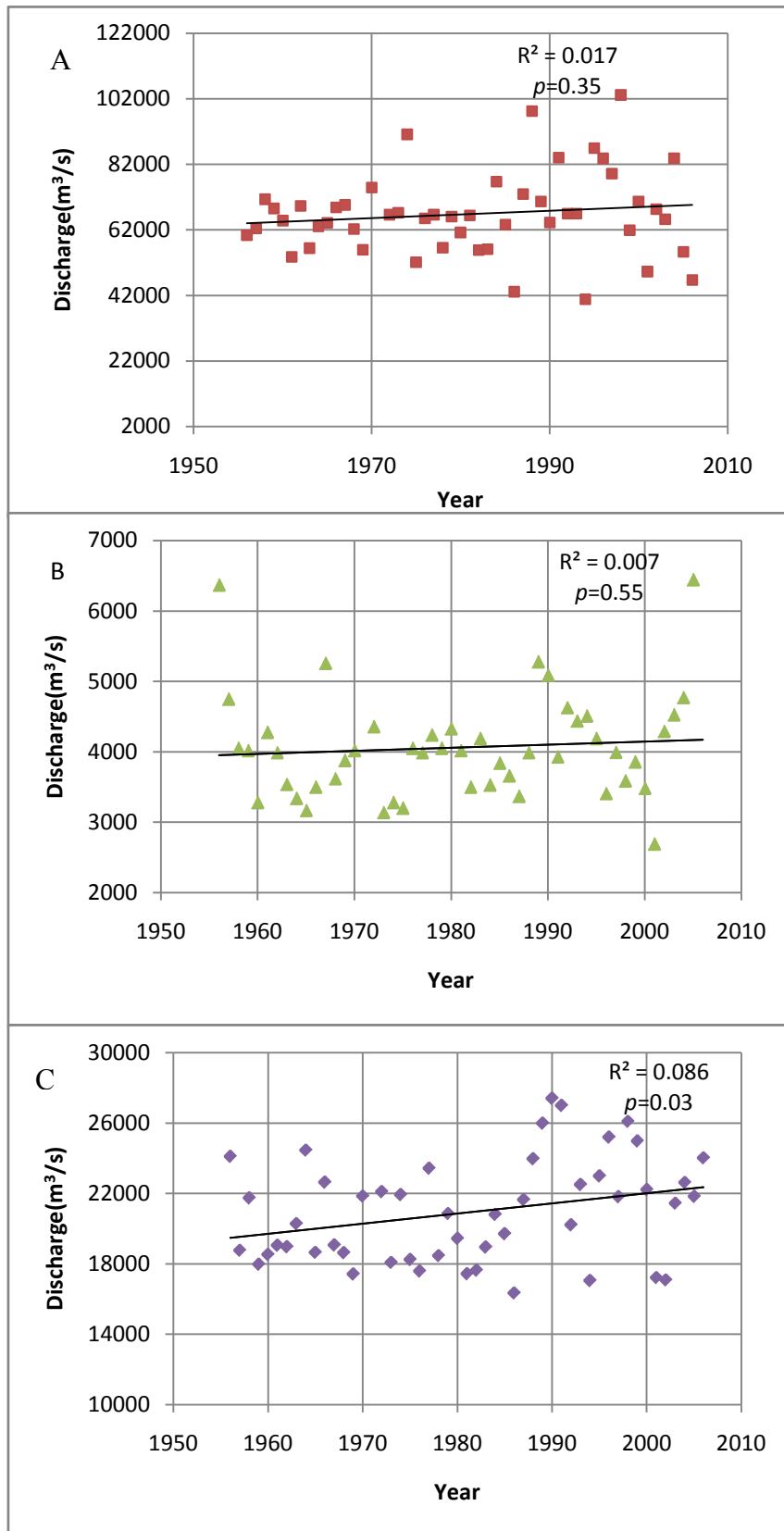


Figure 5-1: Changes in (A) maximum annual discharge, (B) minimum annual discharge and (C) mean annual discharge of the Jamuna River over time

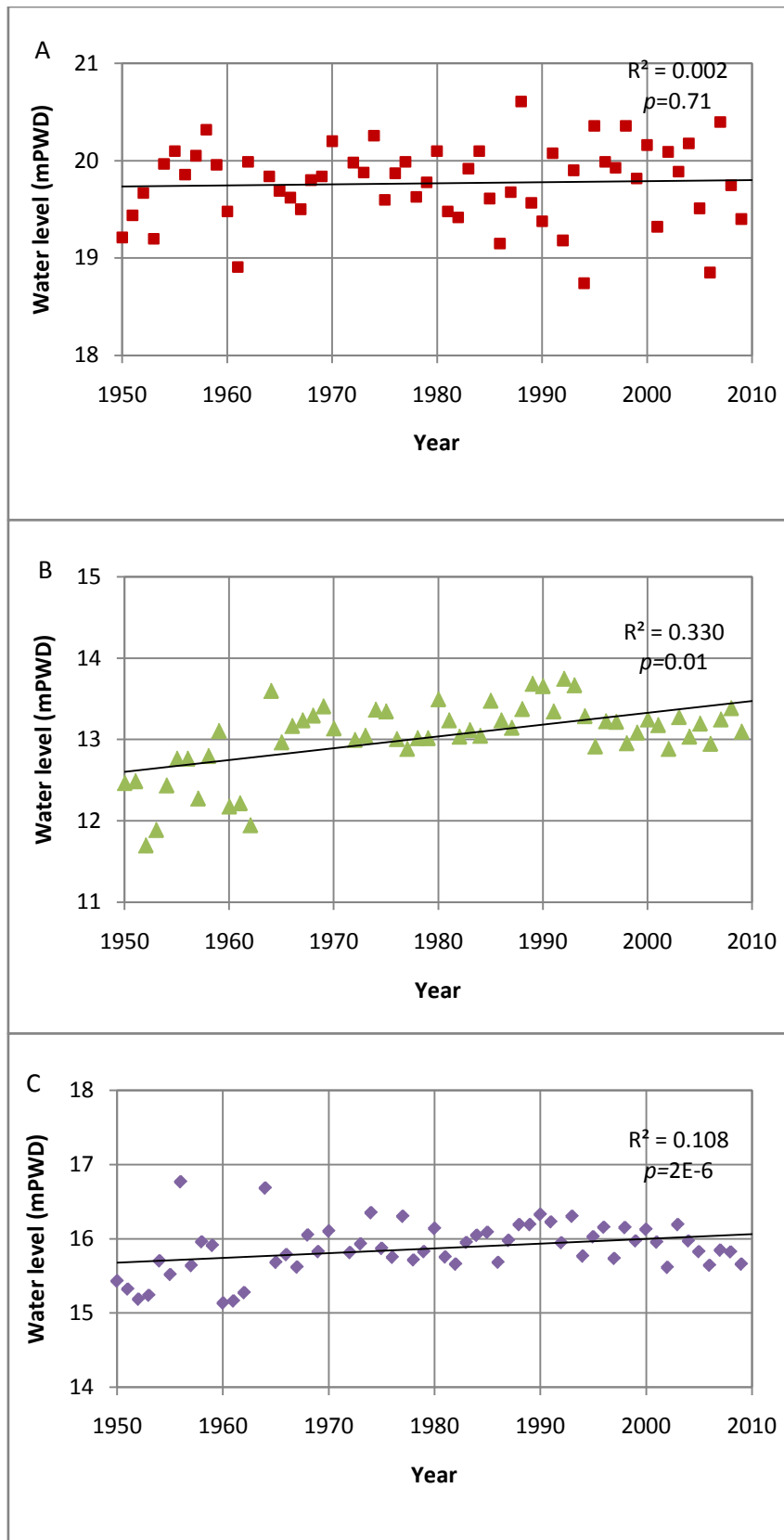


Figure 5-2: Changes in (A) maximum annual water level (B) minimum water level (C) mean annual water level of the Jamuna River over time

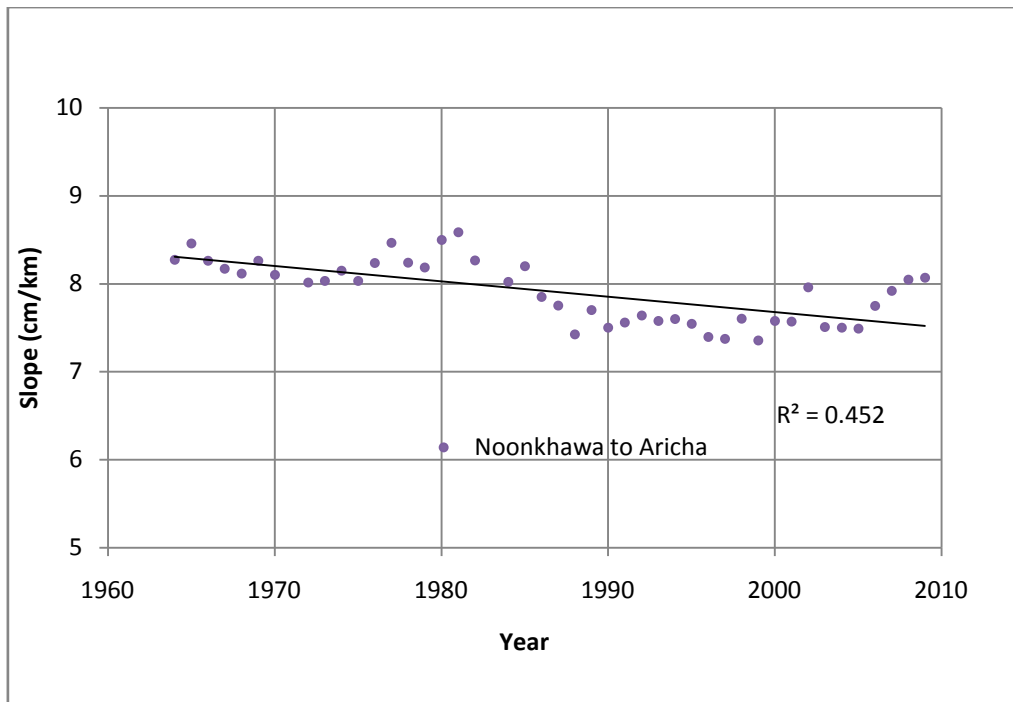


Figure 5-3: Changes in water surface slope over time (at dry period)

The time series analysis of the sediment data (suspended part only) of the river are shown in Figure 5-4. In 1968 the maximum annual bed material load was over 35 000 kg/s where it reduces 3000 kg/s in 2001 which only 9% of the load of the 1968 (Figure 5-4A). The annual minimum load reduces almost 90% (Figure 5-4B). The average load of the river during these few decades was 2649 kg/s. Wash load also shows the same type of trend the mean annual wash load reduces almost 30% from 1972 to 2001. Gupta et al (2012) showed the role of mega dams in reducing sediment fluxes of large Asian rivers. Hence, the construction of dams in the upper basin tributaries of the river may be the cause of sediment reduction. However this process may act as a driver in change of river spatial characteristics.

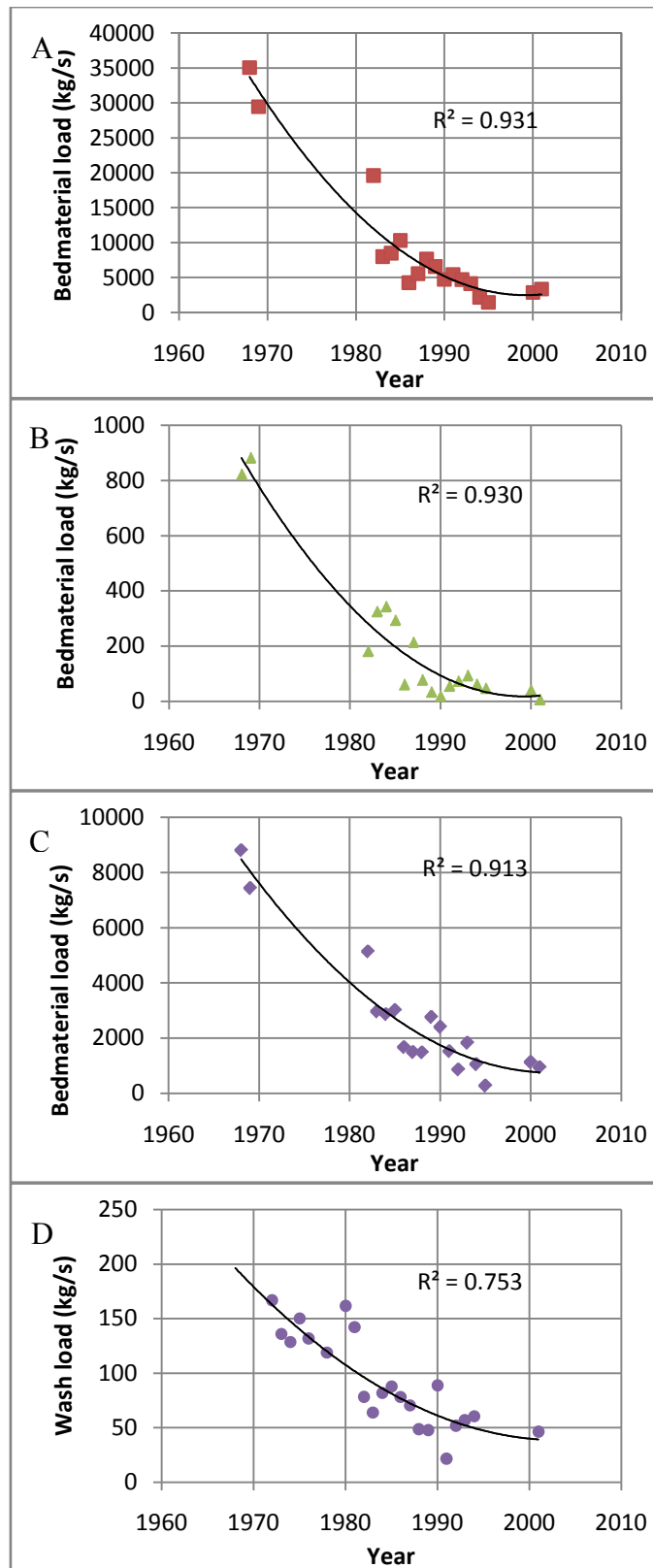


Figure 5-4: Changes in (A) maximum annual Bedmaterial load (B) minimum Bedmaterial load (C) mean annual Bedmaterial load (D) mean annual Wash load of the Jamuna River over time

5.2 Changes in river spatial characteristics

The change in average river width over time is shown in Figure 5-5. As discussed earlier, though there is a slight variation in water level and comparatively high variation discharge in different stations of the river, the river shows a very an increasing trend in its width. This trend was very prominent upto 1992 when the rate was 150 m/y; then the rate of widening slowed down. The widening process continued at the rate of 67 m/y up to 2001, when the average width reached was 10.7 km. Since then, the river width increase at a smaller rate 6.4 m/y. Since the early 1970s, the Jamuna River widened from 8.3 km to 11.8 km in the mid-1990s and now the average width is 10.4 km. Sarker and Thorne (2006) concluded that this change was due of propagation of sand waves caused by 1950 earthquake which has been discussed in sec 3.3.2. However, this study indicates the change in river water surface slope may be one of the reasons of this width change.

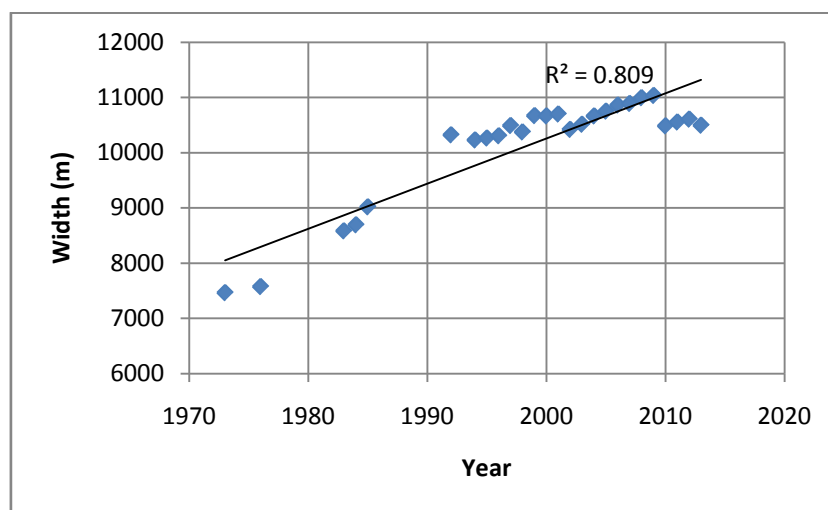


Figure 5-5: Average width of Jamuna with time

Figure 5 -6 shows the results of the time-series analysis of classified dry season satellite images with the annual maximum and minimum flow. This figure demonstrates the changes of water and bar area within the banklines of the study area during the last four decades. Water area mainly represents the area of dry season channel and bar represents the total sand and vegetated land area within the bank line. Like the average width of the river, the bar area shows an increasing trend upto 1992 at a rate of 21.71sq km per year. After that the bar area increases 18.37 sq km per year till 2001. Then it shows almost a constant trend except the yearly variation. But the channel area shows almost a constant trend with an average area 700

sq km in each year. This figure also indicates the change in bar and channel area of the river do not follow the similar trend as that of the flow.

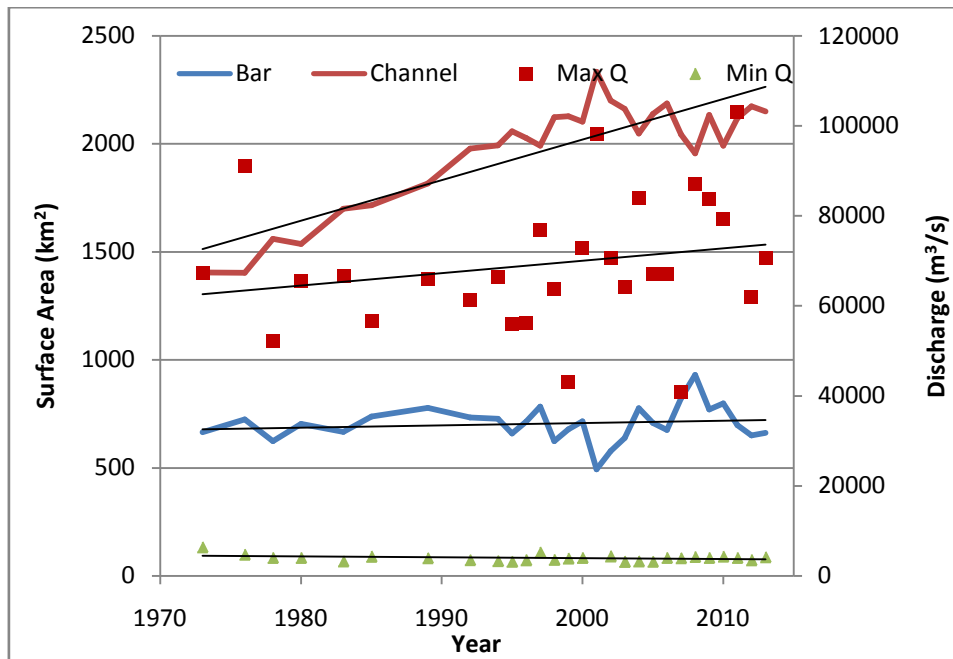


Figure 5-6: Yearly variation of Area of Water and Bar within the bankline with annual maximum and minimum flow

5.3 Relation between the Water Surface Slope and Bar Dynamics

An attempt has been made through this study to relate the changes of bar or channel (Figure 5-6 and 5-3) with the changes of the slope of the channel. Figure 5-7 illustrates such relationship. It can be concluded from this figure that during the last five decades bar shows higher sensitivity than the channel with the changes of slope. With the one unit increase of slope the bar area of the river reduces almost 26% while the channel area increases almost 4.5%.

The explanation of the change in water surface slope is not a straightforward one, the incoming sediment and change in discharge may play an important role behind that. But this change may be a reason of different morphological changes of the river.

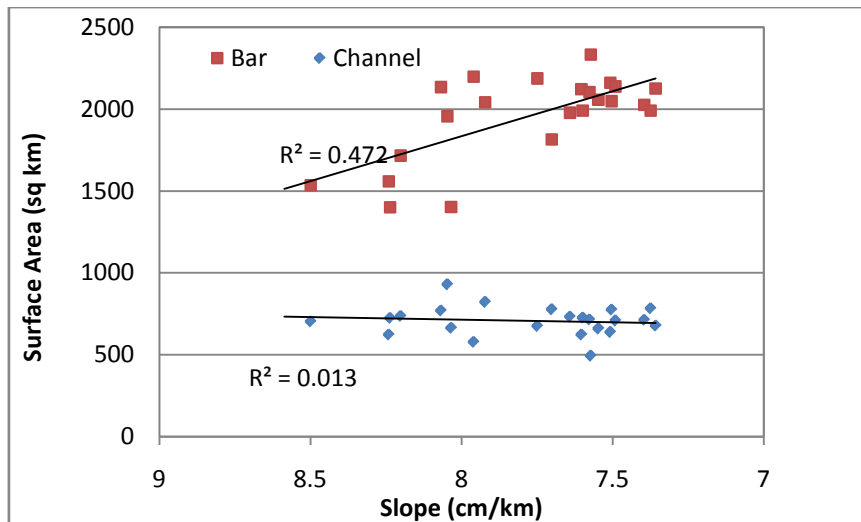


Figure 5-7: Changes in bar and channel area with the slope

5.4 Relation between Sediment load and Bar dynamics

Figure 5-8 shows the relationship between the changes in bedmaterial load with bar and channel area of the river. As like as the river slope during the measured period the bar area shows higher sensitivity than the channel area with the change in bedmaterial load. With the change in every ton/s the bar area reduces almost 2.2% while the channel area increases only 0.43%.

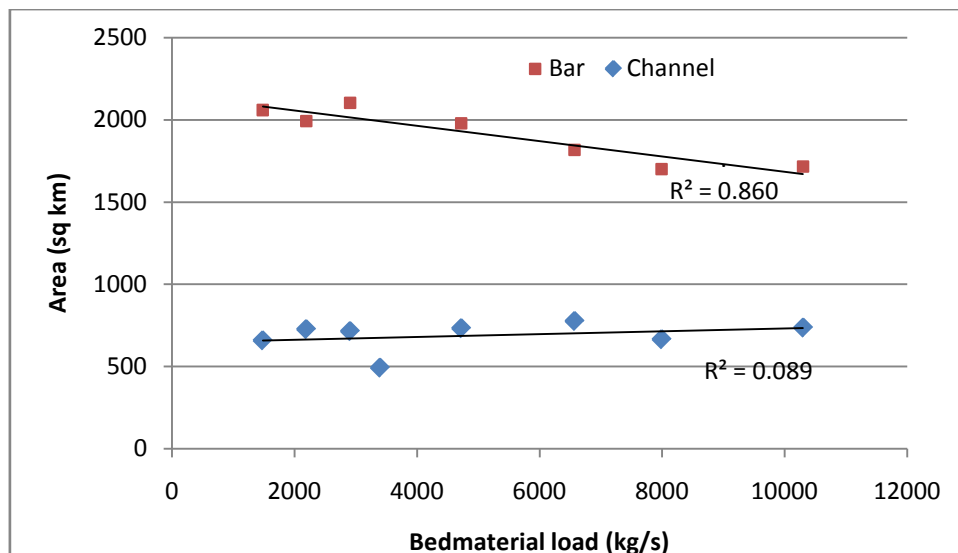


Figure 5-8: Changes in bar and channel area with the sediment load

5.5 Temporal Development of Bars²

5.5.1 Ages of the bars

An attempt has been made through this study to assess the ages of the bars along the entire study area. The result of this analysis is shown in Figure 5-9. From this analysis reveals that the total area of the bars of the river is almost 2150 sq km while the total river area (area within the bankline) 2815 sq km. Maximum river bar are newly developed (Figure 5-10). Almost 55% of the bar area are developed within the last 8 years. 35.5% of the bar the ages from 9-18 years. The areas of the bars equal and above 20 years are only 5.5%. This result is comparable to some previous studies described in sec 2.7. The comparison has been discussed in sec 5.9.

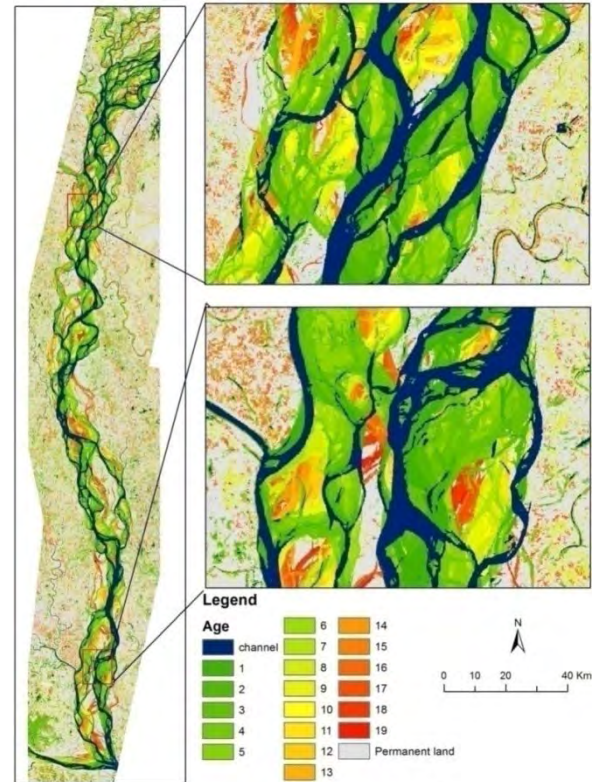


Figure 5-9: Ages of the bars of the study area

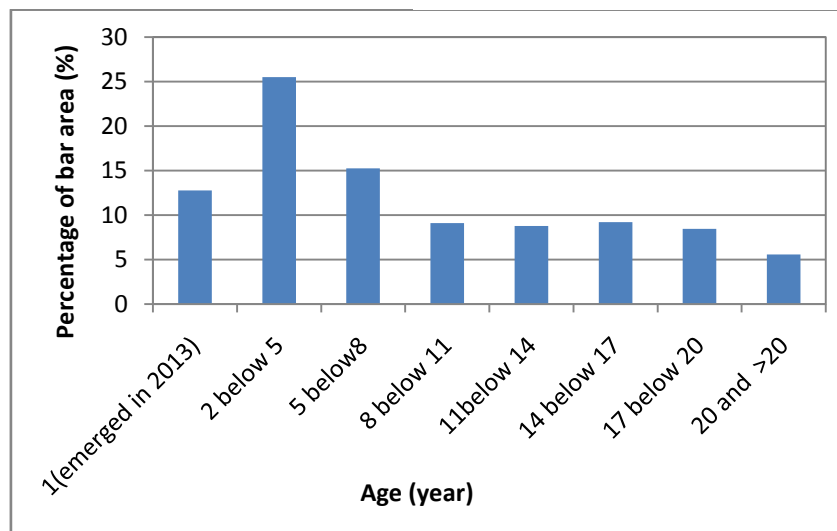


Figure 5-10: Ages of bar area in the study area

² Part of this section has been published in the International Conference of Small scale morphological evolution of coastal, estuarine and river systems (2014)

5.5.2 Vegetation colonization on the bar

As described in chapter two in the way of developing of the braided bar the colonization of the vegetation plays an important role. Sarker et al (2003) mentioned that newly accreted bar, if it does not erode quickly, is initially colonized by grass, particularly catkin grass (*Saccharum spontaneum*, for example). Dense growth of catkin grass can accelerate silt deposition on the top of the bar. Decomposition of the grass also adds humus to the soil and this process accelerates to grow other trees on the bars.

Although this grass grows naturally on newly accreting channels, there are instances where inhabitants or potential inhabitants have planted the grass on newly emerging land to hasten its conversion to agricultural land. However, sometimes some low level vegetation is also found in the newly emerged bars just beside a channel which is shown in Figure 5-11. But these are not the typical bar vegetation. Figure 5-12 shows the time period of the development of vegetation on the bar top. It indicates that at present the almost 52% (1104 sq km) of the bar area are vegetated. The vegetation coverage over the old bars are more. But the area of coverage never go to the 100% because every year the bars (some part or as a whole) are go under water during flooding. Flood deposits sand over the land. Moreover, spill channels also dump bulk of sand. Figure 5-13 shows the ratio between bar area and vegetation area with age. This analysis indicates that maximum 70% of the bar area can be vegetated which can be said as the optimum limit of vegetation coverage of bars in the river like Jamuna.

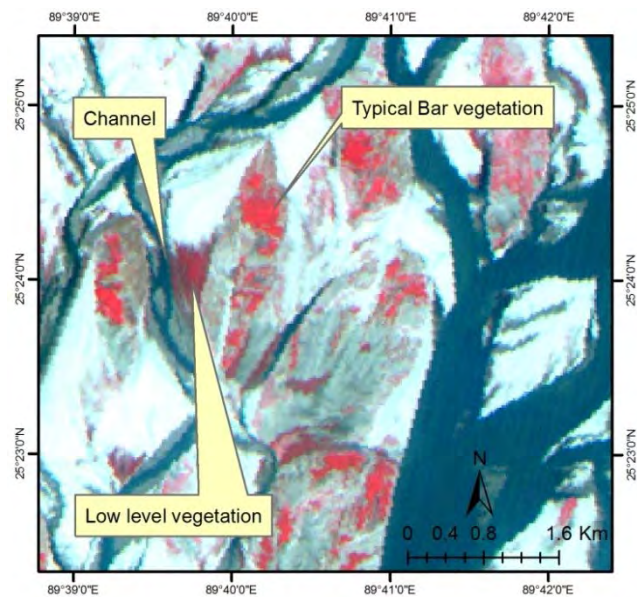


Figure 5-11: Typical and low level vegetation

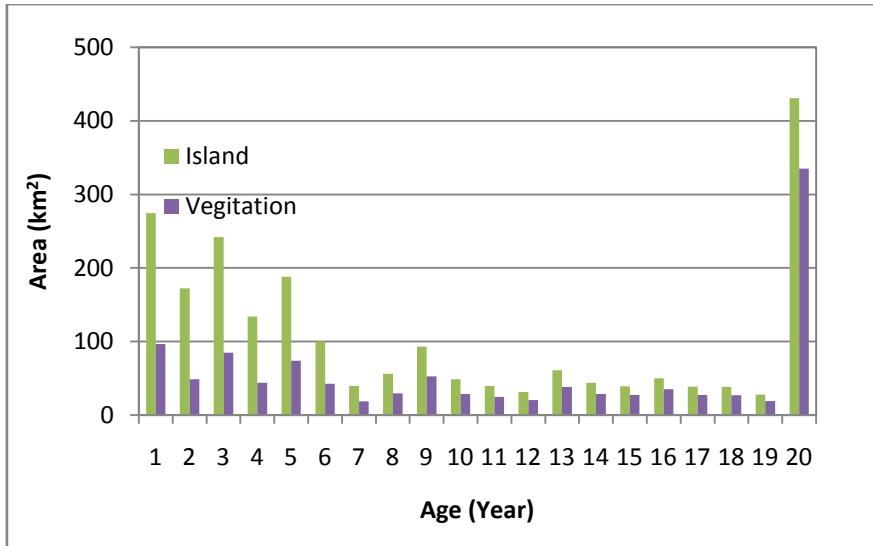


Figure 5-12: The bar area and its vegetation coverage with time

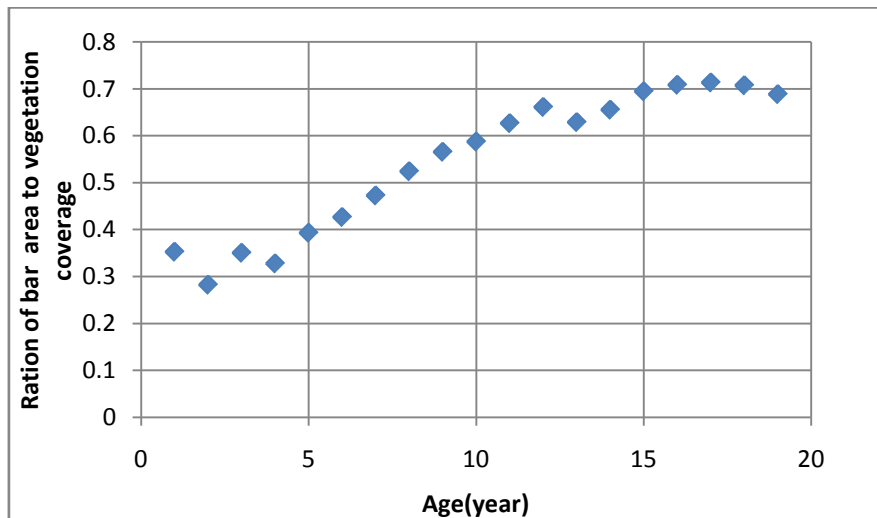


Figure 5-13: Vegetation coverage of land with age

5.6 Vertical growth of bar³

The process of vertical growth of bars is not so straight forward. Every year they go under water. Sometimes the heights of the bars are reduced by creation of cross-bar channels. Moreover, human activities also affect the natural growth of the bar. Figure 5-14 shows the boxplot of relative height (elevation from the low water level to the bar top) of bar with age along the BWDB measured cross-section location. This figure indicates that during the initial stage of bar development, the uncertainty range in vertical growth is very high, but reduces

³ Part of this section has been published in the International Conference of Small scale morphological evolution of coastal, estuarine and river systems (2014)

over time. The data shows very scatter pattern which indicates the complexity relating to this process. Figure 5-15 shows relationship between the mean relative heights of the bar to its age. This figure indicates that a bar can grow almost 5m from the adjacent low water level and it matures within 10 years. The relationship also indicates that the vertical growth of bar are exponential to its age. The relationship developed from this analysis is

$$H = 3.11 * T^{0.157} \dots\dots\dots (5-1)$$

Where, H= Relative height of bar with respect to low water level; T= Age of bar in year

To test this relationship (equation no. 5-1), the topographic data of a bar near Chowhali Thana (Figure 5-16) was collected and a comparison was made between the predicted and observed relative height which is shown in Figure 5-17. The data shows ordinary correlation ($r^2= 0.64$).

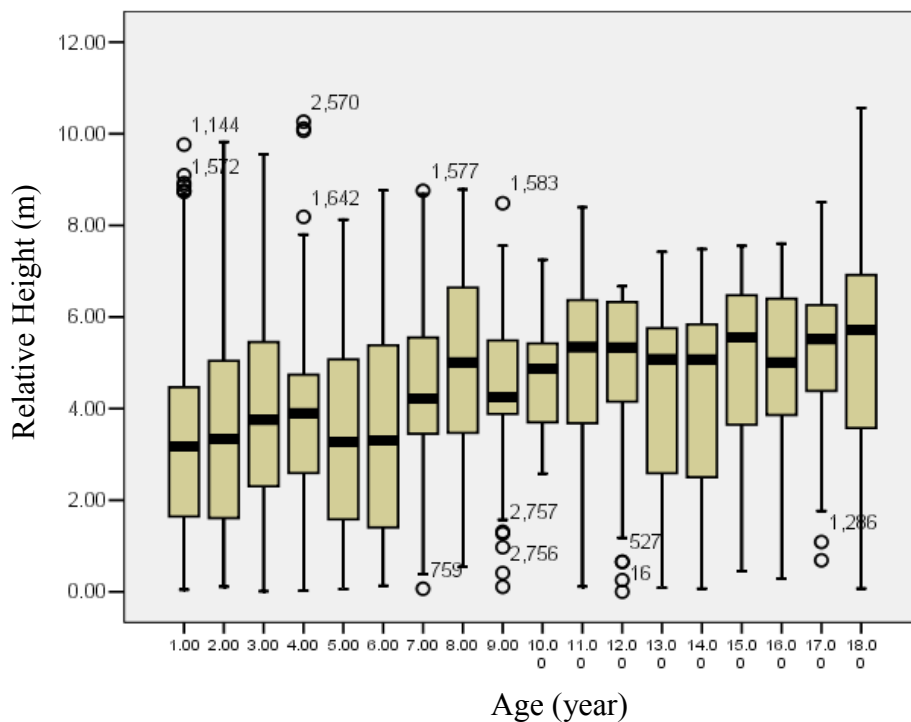


Figure 5-14: Box plot of relative height of the selected bars against age

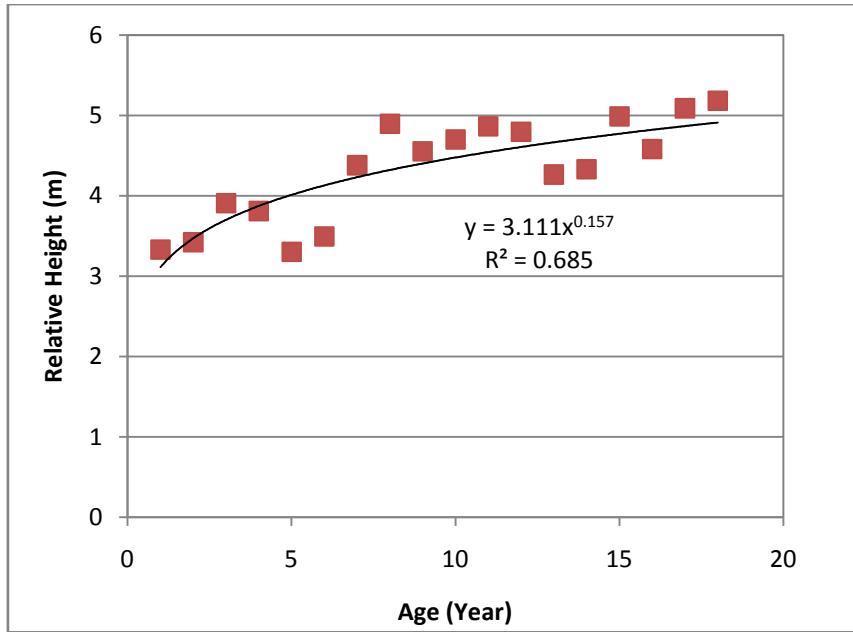


Figure 5-15: Relationship between Relative heights of the selected bars against age

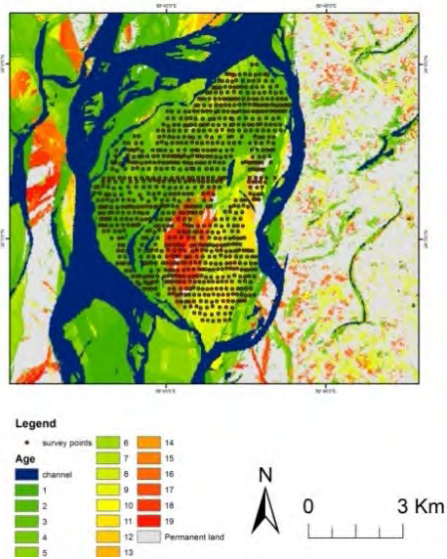


Figure 5-16: Location of topographic survey of Bar at Chowhali

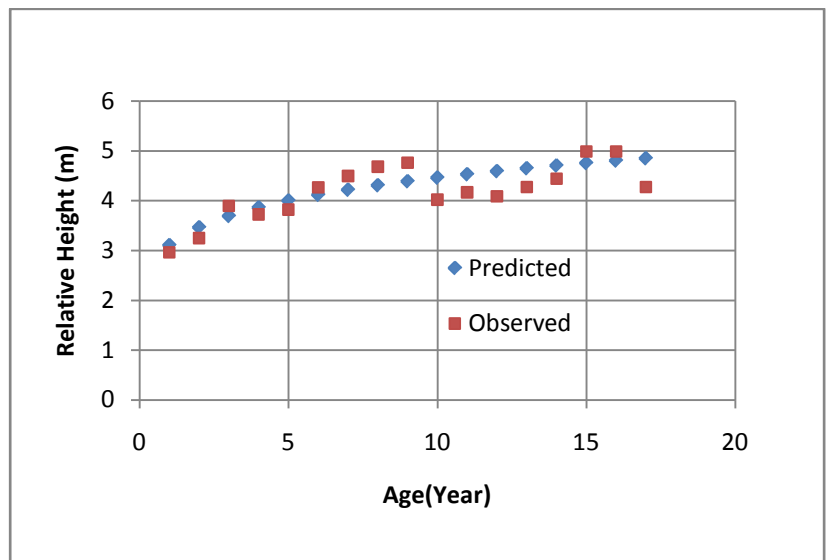


Figure 5-17: Predicted and observed relative height with age

5.6.1 Vertical growth of a structurally intervened and a non-intervened bar

To assess the effect of structural intervention two bars were selected, one is just downstream of the Bangabandhu Bridge another is almost 35 km downstream of the Bridge (shown in Figure 5-18). A very large bar has been developed at the downstream of the right guide bund of the Bangabandhu Bridge. The right guide bund protruded about 4 km into the river, which facilitated to develop about a 20 km long with an area of 82 km² bar (Figure 5-18). The channels separated from the mainland have been declining since the construction of the right guide bund. Only the active channel exists at the east side of the bar.

The analysis showed that growth rate with respect to age of a structurally intervened bar is quite high comparatively to a non-intervened bar (Figure 5-19). The uncertainty range is higher for the non-intervened bar. But the non-intervened bar attains high relative height (mean height 2.7m with standard deviation 0.93m) compared to the structurally intervened bar (mean height 2.2 m with standard deviation 0.73m).

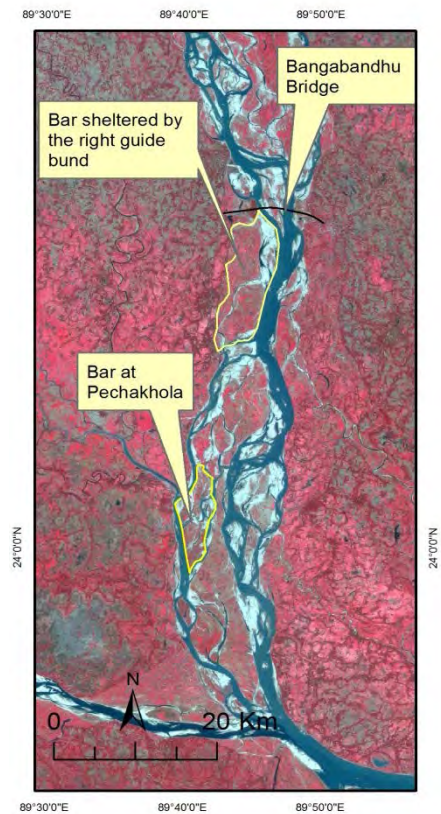


Figure 5-18: Location of selected bar to assess the effect of structural intervention

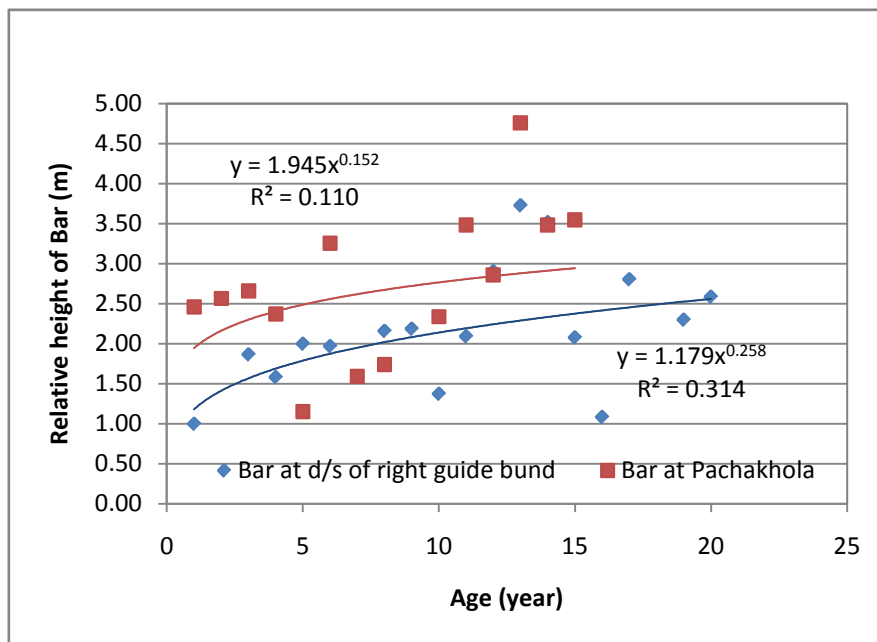


Figure 5-19: Relationship between Relative heights and age of a structurally intervened and non-intervened bar

5.7 Bar dynamics in lateral direction

5.8.1 Spatial Development of bar

During the development, a bar may form as a mid-channel bar, and it may grow, migrate and disappear within a few years. This is true for most of the cases, as the life-span in more than 50% of bars is less than 4 years. In this section the formation process of two types of bars- one is single mid channel bar and another is clusters mid channel bar are discussed.

The development process of a single mid channel derived from satellite imagery analysis is shown in Figure 5-20. A diamond shaped bar emerged in the dry season of 2005 at the downstream of the confluence of two braided channels (A). Elevation appears to be low and the length and width are few hundred of meters.

In the following year, the left confluencing channel disappeared, which facilitated the bar to grow further upstream (B). The bar grew several kilometers long and more than a kilometer wide at both the upstream and the downstream. Vegetation appeared at the middle of the bar where the elevation was low and facilitated the deposition of silt at that location where the soil was moist. Low elevation and deposition of silt and clay indicate the joining of a bar from the upstream.

In 2007, the channel itself widened, indicating that more flow had been diverted through this channel. The bar migrated downstream and split into two or more sections (C). Most of the vegetation disappeared from both the split bars indicating the existence of no low elevated strip within the bar. Vegetation or moist soils appeared on the lee side of the bar.

In 2008, there was a major change in the channel upstream where huge erosion caused an attached bar to develop along the left bank of the channel and the bar completely disappeared

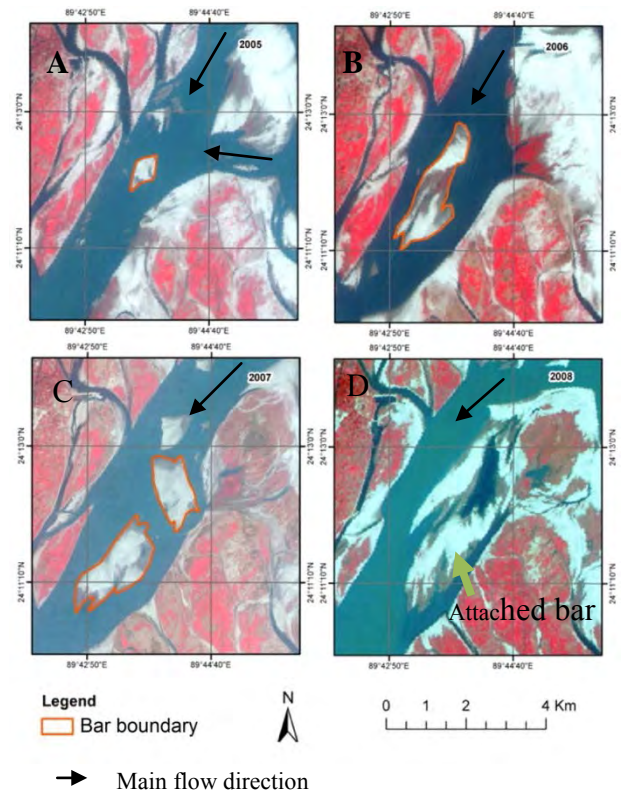


Figure 5-20: Development of a mid-channel bar over time

(D). The life-span of the bar was only three years. Vegetation appeared in this bar was on the moist soil the elevation of which was close to the low water level.

The complex formation process of a cluster of bars in the Jamuna River is presented in Figure 5-21. The boundary of a vegetated bar observed in 2004 satellite images was superimposed on time-series satellite images of 1997. The boundary in 1997 included the downstream part of a cluster of bars, a reach of channel and the upstream part of an attached bar (A). In the following two years there were joining, separating and rejoining of bars, while abandonment and development of channels occurred within this area (B and C). A large and apparently monolithic bar emerged in 2000 (D). This bar was again separated and rejoined by a braided channel by the following years (E, F, G and H). This complex process of bar development has pronounced effects on lateral and vertical growth and the vegetation pattern of the bars.

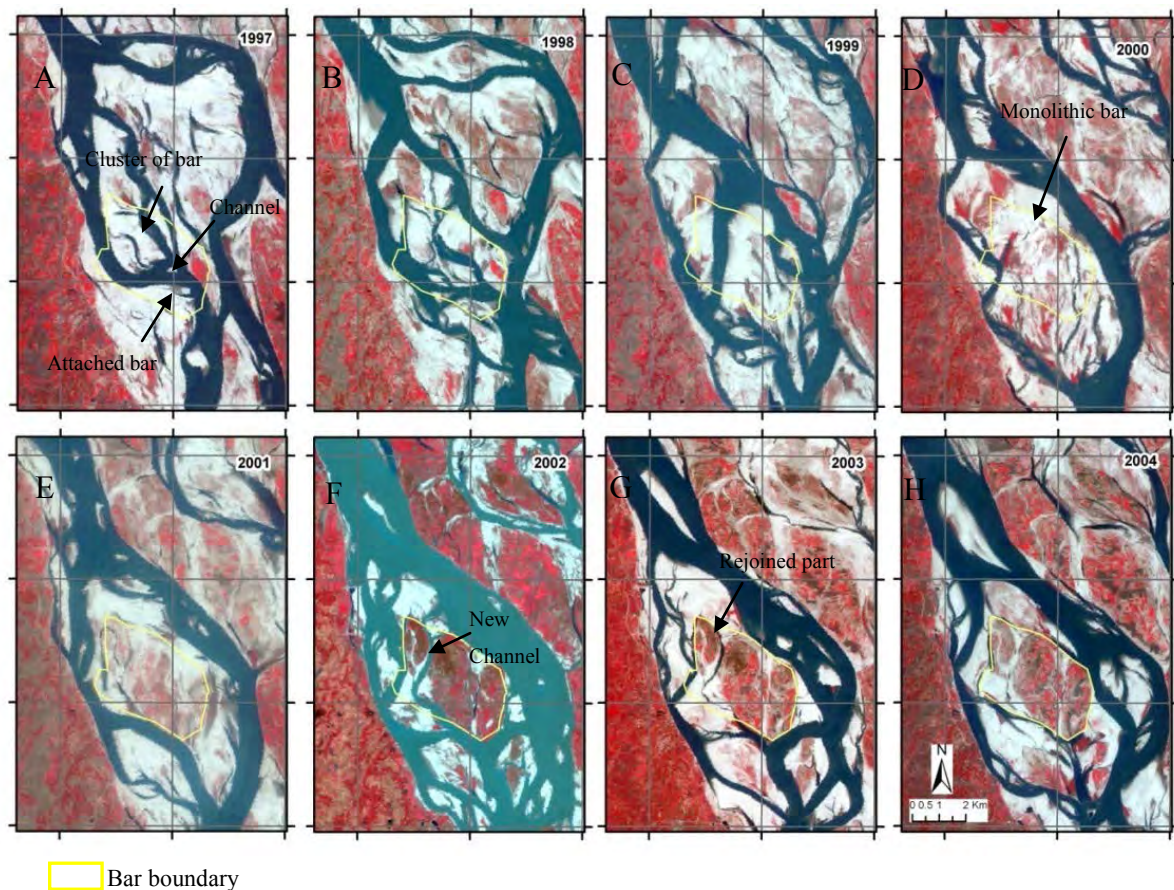


Figure 5-21: Development of a cluster of bars into a bar over time

5.8.2 Unit process related to the development of bar

The analysis of dry season satellite imagery indicates that a bar laterally grows mainly through three dominant processes.

- Adjacent channel shifting
- Growth of cross-bar channels
- Channel abandonment

These processes are shortly described in the following paragraphs

Adjacent channel shifting process

Like the meandering river, the adjacent channel of a bar in the braided river shows a regular shifting process. The channel adjacent to a braided bar shifts its length and sinuosity regularly specially during flooding and this shifting process causes bar accretion and erosion. Figure 5-22 shows such a shifting process in where a bar laterally grows eastward around 675 m from 2011 to 2013.

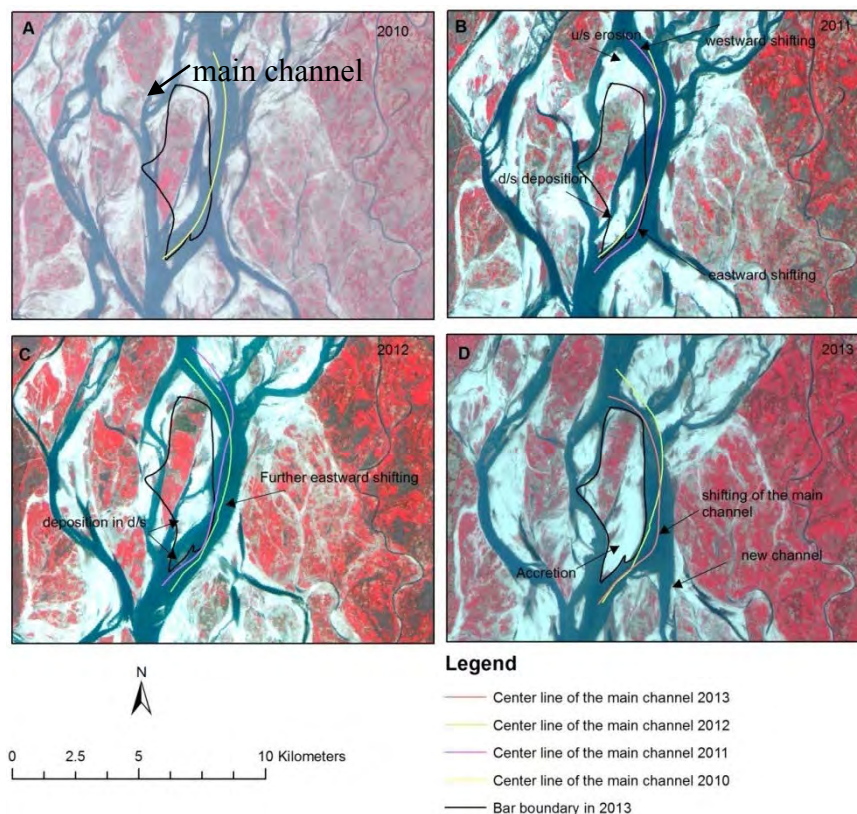


Figure 5-22: Adjacent Channel shifting process and lateral growth of bar

A 2.5 km wide mid channel bar is observed in 2010 (Figure 5-22 A). The main channel of the river flew along the left side of the bar in that time. In 2011, that channel changed its sinuosity, showing westward shifting in u/s and eastward shifting in d/s direction (Figure 5-22 B). As the response of the process, the bar top showed erosion and tail showed deposition. In 2012, the d/s channel moved further eastward and the bar showed depositing in d/s along with the formation of new bar (Figure 5-22 C). In 2013 the main channel moved further eastward with the formation of new bifurcation at the same time the bar tail showed a huge accretion around 2.28 sq km with the amalgamation of the newly formed bar.

Growth of cross-bar channels

The growth of cross-bar channel is playing one of the major roles in the growth of bar both in lateral and vertical direction. During the monsoon almost every bars are overtopped and as consequences numerous cross-bar channel are formed. In those channels the water velocity is normally low than the river main channels; as the consequences higher the sedimentation rate (sec 5.9.5). Figure 5-23 illustrates some impacts of crossbar channel on the growth of bar. Figure 5-23 A shows some small crossbar channels in the year of 2011. These channels became wider and deposited more sand in the successive year (Figure 5-23B). These cross-bar channels are one of the main source of bar top's silt and clay which initiated vegetation colonization. Figure 5-23 C shows some locations over the bar top where the low level vegetation started to grow. Sometimes these channels become wider and split the bar into two or three. Such an example is shown in Figure 5-23 C and D where a crossbar channel became wider and split the bar into two.

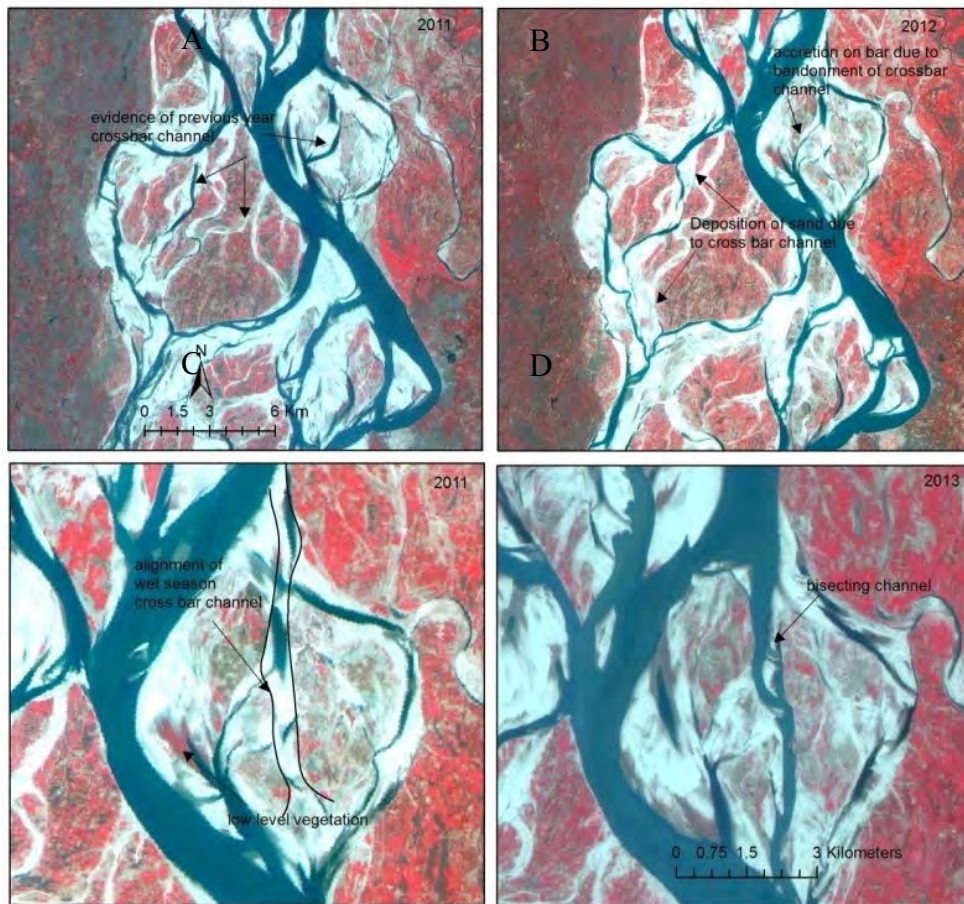


Figure 5-23: Growth of crossbar channel

Channel abandonment

Channel abandonment is a very common phenomenon in a braided river like Jamuna. This phenomenon helps to build complex bar. Sometimes several bars unities through this process to form one complex bar. Such a process is described in Figure 5-24. In Figure 5-24 A two bars are marked as 1 and 2. These bars were separated from the adjacent bars by three channels which are marked as a-a and b-b. In the successive year (Figure 5-24 B) channels a-a and b-b seemed to be abandon where as c-c increased its size. In 2013 the two channels (a-a and b-b) were completely abandon which unites two bars into one (Figure 5-24 C).

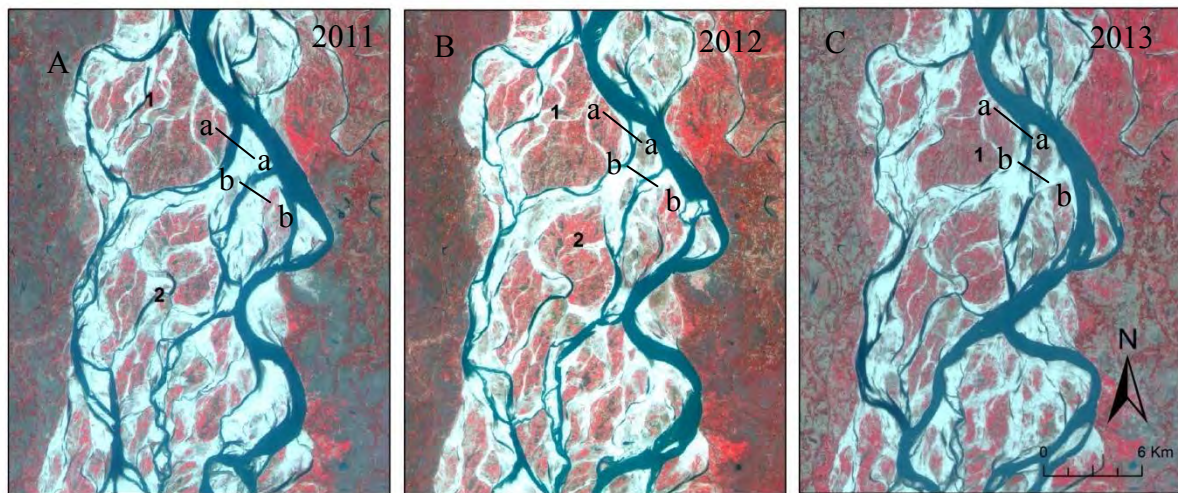


Figure 5-24: Channel abandonment and growth of the bar

It can be summarized from the discussions in section 5.8.1 and 5.8.2 that in a river like Jamuna, several types of bars may form (unit and compound bar are discussed here). The characteristics of these bars may depend on the characteristics of the adjacent channels. Sometimes new bar may form by separately (unit bar) or by joining, separating and rejoining of old bars a new compound bar may form. During these processes one channel may abandon and or development of new channels may occur depending on the characteristics of the river of that time. If the focus is given on individual bar scale, it shows that several process are acting there which may work behind the development of the bar like- Adjacent channel shifting, Growth of cross-bar channels and Channel abandonment. In the next part of this study these processes have been investigated using numerical model. Firstly, focus is given on reach scale development of bar and then bar scale properties have been investigated.

5.8 Numerical Modelling of braiding process⁴

In this study a numerical model was simulated only for the wet period of the year 2011. The assumption worked behind this simulation was the major morphological changes are happened during the monsoon season. A short description of the model has been given in the sec 4.2.5. The numerical simulation was done along 165 km long river reach; 15 km upstream from the Bahadurabad station. Figure 5-25 shows the planform of the river of 2011 and initial bathymetry of the river which is used in the numerical model. It should be noted that the planform of the river shown in Figure 5-25 was the dry season planform of the year 2011 while the bathymetry represents the wet season bathymetry of the river for the same year.

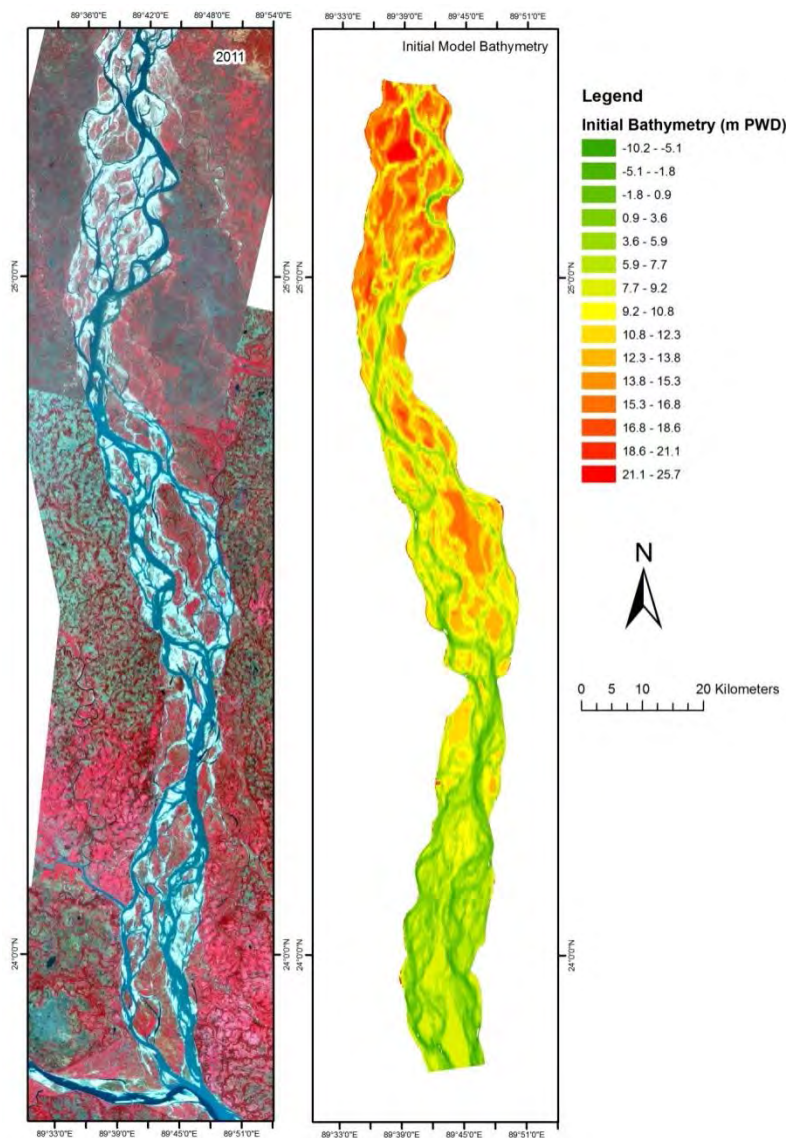


Figure 5-25 Planform of 2011 and initial bathymetry of the river

⁴ Part of this section has been accepted in the 5th International Conference of Water and Flood Management (2015)

5.9.1 Calibration and verification of the Numerical Model

The water level calibration was done along three points Kazipur, Sirajganj and Mathura respectively while the sediment calibration was done only for Bahadurabad station. Figure 5-26 shows the water level calibration results of the model. Here Mathura and Kazipur ($R^2=0.980$ and 0.884 respectively) shows better correlation than the Sirajganj ($R^2=0.87$). The comparison between simulated and observed water level at Sirajganj are shown in Figure 5-27. As no data is available in NWRD or BWDB after 2001, the calibration of sediment was done using the data set of sediment from 1968 to 2001 (described in sec 4.1.3) and the data measured by FAP 6. This calibration is shown in Figure 5-28. It indicates that the model predicts the sediment load better in lower discharge.

Generally calibration and verification of a numerical model requires two independent data sets, one of which is used to calibrate the model and the other to verify the results. In this study the calibration was done using the data sets of 2011 and the model was verified for the hydraulic condition of the year 2012. The verification of the model for the water level at Sirajganj was shown in Figure 5-29. This result indicates that the model predicted the water level well for the average condition rather it predicted higher in case of the peak and through of the hydrograph.

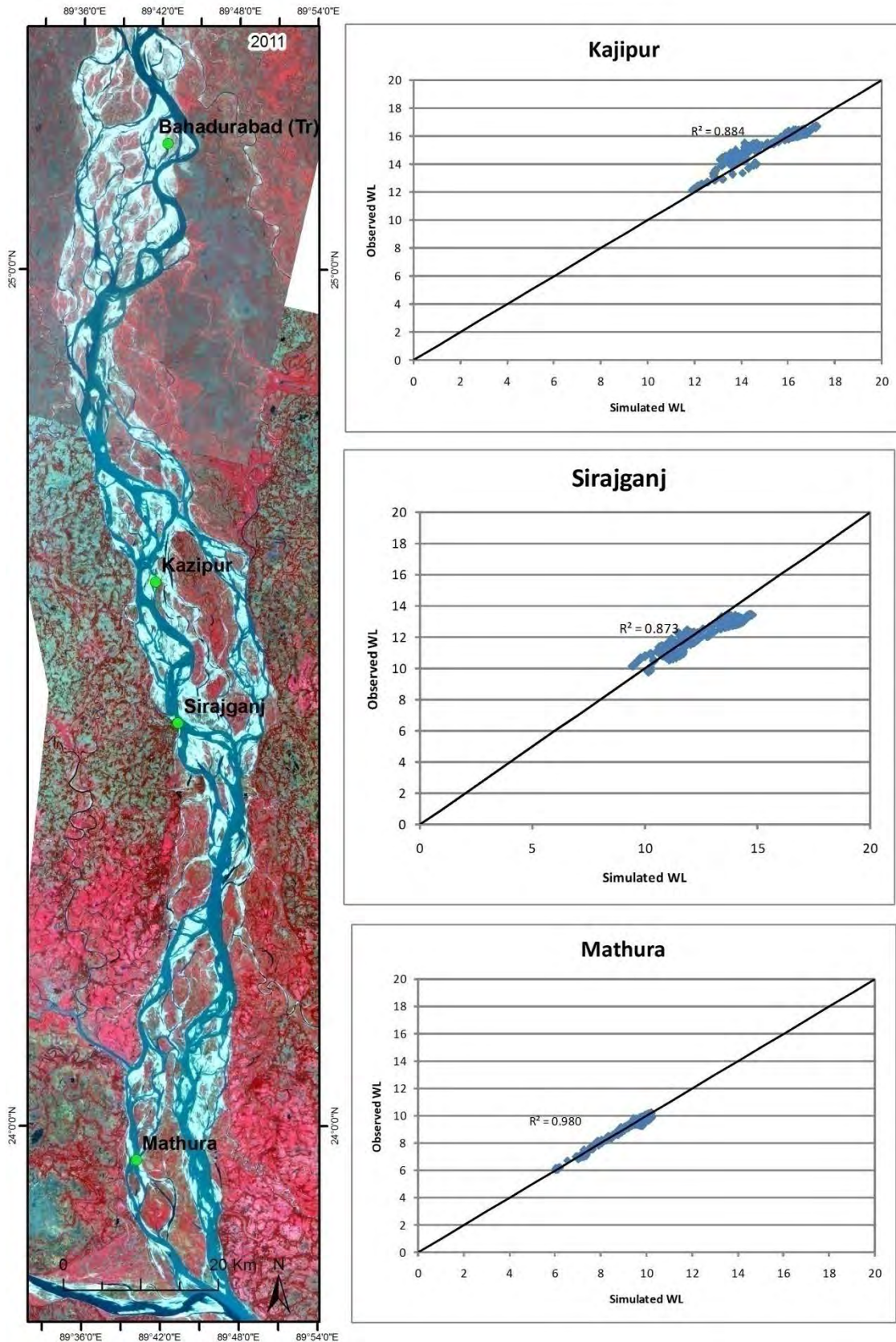


Figure 5-26: Calibration of the numerical model

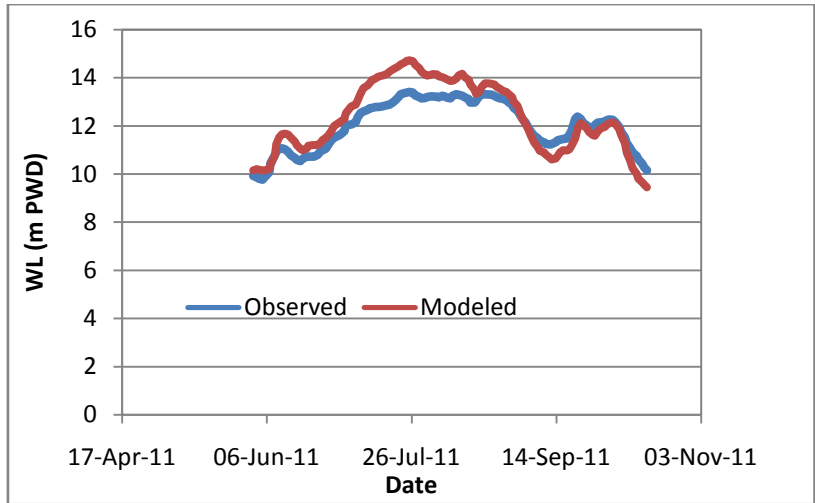


Figure 5-27: Water level calibration at Sirajgonj

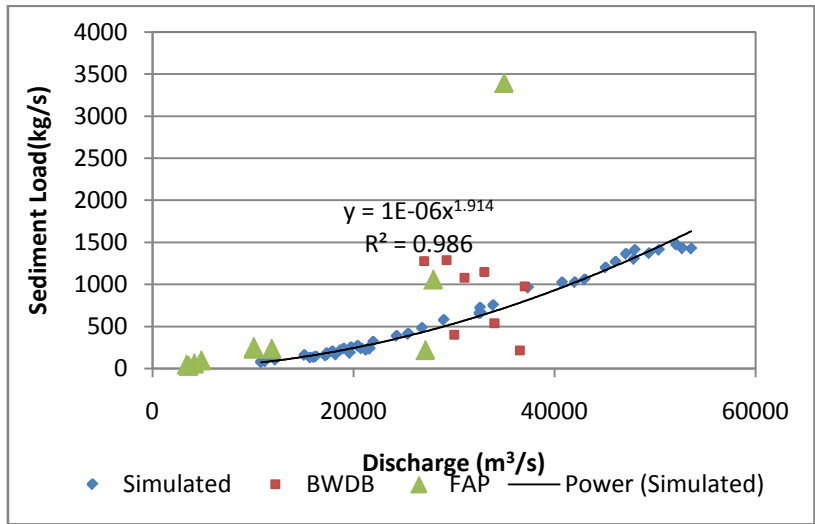


Figure 5-28: Sediment calibration at Bahadurabad

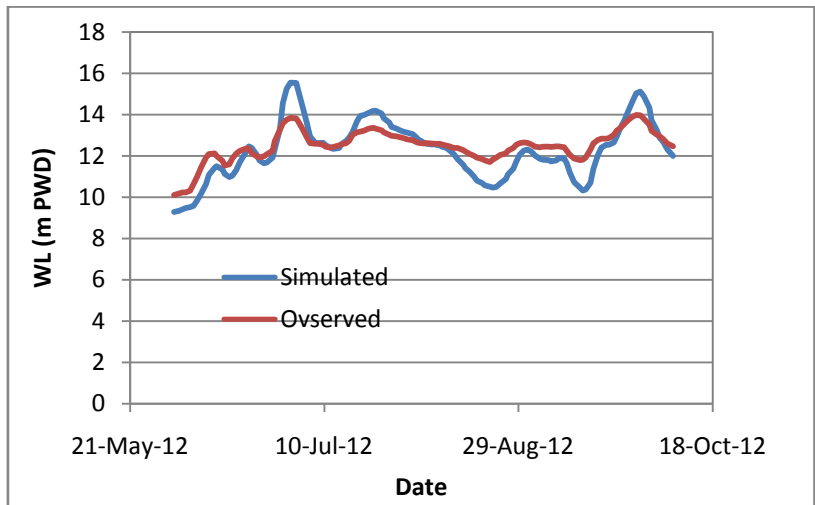


Figure 5-29: Verification of the model for the year 2012 at Sirajgonj

5.9.2 Overall planform of the river

Several behavior of the river relating to the bar development process like adjacent channels shifting, formation of cross-bar channels and channel abandonment were reproduced by numerical modeling and will be described in the following sections. Figure 5-30 shows the comparison between the actual and model planform changes in low flow period. The figure shows substantial difference between observed in modeled channel shape in some part of the river. The river like Jamuna where dynamicity and variability are very high, it is quite difficult to reproduce all the variability through the 2D numerical model.

In this study the numerical model was analyzed basically in two steps. Firstly some reach-scale river properties were analyzed. Along with this changes of bars as a response of these river properties were assessed. Then the focus was given on individual bars scale and attempts have been made to relate the hydraulic properties of the adjacent channels with the bar characteristics.

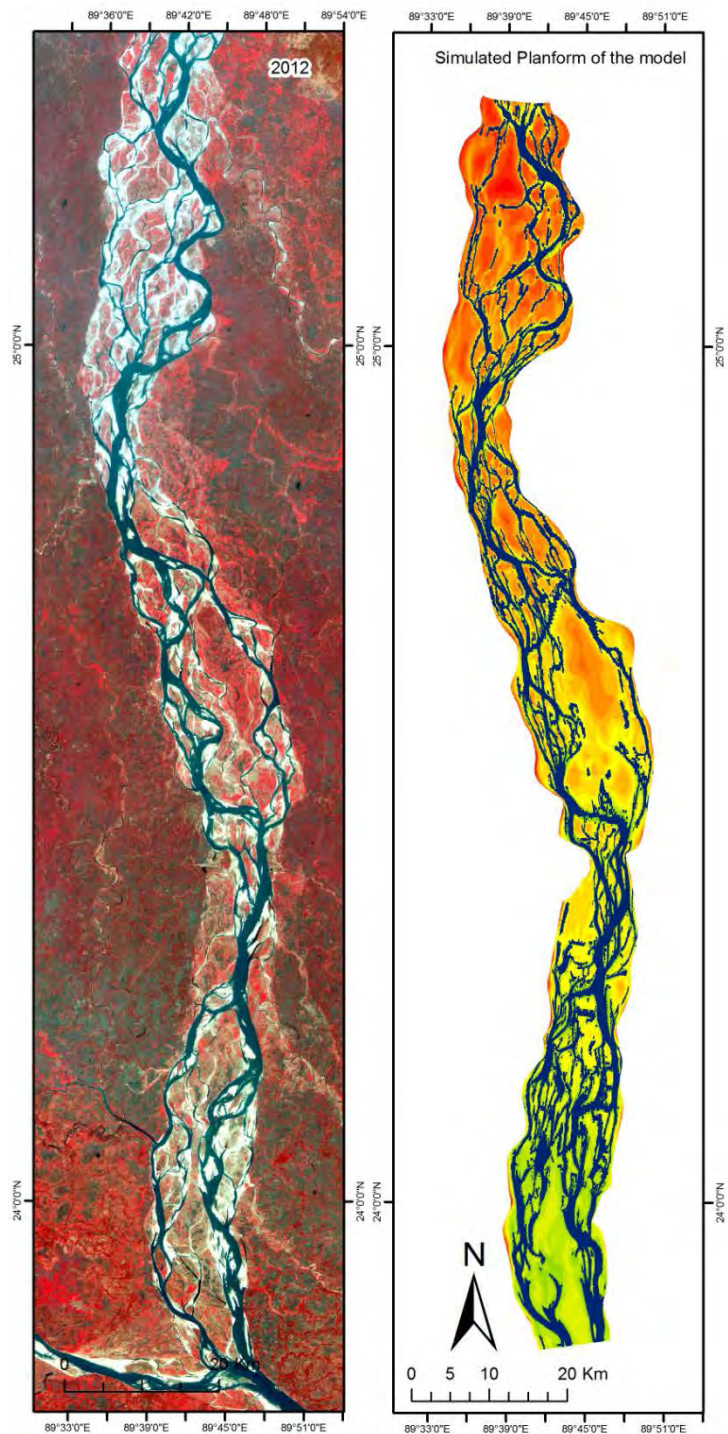


Figure 5-30: Comparison between the planform of 2012 and numerical model

5.9.3 Reach-scale River hydraulic property and Bar

5.9.3.1. Active channel properties and river bar

To assess the relationship of river hydraulic property and bar, some reach scale hydraulic property like active braided index (ABI) and active channel width were analyzed. Both the active braided index (ABI) and active channel width (ACW) was calculated considering the channels in which almost 90% sediment flew during that period as shown in Figure 5-31. The ABI varies around 2 to 7 with the increase of river discharge while the TBI was almost 1.5 (during the monsoon water occupied almost the full width of the year). This value is comparable with the TBI in dry season which has been discussed in sec 3.4.2. Brice (1983) found the braiding index of the river 4 to 6 (FAP24, 1996) while Sarker and Thorne (2006) found it 2 to 2.8 from the dry season satellite imagery analysis.

Active Channel Width (ACW) also increases with the increase of discharge as expected (Figure 5-31). The total average river width was 9.8 km while the most sediment flowing channels occupies almost 80% during the peak flow. This value recedes with the receding discharge. Figure 5-32 shows the relationship of the active width/depth (B_c/h_c) ratio to the active channel braided index ABI. This figure indicates that ABI increases with the increase of B_c/h_c of at a rate of 59%.

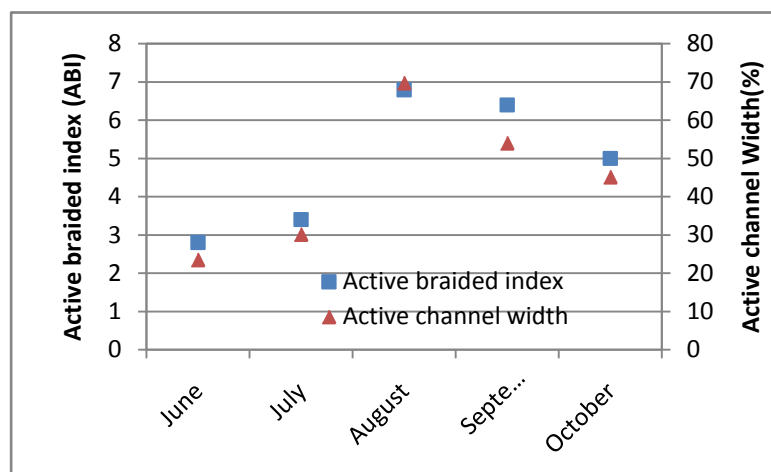


Figure 5-31: Change of ABI and ACW during the simulated period

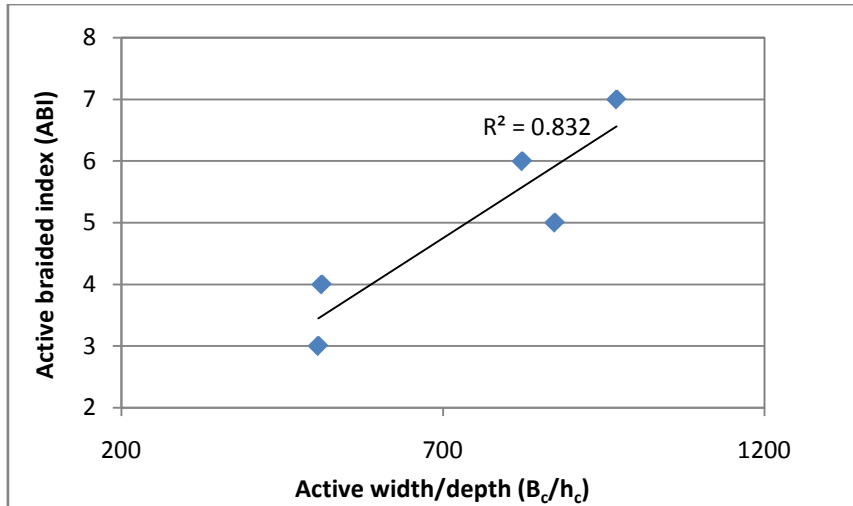


Figure 5-32: Relation between braided index and river width/depth ratio

Several previous laboratory based studies (Ikeda, 1984 and 1990; Yalin, 1992) specified the bar dimension with different semi-empirical formulae which has been discussed in sec 2.5.1. However, in this study the numerical model results shows that the relation between bar amplitude and several hydraulic parameters for unsteady flow is according to equation (5.2)

$$H_b/h_o = 8.8(B/h_o)(B/d)^{-0.3} \dots\dots\dots(5.2)$$

where, H_b = bar height (m), h_o = mean flow depth (m), d =sediment particle diameter (m)

Equation (5.2) signifies that the bar amplitude is quite higher in Jamuna compared to the bar amplitude indicated by Yalin (1992) (equation 2.4) (Figure 5-33).

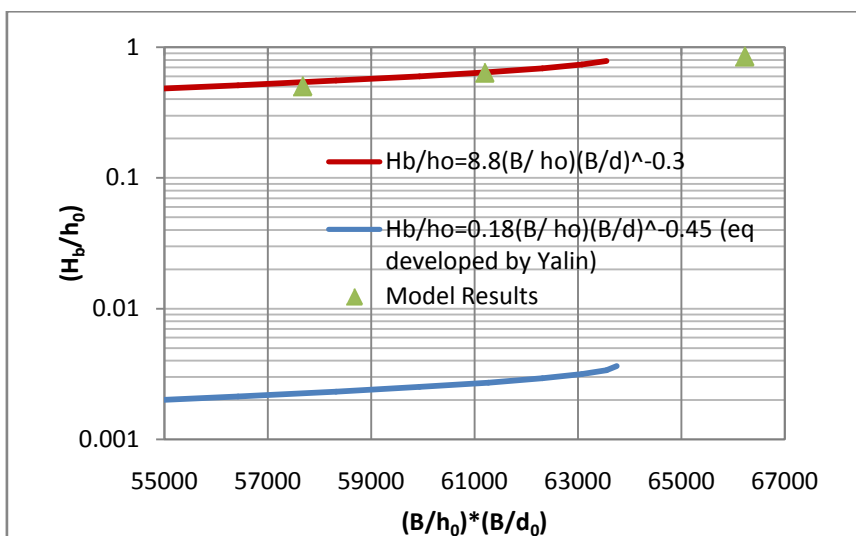


Figure 5-33: Relation between bar amplitude and different hydraulic parameters

The relationship with different hydraulic parameters with the bar length assessed from numerical model studies is shown in equation 5.3.

$$\lambda/B = 19.95(B/h_o)(B/d)^{-0.3} \dots\dots\dots(5.3)$$

where λ = bar length (m)

Equation (5.3) indicates that the bar length is higher for this river compared to the bar length proposed by Ikeda (1990) (equation 2.5) (Figure 5-34).

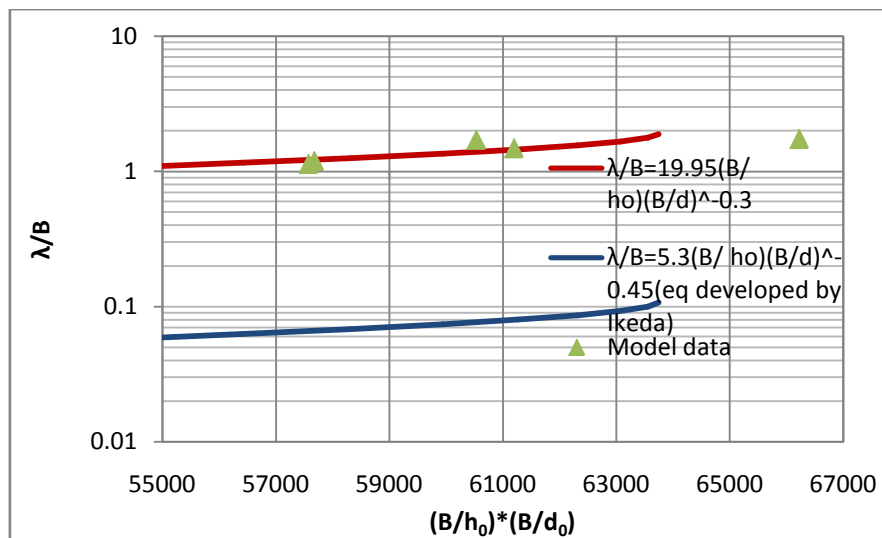


Figure 5-34: Relation between bar length and different hydraulic parameters

Figure 5-35 shows the relationship between bar amplitude and active channel width-depth ratio. For that particular season, the active channel width-depth increases 500 to 970 at the same time the amplitude of bar also increased from 3.4 m to 4.02 m. Bar aspect ratio also increases with the increment of B_c/h_c as shown in Figure 5-36. With one unit increment of B_c/h_c bar aspect ratio increases almost 0.1%. It indicates that large and high amplitude braided bars may form with the high active channel width-depth ratio. Both bar dimensions and braiding intensity are known to depend on the width-depth ratio of the braidplain, as shown by field observations and flume experiments (Bernini, et al., 2006). Fujita (1989) and Ikeda (1990) also found more formative condition for large and high amplitude bars with high channel width-depth ratio but they used the total river width-depth ratio.

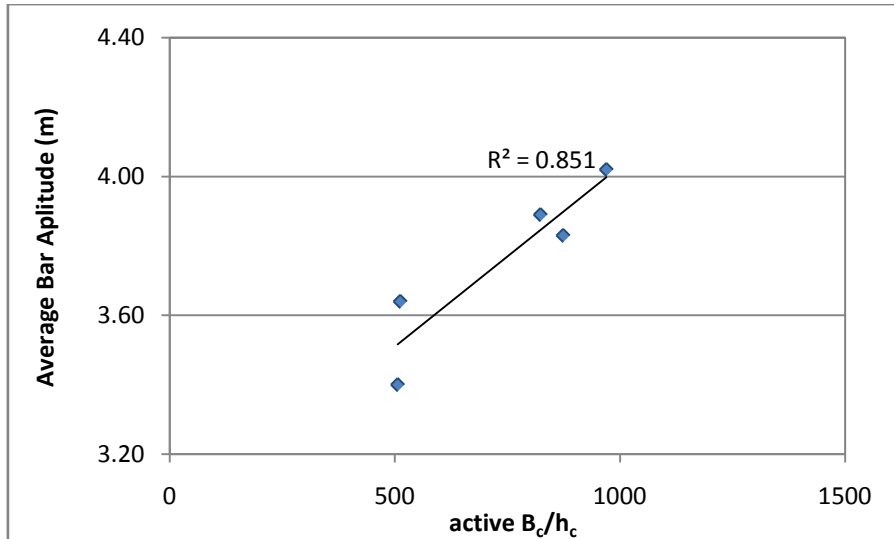


Figure 5-35: Relation between bar amplitude ratio and active B_c/h_c

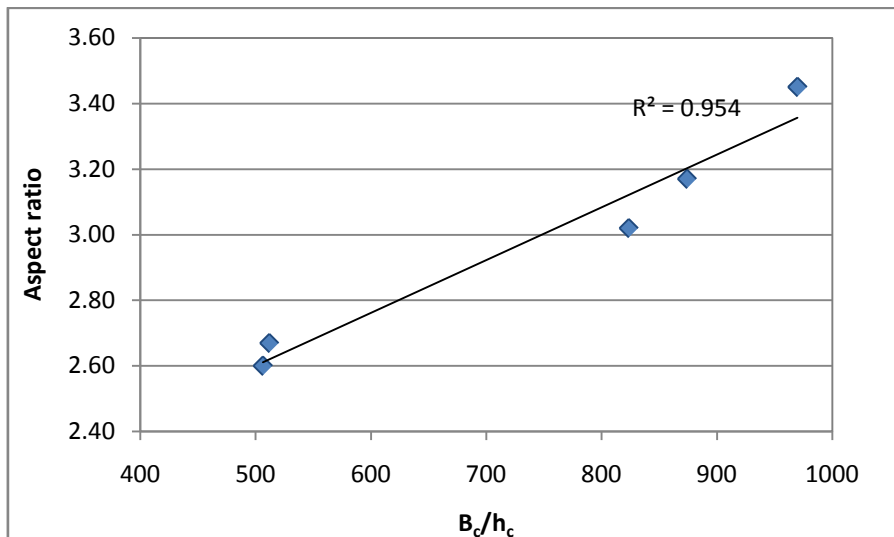


Figure 5-36: Relation between bar aspect ratio and active B_c/h_c

5.9.3.2. Sedimentation within the bankline and bar top

In this study the numerical model was simulated only for 4.5 months. Therefore, the model sedimentation indicates the monsoon sedimentation; when the rate of sedimentation is quite higher. Figure 5-37 shows the cumulative sedimentation and erosion of the model area. Figure 5-38 illustrates the net erosion or sedimentation within the bankline during the entire simulation period. During the simulation period the river experienced a net erosion of 0.12m. As the year 2011 is an average year, hence it can be concluded from the analysis shown in the Figure 5-38, Jamuna does not aggrade during the average monsoon period.

Figure 5-39 shows the cumulative average sedimentation/erosion only on the bar top of the study area. This figure indicates during the simulation period the bars grew vertically almost 1.32 m. The accretion was higher during July to Aug. Then the rate of sedimentation slowed down. However, this rate (3.5 m per year) is comparable to the growth of young bars as described in sec 5.6 which indicates the vertical growth 3.11 m for the young bar (Age is equal to one year).

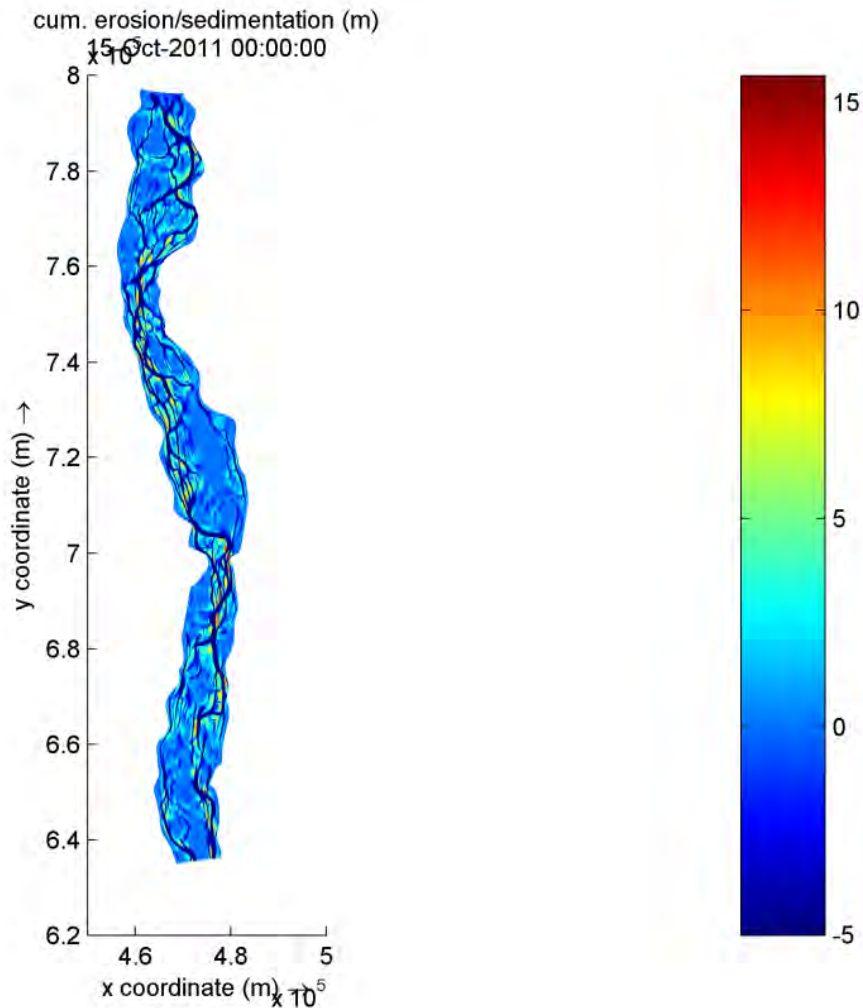


Figure 5-37: Cumulative sedimentation/erosion in the numerical model

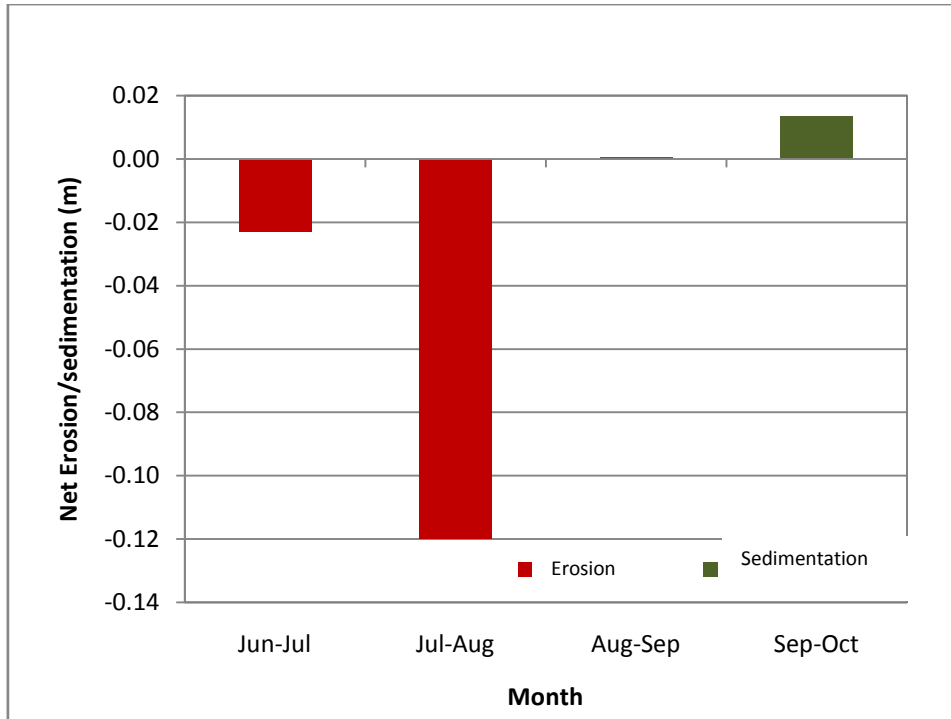


Figure 5-38: Net sedimentation/erosion within the bankline

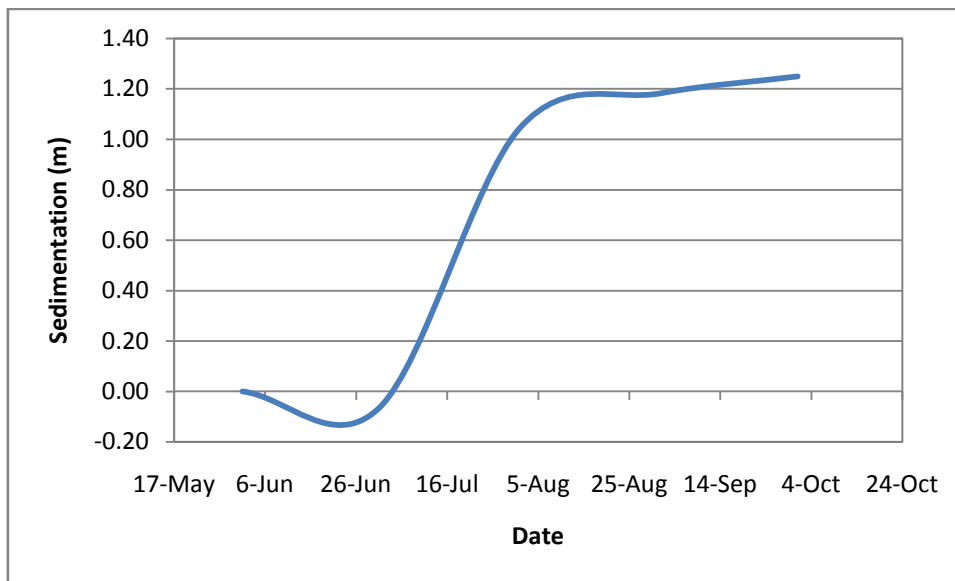


Figure 5-39: Cumulative sedimentation on the bar top

5.9.4 Relation between Adjacent Channel Characteristics and Bar

5.9.3.3. Channel shifting process and Bar size

Adjacent channel shifting process is a very common phenomenon for the growth of the braided bar. Such phenomenon has been searched in the numerical model results and attempt has been made to quantify with hydraulic parameter. Figure 5-40 shows an example of

reproduction of channel shifting process in the numerical model. In Figure 5-40, A and C shows the channel shifting behavior in the base year and successive year in the satellite image whereas B and D shows the reproduction of channel shifting process in the numerical model. Figure 5-41 shows relation of channel shifting and river bars size change. Figure 5-41A, which is the plot of ratio of channel's length to its width vs. bar's length to its width; indicates that with

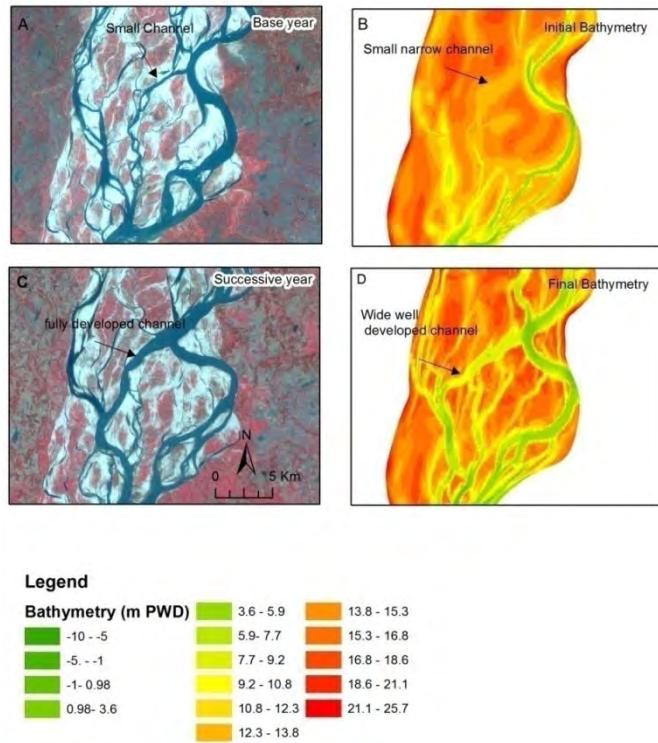
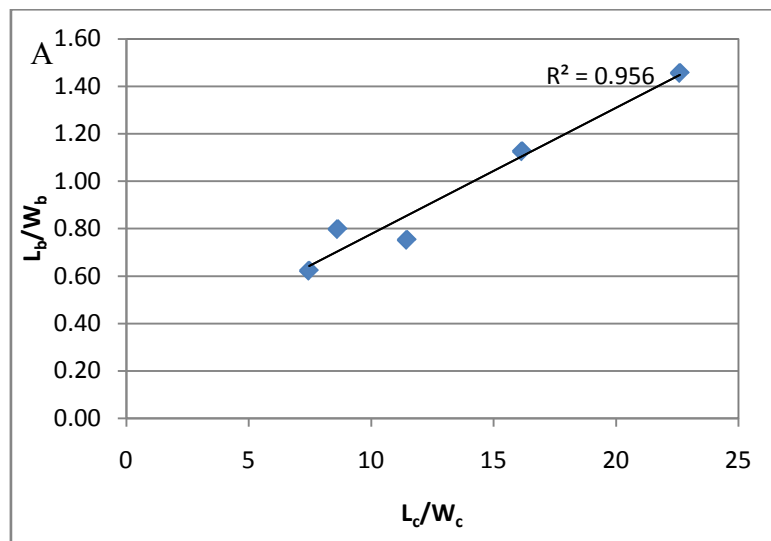


Figure 5-40: Channel shifting process and reproduction in numerical modelling

the increment of one unit change in channel's length-width ratio, bar's length/width

ratio also increases more than 5%. The Figure 5-41B shows the relationship between the bar's width/length ratios to the adjacent channel's unit discharge. With the increment of one unit discharge, the bar's size (width/length ratios) also increases at a rate of 0.7%. The relationship between the average of adjacent channel sinuosity to the bar aspect ratio are shown in Figure 5-41C. With one unit change in adjacent channel sinuosity the bar aspect ratio decreases 1.08 times.



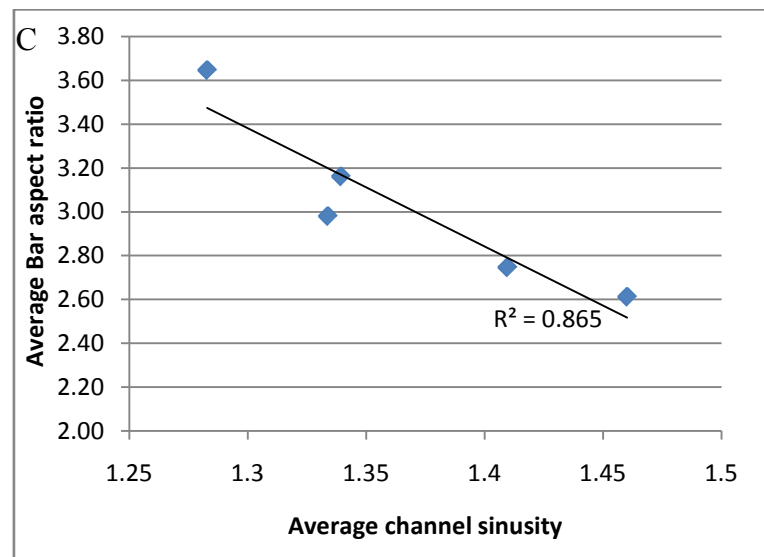
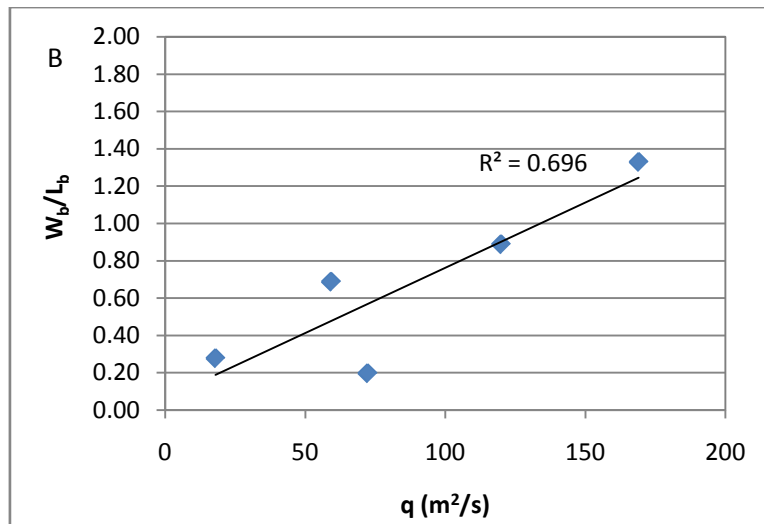


Figure 5-41: Relation between bar and channel hydraulic property where W_b = Width of the bar (m) W_c = Width of the Channel (m) L_b =Length of the bar (m) L_c =Length of the channel (m)

5.9.5 Development of crossbar channel

The growth of crossbar effects mostly the vertical growth of bar. Numerical model results reveal that in the crossbar channel the velocity of flow is lower which makes higher sedimentation rate (Figure 5-42). Moreover these channels spills and make sedimentation in the adjacent bar top.

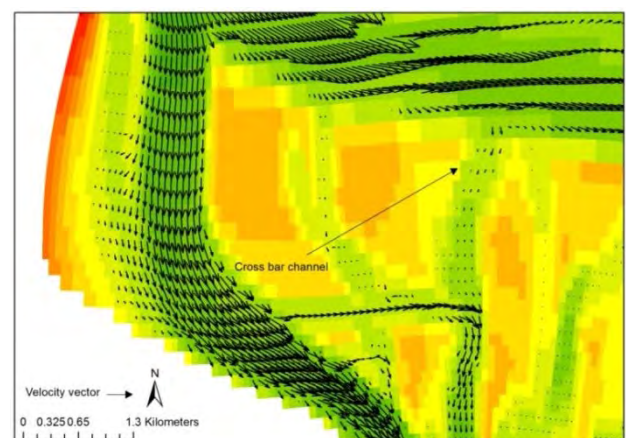


Figure 5-42: Velocity vector in main and cross-bar channel

However, Figure 5-43 shows the reproduction of the bar development process in the numerical model. Figure 5-43 A shows a small crossbar channel in the base year which it became wider in the successive year (Figure 5-43 C). Figure 5-43 B and D show the reproduction of this process in the numerical model.

Moreover, the model results indicate that the formation of cross-bar channel depend on the maximum water depth that the bar experienced during the monsoon. Figure 5-44 shows the relationship of maximum water depth of on bar and the ratio of crossbar channel area to the bar area. This figure indicates that with the change of 1m of water depth the ratio of crossbar channel area/ bar area increases over 35%. At the same time with the increase of water depth maximum bed shear stress on the bar top also increases at a rate of 18%.

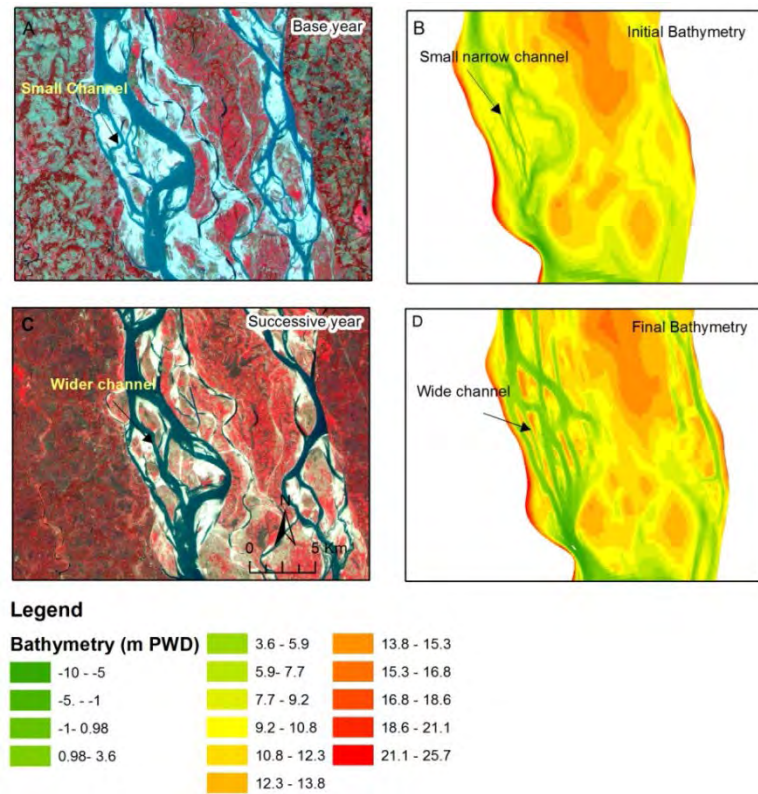


Figure 5-43: Development of crossbar channel and reproduction of the process in the numerical model

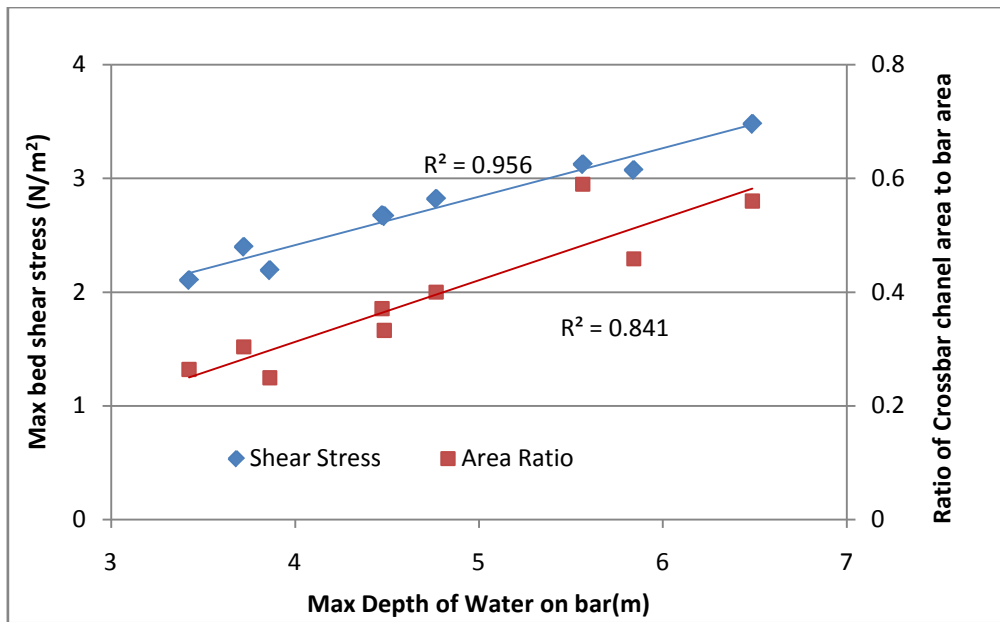


Figure 5-44: Relation between water depth, bed shear stress and crossbar channel area

5.9.6 Channel abandonment and growth of bar

As discussed earlier, the channel abandonment phenomenon helps to build complex bar. Numerical model results indicate that the amount of flows sharing depend on the bifurcation angle with the main flow. Figure 5-45 shows such a new event. Figure 5-45 A shows a bifurcation point where two channels were flowing maintaining almost equal angles (50.56° and 50.35° respectively). But in the successive year, the

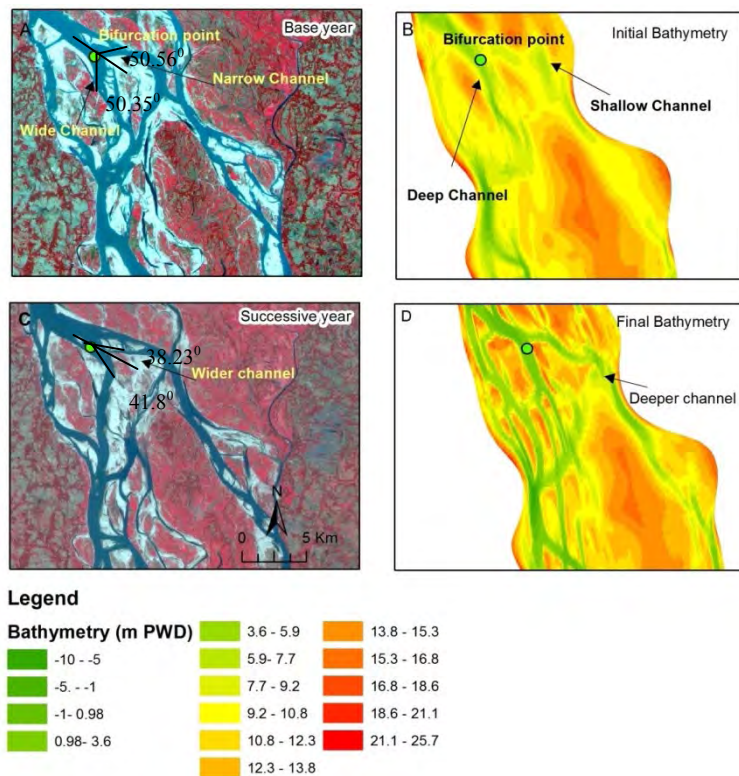


Figure 5-45: Channel abandonment process and reproduction in numerical modelling

point of bifurcation moved 1 km eastward with the change in bifurcation angle of the both

channels (Figure 5-45 C). Comparing the A, B, C and D of Figure 5-45, it can be said that with decreasing the angle the channel with the main flow, it became wider and deeper. Figure

5-46 shows the relation between the channel bifurcation angle and the percentage of flow sharing. This figure indicates with 1° increment in the angle with the main flow the percentage of flow decrease almost 2.3%.

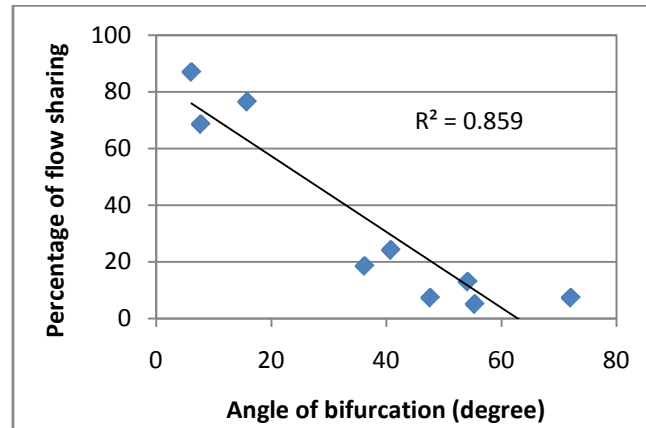


Figure 5-46: Relation between bifurcation angle and percentage of flow

5.9 Discussions

The growth of the braided bars of the Jamuna require complex. The process of bar development can be considered as an integral part of the flood and morpho-dynamics of the river and channels. Through this study, several processes which are responsible for bar growth have been investigated. In the first part of this chapter the results of the hydraulic time series data analysis have been discussed. Then these results have been tried to link with the results dry season satellite imagery analysis. Through the numerical model details of the bar development processes have been investigated.

The time series data of annual discharge (maximum, minimum and mean) shows slightly increasing trend at Bahadurabad (Figure 5-1). Though, Mirza, et al. (2001) found that there is no statistically significant trend in annual peak discharge, this study indicates this rising discharge plays a crucial role in shaping the river morphology. Mirza et al. (1998) also analyzed the time series precipitation data of the Brahmaputra basin using the Mann-Kendall rank statistic, Student's t-test and regression analysis and found no persistent trend (In Brahmaputra basin one subdivision shows a decreasing trend and another shows an increasing trend). CEGIS (2010) explained this small increase as the combined effect of decreased flood flows spilling into the Old Brahmaputra distributary and the construction of flood embankments along its right and left bank.

Though the results of the time series water level data analysis shows almost a constant trend in annual maximum, mean and minimum water level (a slight increasing trend is observed in annual minimum and mean water level but the amount of increment is very, low just a few centimeters), the river's water surface slope (at the date of annual minimum) shows a decreasing trend which is also the same for the bedmaterial load (annual maximum, minimum and average) (Figure 5-2, Figure 5-3 and Figure 5-4). CEGIS (2010) showed that the braiding intensity increased during this period (Figure 3-14). Several qualitative models (Lane, 1955; Schumm, 1969) can be used to predict the possible adjustment as a response of the change in water surface slope and bedmaterial load.

Lane proposed a qualitative relation as depicted in Equation 5.4. It relates the water discharge and channel slope to the bed material size and sediment load in a reach. According to the Lane (1955) if sediment load decreases with increasing river discharge, the river will decrease its the slope by bed degradation.

$$Q_s * d_{50} \propto Q * S \quad (5.4)$$

Where, Q_s = sediment load, d_{50} = bedmaterial size, S = slope, Q = discharge

Schumm (1969) expressed the adjustment of width, depth, meander wavelength, slope and sinuosity to changes in discharge (Q) and sediment load (Q_s) in a series of qualitative relations. According to him, if sediment load decreases with increasing river discharge, the response of the river will be the following

$$Q^+ Q_s^- \approx W^\pm, d^\pm, \lambda^\pm, S^-, P^+, F^- \quad (5.5)$$

Where, W = width, d = depth, S = slope, λ = meander wavelength, P = sinuosity and F representing the width/depth ratio. In these relations, the + sign and - sign indicate an increase and decrease in each of the parameters.

So it can be concluded from the above discussion that the change in water surface slope may be due to decreased sediment load. At the same time as the response of these processes, an increasing or decreasing trend the river width should be happened.

Such a change was also observed in the river width; during the last few decades the width of the river increased significantly (Figure 5-5). The bar area showed higher sensitivity to the widening process than the area of low flow channels. Both sand and vegetated areas increase

as the width of the river increases almost at the same pace. It indicates that the river tried to adjust its width to keep the channel area almost same throughout this period. From 1973 to 2013 the channel area changed at an average rate of 1.08 sq km per year while the bar area increased at an average rate of 18.78 sq km per year (Figure 5-6). The bar area shows more sensitivity with the change in water surface slope and change in bed material load (Figure 5-7 and Figure 5-8). From the above discussion it can be concluded that in case of braided river like Jamuna, the river response to fluvio-morphological parameter changes occurs mainly through the adjustment of its braid bars.

The temporal analyses of the river bar reveal that most of the bars (more than 53%) are young; age ranges from 0-8 years with an average of 4.5 years (Figure 5-10). Only 5.56% ages above 20 years. This result is comparable to some previous studies described in sec 2.7. ISPAN (1995) used satellite images to assess the ages of bars that existed in the early 1990s. According to them the average age of 38% of the bars, observed in 1992 dry season satellite image, were within three years but they found that only 14% of the bars were older than 20 years. Hasan et al. (1999) and Sarker et al. (2003) updated the analysis of ISPAN (1995) works. They extended the analyses of bar ages and persistence for the bars appearing on satellite images of 2000. They found that the ages of more than 56% of the bar areas were within three years and only 6% of bar areas above 19 years. They further found that 34% of the bars persisted for 3 to 6 years, which was the highest among other groups of years. This study found highest age groups of bar ranges from 2 to 5 years (25.5%)

Figure 5-12 and Figure 5-13 indicate that the bars of Jamuna are not fully covered by vegetation; the maximum 70% coverage is found and it happens within the first 8 years. The vertical growth of the bar also reaches its maximum level within that period of time when the average height of the bars above low water level would go upto 5 m (Figure 5-14 and Figure 5-15). Though EGIS (1997) and Hasan et al. (1999) found a 5 years period to reach this average height but they found average height of the bars above low water level would go upto 5.5 m, which is very close to the findings of this study. It can be drawn as conclusion that in Jamuna an average braid bar matures with 8 years both in terms of vegetation coverage and vertical growth. If the bar is structurally intervened the rate of growth is faster than the natural one the accumulation of sediment over the bartop is quite less compared to the non-intervened bar (Figure 5-19).

The development of bars in a dynamic river like Jamuna does not follow a uni-direction process (Figure 5-20 and Figure 5-21). However, the major processes related to the bar development are adjacent channel shifting, growth of crossbar channels and channel abandonment (Figure 5-22, Figure 5-23 and Figure 5-24). However, these processes are essentially related to the overall morphology of the river.

2D numerical model can reproduce the major planform characteristics but here the period of numerical simulation was very small (Figure 5-30). But there is substantial difference between observed in modeled channel shape in some part of the river. The river like Jamuna where variability is very high, it is very difficult to reproduce all the variability through the 2D numerical model. However, through 2D numerical model it is possible to investigate some major bar developing phenomena (Figure 5-40, Figure 5-43 and Figure 5-45).

Several previous studies related the bar development phenomenon on river width/depth ratio (described in sec 2.5.1). However, Bertoldi et al. (2009) showed that active channel (the channels in which most of the sediment flow) can be used for better understanding of the braided river. Hence, in this study several river properties have been investigated by relating to the active channel property. Both the active braided index (ABI) and active channel width increase with the increase of discharge and recede as the discharge falls down during the simulation period (Figure 5-31 and Figure 5-32). The analysis also showed that bar amplitude and aspect ratio are seemed to be related to these active channels properties. Both the bar amplitude and aspect ratio increases with the increment of width-depth ratio of these channels (Figure 5-35 and Figure 5-36).

Though it is traditionally believed that braiding is caused by high sediment loads that the river cannot carry, resulting in deposition on the bed as internal bars and general channel aggradations (Parker, 1976); this study indicates that the river Jamuna is a degrading one for the average flooding year (Figure 5-38). During the simulation period the river experienced a net degradation of 0.12 m.

In this study the numerical model were simulated only for wet period. The sedimentation rate over the bar top is seemed to be higher during this period. The results of the numerical model indicated that the rate of sedimentation during wet season is an average 3.5 m in a year (Figure 5-37 and Figure 5-39). The BWDB data and Satellite images analysis indicates the bar will grow 3.1 m only for the 1st year from its emergence (Figure 5-15).

These numerical model revealed that the development of bar in lateral direction depend on the adjacent channel hydraulic property (Figure 5-41). With one unit change in channel length-width ratio, bar's width/length ratio also increases more than 5%. With the change in discharge the adjacent channels adjust their sinuosity causing the lateral growth of bar. But the flow and water depth of the adjacent channel depend on the hydro-morphological characteristics of the river.

However, the growth of crossbar channels depends on the amount of inundation that the bar experienced during the monsoon. In fact, high water caused higher bed shear stress which initiates the formation of crossbar channel on the bar top (Figure 5-44). Another bar development process- abandonment of the adjacent channel is mainly depending on the bifurcation angle with the main channel (Figure 5-46).

Like the other large rivers in the world, the Jamuna is also subjected to future changes like climate anomalies, human interventions etc. If such changes occur hydro-morphological condition of the river will be altered. If the discharge of the river increase due to future climate change, this study indicates the braiding intensity will be increased. At the same time there is a high chance to decrease the sediment load due to future human interventions which will affect the river and hoped to be act as a d river to continue existing morpho-dynamic process of adjustment.

Chapter 6

Conclusions and Recommendations

6.1 Conclusions

Through this study the growth of bars in lateral and vertical direction of the Jamuna River were studied using time-series satellite images, bathymetric surveys, cross-bed profiling data and numerical model within limited time and resources. The process of bar development can be considered as an integral part of the flood and morpho-dynamics of the river. Attempts have been made through this study to relate the dynamics of the bars with the dynamics of the whole river and the adjacent channels. Within the limitation of data and resources, it was not possible to address all the issues properly. Nevertheless, this study has been able to highlight some important issues which have been summarized below.

- Though during the last few decades river's discharge and water level did not change significantly, river's sediment load decreased almost 90%. As a response of the process, river reduces its water surface slope and increased its width at an average 75.67 m/y.
- The bar area showed higher sensitivity to this process. The channel area increased at an average rate of 1.08 sq km per year while the bar area increased at an average rate of 18.78 sq km per year.
- Temporal analysis of bars shows that at present maximum ages of the ranges from 1 to 5 years. Within the bar, the optimum limit that the vegetation can cover is highest 70% of the bar area.
- The vertical growth of bar stabilizes from 8 to 10 years. This range of age matches well with the colonization of vegetation of the bars. The average time required for about 70% vegetation coverage is also 8 to 10 years. This study also found the average height of the bars above low water level would be around 5 m. The growth rate of a structurally intervened bar is faster than the natural one but the accumulation of sediment over the bar top is quite less compared to a non-intervened bar.
- The numerical model can simulate several bar phenomenon like adjacent channel shifting, formation of cross-bar channels and channel abandonment.
- The numerical model results indicated that the river Jamuna is a degrading one; during the simulation period the river experienced a net degradation of 0.12 m. The

results of the numerical model also indicated that the average rate of sedimentation over the bar top during wet season was 3.5 m/year.

- Here reach scale river property was linked to the active channel property. Both the bar amplitude and aspect ratio were related to the active channel width-depth ratio. With one unit change in active channel width-depth ratio both the bar amplitude and aspect ratio increased about 0.1 %.
- The growth of bar in lateral direction depend on the hydraulic property of the adjacent channel. With the increment of channel length/width ratio, bar's length/width ratio increased at a rate of 5%. With one unit change in adjacent channel sinuosity the bar aspect ratio decreases 1.08 times.
- The growth of crossbar channel depends on the water depth that the bar experienced during monsoon. With the change of 1 m of water depth the ratio of crossbar channel area/ bar area increases over 35%.
- Adjacent channel abandonment process is mainly depend on the bifurcation angle with the main channel; with 1° increase in the angle with the main flow the percentage of flow decrease almost 2.3%.

6.2 Recommendations

The process of braided bar development is as an essential part of the morpho-dynamics of the river. Through this study the vertical and lateral growth of bars has been investigated. Based on the findings of the study the following recommendations are proposed for further studies.

- The interaction between the floodplain and river play in important role for the growth of bar i.e. act as local sediment sources (bank erosion), therefore it should be considered.
- There are several interventions in the river like revetments and groins. The effect of these interventions on channel and bar dynamics should be identified clearly for proper understanding of the natural process of bar growth.
- This study indicates numerical model can be used as a very effective tool for the future predictions of the channel and bar dynamics due to extrinsic and intrinsic factors. But in this study the numerical model was simulated for a very short period, only for one wet period due to difficulties in computational facility. For long term

prediction of the morphological process of the river, numerical model can be simulated for longer periods.

- In this study the numerical model was simulated assuming the fixed banks. But the banks of the Jamuna are highly erodible. Hence, it may be included during future studies.
- The river Jamuna is subjected to future changes like climate anomalies, human interventions etc. If such changes occur hydro-morphological condition of the river will be altered. For an example if the discharge of the river increases due to future climate change, this study indicates the braiding intensity will be increased. So before any interventions in the river, it should be considered that the river may not behave as the same as it do now. Hence detail study is needed prior to any intervention.

Reference

- Ashmore, P. E. (2000). Braiding phenomena: statics and kinetics. In: *Gravel Bed Rivers V* (Ed. by P.M. Mosley), pp. 95–114. New Zealand Hydrological Society, Wellington.
- Ashmore, P. E. (1982). Laboratory modelling of gravel braided stream morphology. *Earth Surf. Proc.*, 7, 2201–2225
- Ashmore, P. E. (1991). How do gravel-bed rivers braid?. *Canadian Journal of Earth Sciences*, 28(3), 326–341.
- Ashworth, J. P., G. H. Sambrook Smith, J. L. Best, J. S. Bridge, S. N. Lane, I. A. Lunt, A. J. H. Reesink, C. J. Simpson, and R. E. Thomas (2011). Evolution and sedimentology of a channel fill in the sandy braided South Saskatchewan River and its comparison to the deposits of an adjacent compound bar, *Sedimentology*, 58(7), 1860–1883, doi:10.1111/j.1365-3091.2011.01242.x.
- Ashworth, J. P., J. L. Best, J. E. Roden, C. S. Bristow, and G. J. Klaassen (2000). Morphological evolution and dynamics of a large, sand and silt braided bar, Jamuna River, Bangladesh, *Sedimentology*, 47(3), 533–555, doi:10.1046/j.1365-3091.2000.00305.x.
- Ashworth, J. P., Best, J. L., Roden, J. E., Bristow, C. S. and Klaassen, G. J. (2000). Morphological evolution and dynamics of a large, sand and silt braided bar, Jamuna River, Bangladesh. *Sedimentology*, 47, 533–555.
- Barua, D.K. (1994). On the environmental controls of Bangladesh river systems, *Asia Pacific Journal on Environment and Development*, 1, 81–98.
- Begum, S. and Fleming, G. (1997). Climate change and sea level rise in Bangladesh, Part I: numerical simulation, *Marine Geodesy*, 20, 33–53.
- Bernini, A., Caleffi, V., and Valiani, A. (2006). Numerical modelling of alternate bars in shallow channels. In: *Braided Rivers: Process, Deposits, Ecology and Management* (Eds Sambrook Smith, G.H., Best, J.L., Bristow, C.S. and Petts, G.), Special Publication of the International Association of Sedimentologists, No. 36, Blackwell, Oxford, 289–310.
- Bertoldi, W., L. Zanoni, and M. Tubino (2009). Planform dynamics of braided streams, *Earth Surf. Processes and Landforms*, 34(4), 547–557, doi:10.1002/esp.1755.
- Best, J. L., J. Woodward, J. P. Ashworth, G. H. Sambrook Smith, and C. J. Simpson (2006). Bar-top hollows: A new element in the architecture of sandy braided rivers, *Sediment Geology*, 190(1–4), 241–255, doi:10.1016/j.sedgeo.2006.05.022.

- Best, J. L., J. Woodward, J. P. Ashworth, G. H. Sambrook Smith, and C. J. Simpson (2006). Bar-top hollows: A new element in the architecture of sandy braided rivers, *Sediment Geology*, 190(1-4), 241–255, doi:10.1016/j.sedgeo.2006.05.022.
- Best, J. L., Ashworth, P.J., Bristow, C.S. and Roden, J.E. (2003). Three-dimensional sedimentary architecture of a large, midchannel sand braid bar, Jamuna River, Bangladesh, *Journal of Sedimentary Research*, 73, 516–530.
- Blondeaux, P., and Seminara, G. (1985). A unified bar bend theory of river meanders, *J. Fluid Mech.*, 157, 449–470, doi:10.1017/S0022112085002440.
- Brice, J.C. (1982). *Stream Channel Stability Assessment*. Washington, D.C.: Federal Highway Administration, Report No. FHWA/RD-82/021
- Brice (1983). Planform properties of meandering rivers. In C.M. Elliott, ed., *River Meandering*. New York: American Society of Civil Engineers, pp. 1–15.
- Bridge, J.S. (1993). The interaction between channel geometry, water flow, sediment transport and deposition in braided rivers. In: *Braided Rivers* (Eds Best, J.L. and Bristow, C.S.), Special Publication of the Geological Society of London, No. 75, London, 13–71.
- Bristow, C.S. (1987). Brahmaputra River: channel migration and deposition. In: *Recent Developments in Fluvial Sedimentology* (Eds Ethridge, F.G., Flores, R.M. and Harvey, M.D.), Special Publication of the Society of Economic Palaeontologists and Mineralogists, No. 39, Tulsa, OK, 63–74.
- Cant, D.J. and Walker, R.G. (1978). Fluvial processes and facies sequences in the sandy braided South Saskatchewan River, Canada. *Sedimentology*, 25, 625–648.
- Center for Environmental and Geographic Information Services (CEGIS) (2007). *Long-term Bank Erosion Processes of the Jamuna River*, Prepared for JMREMP, BWDB, Dhaka, Bangladesh
- Center for Environmental and Geographic Information Services (CEGIS) (2010). *Impact of Climate Change on Morphological Processes in Different rivers of Bangladesh*, prepared for Asian Development Bank, Dhaka, Bangladesh.
- Center for Environmental and Geographic Information Services (CEGIS) (2011). *Effectiveness of River Bank Protection Structures on Navigation*, prepared for Northwest Hydraulic Consultants Ltd, Dhaka, Bangladesh.
- Choudhury, A.M., Haque, M.A. and Quadir, D.A. (1997). Consequences of global warming and sea level rise in Bangladesh, *Marine Geodesy*, 20, 13–31.
- Coleman, J.M. (1969). Brahmaputra River: channel processes and sedimentation, *Sedimentary Geology*, 3, 129–239.

- Colombini, M., Seminara, G. and Tubino, M. (1987). Finite-amplitude alternate bars. *J. Fluid Mech.*, 181, 213–232.
- Crosato, A., and E. Mosselman (2009). Simple physics-based predictor for the number of river bars and the transition between meandering and braiding, *Water Resour. Res.*, 45, W03424, doi:10.1029/2008WR007242.
- Crosato, A., and M. S. Saleh (2010). Numerical study on the effects of floodplain vegetation on river planform style, *Earth Surf. Processes Landforms*, 36(6), 711–720, doi:10.1002/esp.2088.
- Crosato, A., E. Mosselman, F. B. Desta, and W. S. J. Uijttewaal (2011). Experimental and numerical evidence for intrinsic nonmigrating bars in alluvial channels, *Water Resour. Res.*, 47, W03511, doi:10.1029/2010WR009714.
- Crosato, A., F. B. Desta, J. Cornelisse, F. Schuurman, and W. S. J. Uijttewaal (2012). Experimental and numerical findings on the long-term evolution of migrating alternate bars in alluvial channels, *Water Resour. Res.*, 48, W06524, doi:10.1029/2011WR011320.
- Delft Hydraulics (1999). Delft3D users' manual, *Delft Hydraulics*, The Netherlands.
- Engelund, F. and Hansen, E. (1967). *A Monograph of Sediment Transport in Alluvial Streams*. Teknisk Forlag, Copenhagen.
- Environmental and GIS Support Project for Water Sector Planning (EGIS) (1997). *Morphological Dynamics of the Brahmaputra-Jamuna River*. Prepared for Water Resources Planning Organization, Dhaka, Bangladesh, 76 pp.
- Environmental and GIS Support Project for Water Sector Planning (EGIS) (2000). *Remote Sensing, GIS and Morphological Analyses of the Jamuna River, Part II*. Dhaka, Bangladesh.
- Federici, B. and Seminara, G. (2002). Sulla natura convettiva dell'instabilità delle barre fluviali. *28° Convegno di Idraulica e Costruzioni Idrauliche*, 3, 87–94, Potenza, Italy.
- Flood Action Plan 24; Delft Hydraulics, DHI and Leeds University (1996a). FAP24 River Survey Project, Special Report 9, *Bedform and bar dynamics in the main rivers of Bangladesh* (prepared for FPCO), Dhaka, Bangladesh, 107 pp.
- Flood Action Plan 24; Delft Hydraulics and DHI (1996b). FAP24 River Survey Project, Final Report, Main Volume (prepared for FPCO), Dhaka, Bangladesh, 280 pp.
- Foufoula-Georgiou, E., & Sapozhnikov, V. (2001). Scale invariances in the morphology and evolution of braided rivers. *Mathematical Geology*, 33(3), 273-291.
- Fredsøe, J. (1978). Meandering and braiding of rivers. *J. Fluid Mech.*, 84(4), 609–624.

- Germanoski, G. and Schumm, Fujita, Y. and Muramoto, Y. (1985) *Studies on the process of development of alternate bars*. Bull. Disaster Prevent. Res. Inst., 35, 55–86.
- Fujita, Y. (1989). Bar and channel formation in braided streams. In: River Meandering (Eds Ikeda, S. and Parker, G.), *Water Research Monograph*, No. 12, American Geophysical Union, Washington, DC, 417–462.
- Furbish, D.J. (2003). Using the dynamically coupled behaviour of land-surface geometry and soil thickness in developing and testing hillslope evolution models. In: *Predictions in Geomorphology* (Ed. P.R. Wilcock and R.M. Iverson), pp. 169–181. Monograph 135, American Geophysical Union, Washington, DC.
- Germanoski, D., & Schumm, S. A. (1993). Changes in braided river morphology resulting from aggradation and degradation. *The Journal of Geology*, 451-466.
- Goodbred Jr, S.L. and Kuehl, S.A. (2000a). The significance of large sediment supply, active tectonism, and eustasy on sequence development: Late Quaternary stratigraphy and evolution of the Ganges-Brahmaputra delta, *Sedimentary Geology*, 133, 227–248.
- Goodbred Jr, S.L. and Kuehl, S.A. (2000b). Enormous Ganges- Brahmaputra sediment load during strengthened early Holocene monsoon, *Geology*, 27, 559–562.
- Goodbred Jr, S.L., Kuehl, S.A., Steckler, M.S. and Sarker, M.H. (2003). Controls on facies distribution and stratigraphic preservation in the Ganges-Brahmaputra delta sequence, *Sedimentary Geology*, 155, 301–316.
- Gupta, A. (Ed.). (2008). *Large rivers: geomorphology and management*. John Wiley & Sons.
- Gupta, H., Kao, S. J., & Dai, M. (2012). The role of mega dams in reducing sediment fluxes: A case study of large Asian rivers. *Journal of Hydrology*, 464, 447-458.
- Halcrow, Sir William and Partners, (1991). *River training studies of the Brahmaputra River*, Second interim report, Annex 4, Morphological studies of the Bangladesh Water Development Board.
- Hassan, A., Martin, T. C., & Mosselman, E. (1999). Island topography mapping for the Brahmaputra-Jamuna River using remote sensing and GIS. *Geological Society*, London, Special Publications, 163(1), 153-161.
- Heun, M. et al. (1997). Site of Einkorn wheat domestication identified by DNA fingerprinting. *Science* 278 (5341), 1312–1314.
- Holeman, J.N., (1968). The Sediment Yield of Major Rivers of the World, *Water Resources Research*, Vol.4, No.4, p. 737-747.

- Hooke J. M., (1997). Styles of channel change. In *Applied fluvial geomorphology for river engineering and management* (Eds Thorne C, Hey R and Newson M), Wiley, Chichester 237–68
- Ikeda, S. (1990) *Experiments by Engels on alternate bars*. Summer School on Stability of River and Coastal Forms, La Colombella, Perugia, Italy, 3–14 September.
- Imran, M., Hasan, M.E. and Maniruzzaman, M. (2002). Microfinance in the Brahmaputra-Jamuna Chars: The Context, the Providers and Way Forward, *Finance for the Poor*, Vol. 3, No. 2. http://www.adb.org/Documents/Periodicals/Microfinance/finance_200232.pdf.
- ISPAN (FAP 16 and FAP 19) (1993). *The Dynamic Physical and Human Environment of Riverine Charlands: Jamuna*, Dhaka, Bangladesh.
- ISPAN (FAP 16 and FAP 19) (1995). *A Study of Sedimentation in the Brahmaputra-Jamuna Floodplain*, Dhaka, Bangladesh.
- Jagers, H.R.A. (2003). *Modelling planform changes of braided rivers*, PhD thesis, University of Twente, The Netherlands, 313pp.
- Kabir, M. R., & Ahmed, N. (1996). Bed shear stress for sediment transportation in the River Jamuna. *Journal of Civil Engineering*, The Institution of Engineers, Bangladesh CE24, 55-68.
- Kelly, S. (2006). Scaling and hierarchy in braided rivers and their deposits: Examples and implications for reservoir modeling, In *Braided Rivers: Process, Deposition, Ecology and Management*, edited by G. H. S. Smith et al., pp. 75–103, Blackwell, Oxford, UK, doi:10.1002/9781444304374ch4, (to appear in print)
- Khan S R, Kudrass H R (1999). *Holocene sedimentation of the lower Ganges-Brahmaputra river delta, Bangladesh*. SONNE-SO126 cruise Final Report, Federal Institute for Geosciences and Natural Resources, Stilleweg 2, 30655, Hanover, Germany
- Khan, N.I. and Islam, A. (2003). Quantification of erosion patterns in the Brahmaputra-Jamuna River using geographical information system and remote sensing techniques, *Hydrological Processes*, 17, 959–966.
- Klaassen, G.J. and Masselink, G. (1992). Planform changes of a braided river with fine sand as bed and bank material, Proc. *5th international Sump. River Sedimentation*, Karlsruhe, FR Germany, 459-471.
- Klaassen, G.J. and Vermeer, K. (1988). Confluence scour in a large braided river with fine bed material. Proceedings of the *International Conference on Fluvial Hydraulics*, Budapest, Hungary, International Association of Hydraulic Research, Budapest, 395–408.

- Kleinhans, M. G., and J. H. Van den Berg (2011). River channel and bar patterns explained and predicted by an empirical and a physics-based method, *Earth Surf. Processes and Landforms*, 36(6), 721–738, doi:10.1002/esp.2090.
- Lane, E.W. (1955). Importance of Fluvial Morphology in Hydraulic Engineering, *ASCE, Proceedings*, Vol. 81, Paper 795, pp 1-17.
- Langendoen, E. J. (2001). Evaluation of the effectiveness of selected computer models of depth-average free surface flow and sediment transport to predict the effects of hydraulic structures on river morphology, *J. Geophys. Res.*, 111, F04006, doi:10.1029/2005JF000416.
- Lesser, G. R., Roelvink, J. A., Van Kester, J. A. T. M., & Stelling, G. S. (2004). Development and validation of a three-dimensional morphological model. *Coastal engineering*, 51(8), 883-915.
- Leopold, L. B., Wolman, M. G., and Miller, J. P. (1964). *Fluvial processes in geomorphology*, W. H. Freeman and Company, San Francisco, California.
- Leopold, L.B. and Wolman, M.G. (1957). *River channel patterns: braided, meandering and straight*, Professional Paper United States Geological Survey, 262-B, 51 pp.
- Meshkova, L. V., and P. A. Carling (2013). Discrimination of alluvial and mixed bedrock-alluvial multichannel river networks. *Earth Surf. Processes and Landforms*, 38, 1299 – 1316, doi:10.1002/esp.3417.
- Meyer-Peter, E., and R. Mueller (1948). Formulas for bed-load transport, in Proceedings 2nd Meeting of the International Association for Hydraulic Structures Research, edited by International Association for Hydraulic Structures Research, pp. 39–64, *Int. Ass. for Hydr. Struct. Res.*, Stockholm, Sweden.
- Mirza, M.M.Q. (2002). Global warming and changes in the probability of occurrence of floods in Bangladesh and implications, *Global Environmental Change*, 12, 127–138.
- Mirza, M. Q., Warrick, R. A., Ericksen, N. J., & Kenny, G. J. (1998). Trends and persistence in precipitation in the Ganges, Brahmaputra and Meghna river basins. *Hydrological Sciences Journal*, 43(6), 845-858.
- Mirza, M.M.Q., Warrick, R.A., Ericksen, N.J. and Kenny, G.J. (2001). Are floods getting worse in the Ganges, Brahmaputra and Meghna basins?, *Environmental Hazards*, 3, 37–48.
- Morgan, J.P. and McIntire, W.G. (1959). *Quaternary geology of the Bengal Basin, East Pakistan and India*, Bulletin of the Geological Society of America, 70, 319–342.
- Mosley, M. P., (1976). An experimental study of channel confluences, *Journal of Geology*, 84, 535–562.

- Muramoto, Y. and Y. Fujita. (1977). *Study on meso scale river bed configuration*, Annuals, Disast. Prev. Res. Inst., Kyoto Univ., 20B-2, 243-258.
- Muramoto, Y. and Y. Fujita, A. (1978). classification and formative conditions of river bed configuration of meso scale, Proc. 22nd Japanese Conf. on Hydraulics, Japan Soc. Civ. Eng., 275-282.
- Murray, A. B., & Paola, C. (1994). A cellular model of braided rivers. *Nature*, 371(6492), 54-57.
- Murray, A. B., & Paola, C. (1997). Properties of a cellular braided-stream model. *Earth Surface Processes and Landforms*, 22(11), 1001-1025.
- Nicholas, A. P., Ashworth, P. J., Sambrook Smith, G. H., & Sandbach, S. D. (2013). Numerical simulation of bar and island morphodynamics in anabranching megarivers. *Journal of Geophysical Research: Earth Surface*, 118(4), 2019-2044.
- Parker, G. (1976). On the cause of characteristics scales of meandering and braiding in rivers, *Journal of Fluid Mechanics*, vol. 76, part 3, p. 457-480.
- Rahman, M.M., Murata, H., Nagata, N. and Muramoto, Y. (1998). Local Scour around Spur-dike-like Structures and their Countermeasures using Sacrificial Piles, *Annual Journal of Hydraulic Engineering*, Vol. 42, 991-996.
- Rashid, H. (1991). *Geography of Bangladesh (2nd edition)*, Published by University Press Ltd., Dhaka, Bangladesh
- Repetto, R. (2000). *Unit processes in braided rivers* (Doctoral dissertation, Ph. D. thesis, Univ. of Genova, Italy).
- Rice, S. P., Church, M., Wooldbridge, C.L. and Hickin, E. J. (2009). Morphology and evolution of bars in a wandering gravel-bed river; lower Fraser river, British Columbia, Canada, *Sedimentology*, 56(3), 709–736, doi:10.1111/j.1365-3091.2008.00994.
- Richardson, W. R.R., Thorne, C.R. and Saleem, M. (1996), Secondary Flow and Channel Changes around a bar in the Brahmaputra River, Bangladesh, In: Ashworth, P.J., Bennett, S.J., Best J.L., McLelland, S.J., *Coherent Flow Structures in Open Channels*, pp. 519-543, John Wiley and Sons Ltd.
- Richardson, W.R. and Thorne, C.R. (2001). Multiple thread flow and channel bifurcation in a braided river: Brahmaputra–Jamuna River, Bangladesh. *Geomorphology*, 38, 185–196.
- Robson, B. J., Bukaveckas, P. A. and Hamilton, D.P., 2008. Modelling and mass balance assessments of nutrient retention in a seasonally-flowing estuary (Swan River Estuary, Western Australia). *Estuarine, Coastal and Shelf Science* 76: 282-292.

- Roden J. E. (1998). *Sedimentology and Dynamics of Mega-sand Dunes, Jamuna River, Bangladesh* . Unpubl. PhD Thesis, University of Leeds.
- Roelvink, J. A. (2006), Coastal morphodynamic evolution techniques, *Coastal Eng.*, 53(2-3), 277–287, doi:10.1016/j.coastaleng.2005.10.015.
- Rosgen, D. L. (1994). A classification of natural rivers, *Catena* 22: 169--199.
- Sarker, M .H. (1996). *Morphological processes in the Jamuna River*, MS c t hesis, International Institute f or Hydraulic a nd Environmental Engineering, D elft, T he Netherlands, 175 pp.
- Sarker, M.H. and Thorne, C.R. (2006). Morphological response of the Brahmaputra-Padma-Lower Meghna River system to the Assam earthquake of 1950. In: *Braided Rivers: Process, Deposits, Ecology and Management* (Eds Sambrook Smith, G.H., Best, J .L., Bristow, C .S. a nd Petts, G .), Special Publication of t he International Association of Sedimentologists, No. 36, Blackwell, Oxford, 289–310.
- Sarker, M.H. Klassen, G.J. Noor, F. a nd Islam, M .S. (2011). Impact of t he Bangabandhu Bridge on t he Morphology of t he Jamuna River, Bangladesh. *Proc. of t he 3rd International Conference on Water and Flood Management*, IC WFM- 2011, held a t Bangladesh, 8-10 January 2011, Volume One, Pp-325-338.
- Sarker, M .H., 2009. (unpublished). *Morphological response of t he Brahmaputra-Jamuna-Padma- Lower Meghna River to the Assam earthquake of 1950*, PhD thesis, University of Nottingham, UK.
- Sarker, M.H., Huque, I., Alam, M. and Koudstaal, R. (2003). Rivers, chars, and char dwellers of Bangladesh, *International Journal of River Basin Management*, 1, 61–80.
- Sarker, M.H., Thorne, C.R., Aktara, M.N. and Ferdous, M.R. (2013) Morpho-dynamics of the Brahmaputra–Jamuna R iver, B angladesh, *Geomorphology* (in p ress). <http://dx.doi.org/10.1016/j.geomorph.2013.07.025>
- Sapozhnikov, V ., Murray, B., Paola, C. a nd Foufoula-Georgiou, E . (1998). Validation of braided-stream models: spatial state-space plots, self-affine scaling a nd island shapes. *Water Resour. Res.*, 34, 2353–2364.
- Schumm, S. A. (2005). *River variability and complexity* (Vol. 65). Cambridge: Cambridge University Press.
- Schumm, S.A. (1969). River Metamorphosis, *Journal of the Hydraulic Division*, Proc. of the ASCE, Vol. 95, No. HY1, 255-273
- Schumm, S.A. (1977). *The Fluvial System*, John Wiley & Sons, NY.

- Schumm, S.A. and Winkley, B.R. (1994). The character of large alluvial rivers. In: *The Variability of Large Alluvial Rivers* (Eds Schumm, S.A. and Winkley, B.R.), American Society of Civil Engineers, New York, 1–13.
- Schuurman, F., Marra, W. A., & Kleinhans, M. G. (2013). Physics based modeling of large braided sandbed rivers: Barp pattern formation, dynamics, and sensitivity. *Journal of Geophysical Research: Earth Surface*, 118(4), 2509-2527.
- Seijmonsbergen, A.C. (1999). The influence of neo-tectonics on river patterns in Bangladesh; a preliminary study based on Landsat MSS imagery, *Geologie en Mijnbouw*, 77, 129–135.
- Ter-Stepanian, G. (1988). Beginning of the technogene. *Bull. Eng. Geol. Environ.* 38 (1), 133–142.
- Thomas R., Nicholas A.P. (2002). Simulation of braided river flow using a new cellular routing scheme. *Geomorphology* 43: 179–195.
- Thorne, C. R., Hey, R. D., and Newson, M. D. (Eds.) (1997). *Applied fluvial geomorphology for river engineering and management*. Chichester: Wiley.
- Thorne, C.R., M.M. Hossain and Russell, A.P.G. (1995). Geomorphic Study of Bank Line Movement of the Brahmaputra River in Bangladesh, *The Journal of NOAMI*, Vol. 12 no. 1&2, p.1-10.
- Thorne, C.R., Russell, A.P.G., Alam, M.K. (1993). Planform pattern and channel evolution of the Brahmaputra River, Bangladesh. In: *Braided Rivers* (Eds Best, J.L. and Bristow, C.S.), Special Publication of the Geological Society of London, No. 75, 257–276.
- Tubino, M., R. Repetto, and G. Zolezzi (1999). Free bars in rivers, *J. Hydraul. Res.*, 37(6), 759–775, doi:10.1080/00221689909498510.
- Uddin, M.N. and Rahman, M.M. (1993). Socio - Economic Impact of Erosion along the Right Bank of the Jamuna River in Bangladesh, *DUET Journal*, Vol. 1, Issue 2, 2011.
- Umitsu, M. Late Quaternary sedimentary environments and landforms in the Ganges delta. *Sedimentary Geology*, 83, 177–186.
- Van Ballegooyen R.C, Taljaard, S., Van Niekerk, L. and Huizinga P. (2004). Using 3D Modelling to predict physico-chemical responses to variation in river inflow in smaller, stratified estuaries typical of South Africa. *Journal of Hydraulic Research* 42 (6): 563-577.
- Van der Wegen, M., and J. A. Roelvink (2008). Long-term morphodynamic evolution of a tidal embayment using a two-dimensional, process-based model, *J. Geophys. Res.*, 113, C03016, doi:10.1029/2006JF003983.

- Van Maren, D. S. (2007). Grain size and sediment concentration effects on channel patterns of silt-laden rivers, *Sediment. Geol.*, 202(1-2), 297–316, doi:10.1016/j.sedgeo.2007.04.001.
- Van Rijn, L. C. (2000). *General view on sediment transport by currents and waves*, Rep. Z2899, Delft Hydraulics, Delft, The Netherlands.
- Van Rijn, L. C. (1984). Sediment transport, Part I: Bed load transport, *J. Hydraul. Eng.*, 110(10), 1431–1456, doi:10.1061/(ASCE)0733-9429(1984)110:10(1431).
- Winkley, B. R. (1994). Response to the lower Mississippi River to flood control and navigation improvements. In S. A. Schumm and B. R. Winkley, eds., *The Variability of Large Alluvial Rivers*. New York: American Society of Civil Engineers, pp. 45--74.
- Yalin, M.S. (1992). *River Mechanics*. Pergamon Press, Oxford.